The effect of storms on fine sediment dynamics in the Dutch Coastal Zone

Anneliese K. Schmidt

Masters thesis in hydraulic engineering

2021

TU Delft

Deltares

The effect of storms on fine sediment dynamics in the Dutch Coastal Zone

by

Anneliese K. Schmidt

Student number: 4789814

in partial fulfilment of the requirements for the degree of

Master of Science

in Civil Engineering

at the Delft University of Technology,

to be defended publicly on 13 January 2021 at 16:00

Supervisor:	Erik Hendriks	TU Delft/Deltares
Thesis committee:	Stefan Aarninkhof	TU Delft
	Bram van Prooijen	TU Delft
	Thijs van Kessel	Deltares

An electronic version of this thesis is available at repository.tudelft.nl

Cover image from NASA Earth Observatory A Sea of Color and Wind (nasa.gov)

SUMMARY

The North Sea is a heavily used area, with wind parks, shipping routes, fishing, sand mining, and many future constructions planned. The Dutch Coastal Zone, the area of the North Sea containing the Dutch coast, is home to several natural areas, alongside extensive human-built flood defenses. Maintaining balance between these areas requires that we understand the complex dynamics of the system. This way, we can efficiently build what is required, while preserving the natural areas and their ecosystems.

The Dutch Coastal Zone is about 70km wide, running parallel to the Dutch coast. It is relatively shallow and periodically stratified between the Rhine outflow at Rotterdam and IJmuiden. Its seabed mostly consists of sand (median grain size ~ 300 µm), with a fraction of fine sediment (median grain size < 63 µm) varying in space and time. The fine sediment fraction is important for the ecological functioning of the area, as turbidity strongly increases when it is suspended in the water column which hinders light penetration. Fine sediments are also responsible for the siltation of approach channels to important ports in the area. The yearly climate can be divided into a summer and a winter period, where the winter period has higher waves and wind speeds than the summer period. Previous research has shown that there is a higher concentration of fine sediment in the water column in winter, which is likely caused by the more frequent occurrence of storms and/or patterns in biological activity. However, the exact dynamics of fine sediments during these storms are still incompletely understood. It is also unclear how sediment stirred up by human interference behaves, and how it is transported through the system.

This project sets out to analyze the behavior of fine sediments in the water column due to storms in the Dutch Coastal Zone, using a combination of field data and modeling. To interpret this data, we conceptualize the seabed using the two-layer model concept of van Kessel et al (2011). In this model, a thin top layer, consisting purely of fines, resides on top of a thicker lower layer, which is composed of a mixture of sand and fines. This expresses the heterogeneity in the vertical sediment distribution, caused by the mixture of sediment sizes. In this model, we assume that the top layer, called the 'fluff layer', is resuspended at every tide and deposited again during slack when conditions are calmest. The lower layer, called the 'buffer layer', is much more stable, eroding only during very energetic conditions such as storms.

With existing knowledge of fine sediment dynamics, we created a theoretical model of the response of the seabed. Initially, both the fluff and buffer layer contain fine sediment. During the storm, the fluff and part of the buffer are eroded. When the sediment settles, the sand settles first followed by the fine sediment. The resulting bed is stratified by settling velocity, and the fines which were stored in the portion of the buffer layer that was eroded are now in the fluff layer. Gradually by some process, the portion of fines eroded from the buffer layer during the storm is re-entrained into the buffer layer. We assume that for each tidal cycle following the storm, the maximum suspended sediment measured is representative of what is available in the fluff layer. This suspended amount decreases over time, and through this value we can follow the recovery of the system.

We quantify reaction to storms and subsequent recovery from our theoretical model using data gathered off the coast of Egmond aan Zee over 2 years in 10.5 m water depth, using a frame equipped with sensors in the bottom 2 m. Storms are defined in this project as energetic events (wave heights > 1 m at 1 km offshore), with clear peaks. We analyze individual events, and briefly touch on the effects of storms occurring in succession. We observe in the field data that individual storm events have corresponding peaks in suspended sediment near the bottom. Over several tidal cycles following the storm, the sediment concentrations gradually decrease until pre-storm conditions are reached. This decrease per tide can be described with an exponential decay function, with a decay constant of around 0.1 per half tidal cycle, which appears to fluctuate seasonally by ± 0.03. A computational model, delwaq and Delft-3D, was used to determine the impact of advection on the reaction and recovery from the storm. We use a closed cell 1 dimensional model, with realistic boundary conditions, to determine the impact of advection which plays a role in the recovery of the storm. From the model we also determine that a varying floc size may be responsible for the reaction of SPM to storm conditions observed in the field data.

With these new insights, we better understand how and on what time scale storms affect the fine sediment dynamics in the water column which contributes to critical knowledge of fine sediment transport in the North Sea.

TABLE OF CONTENTS

1 INTRODUCTION: SETTING AND RESEARCH QUESTIONS

The North Sea is a shallow sea adjoining the Eastern Atlantic between the UK, the Netherlands, Germany, and parts of Scandinavia. The area between England, the Netherlands, and Belgium is known as the Southern North Sea. (Figure 1). The sediment found here is a mix of sand, 100-400 µm grain size, and mud deposits (Dankers, 2005). The region of interest for this project is the Dutch Coastal Zone (DCZ), the 70 km wide area of the North Sea parallel to the coast of the Netherlands (Visser et al., 1991). This area includes many man-made structures to protect the low-lying Netherlands and enable trade, including the Delta works, the Rotterdam port extension Maasvlakte2, the Sand Motor, North Sea Canal, wind parks, and the ports of Scheveningen and IJmuiden. However, it also hosts several Natura2000 areas such as the Wadden Sea in the north of the country, and the southwestern Delta**.** Given the numerous existing and many planned human interventions there is a strong interest in understanding the dynamics of this system in detail. With better understanding, we will be able to predict how the system will react to the construction of new projects, build more efficiently with nature, and adapt to rising sea levels and a changing storm climate (Grabemann & Weisse, 2008; Sterl et al., 2009). This understanding is therefore crucial for the protection and development of the Dutch coast.

Figure 1: Satellite imagine North Sea with several important features labeled (google earth engine). Note the sediment plumes, seen as areas of lighter blue/beige along the coast of both the Netherlands and England.

The role of fine sediments, such as mud and silt, in this system has been the focus of intense research. Fine sediments affect the ecosystem in this area, where increased turbidity and sediment concentrations decrease primary production and otherwise harm a multitude of marine species (Lummer et al., 2016). For harbours, the presence of fine sediment entails continual dredging as they silt up their entrance channels and basins (Bijker, 1980; de Nijs et al., 2009).

The behaviour of fine sediments (D50 < 63 µm) is different from that of sand, which have a D50 around 300 µm. The larger surface-to-volume ratio of fine sediment particles implies that interactions with biology and other particles become important. It is known that surface sediment concentrations are higher in winter than in summer (Visser et al., 1991), though the reasons for this observation are debated. Suggested reasons are increased storm activity keeping the sediment suspended and available during winter (Van Raaphorst et al., 1998; Visser et al., 1991), and/or differences in biological activity aiding in settling the sediment and entraining it into the bed during summer (Fettweis et al., 2014, Witbaard et al, 2016). Species such as clams, worms, and diatoms all affect aspects of sediment dynamics.

The wave climate along the Dutch coast is dominated by wind, with larger waves in winter than in summer and winds predominantly from the south west. The tidal range is semi-diurnal with a range of 1.1 to 1.9 m between neap and spring. Hurricanes, or ex-hurricanes, occasionally reach the Dutch coast causing increased wind and wave conditions (van der Hout et al., 2017). Due to the shallowness of the North Sea the winds can drive water to-wards the coast causing an increase in water height and amplifying the flood tidal currents (Zhu et al., 2016). This is known as storm surge.

Previous studies have looked at behaviors of fine sediment on yearly time scales in the DCZ (van Alphen, 1990; van der Hout et al., 2017; Van Raaphorst et al., 1998; Visser et al., 1991), but only one looked at the time scale of individual storms (Fettweis et al., 2010). The cited study used data from the Belgian Coastal Zone (BCZ), where there are, in general, higher concentrations of fine sediment. The sediment in this system stays suspended for a long time following the storm, which appears to introduce these high levels of sediment into the water (Figure 2). It is unclear whether we see similar patterns in the DCZ, presumably because the bed has a lower fines content than the BCZ.

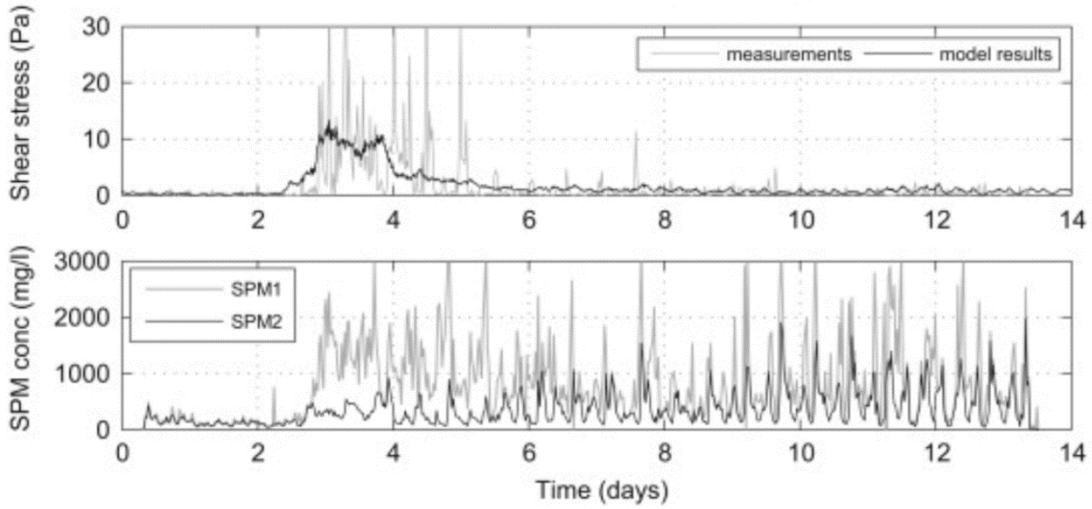

Figure 2 Times series of shear stress (top) and SPM concentration (bottom) from Fettweiss et al. 2010. Here we see the increase in SPM due to the storm, and how the higher concentrations remain until at least the end of the measurements.

1.1 PROBLEM STATEMENT AND RESEARCH QUESTIONS

The short-term effects of storms on fine sediment dynamics in mixed sediment nearshore environments have not been studied. Prior studies of fine sediment dynamics have primarily looked at the erosion and deposition relative to shear stress, longer term behaviour, developing models to match observations. Only one project has looked at a similar question, in the Belgian Coastal Zone (Fettweis et al., 2010). We do know that storms erode the bed, causing peaks in suspended sediment, and increase the mass of fines available in the upper layer of the bed for some time following the storm. But we do not know the timing of the peak of suspended sediment, or for how long following the storm this sediment is available for.

Therefore, the following research questions are posed:

1. How does the system react to the occurrence of a storm?
    a. Is there a lag between the peak of the storm and the peak in suspended sediment?
2. How does the system recover from a storm?
    a. How long does it take for the suspended sediment to return to pre-storm values?
    b. Is the recovery time consistent for different storms?
3. Are there (seasonal) differences in the reaction and/or recovery?
    a. Are differences related to the presence of diatoms?

Answering these questions will enable us to better understand the dynamics of fine sediments during and directly after storm events.

1.2 Approach

This project focuses on storms, irregular events with wave heights larger than 1 m, which cause high stresses and erode parts of the bed which are normally stable. To answer the research questions, we select a 19-month in-situ dataset from a location in the DCZ near Egmond aan Zee. This dataset consists of measurements of suspended sediment concentrations, velocity, wave height, chlorophyll-a, and bed composition. Data was gathered by a frame equipped with optical backscatter sensors, acoustic doppler velocimeters, pressure sensors, which measure in the water column, along with sediment samples taken on a 3 to 6-week interval. The comprise a unique long-term dataset allowing for detailed study of fine sediment dynamics under a variety of conditions. These measurements can provide us with insight on events and behaviors currently not included in the models, especially those surrounding storms.

After we analyze the sediment behavior from field data, a numerical model is applied to mimic the system behavior and to test the sensitivity, and specifically the effect of advection and settling velocity. Again, the focus is on storm conditions. We use the Delft3D suite with model settings for fine sediments that were calibrated for the DCZ near IJmuiden. The model is applied without accounting for horizontal gradients, i.e. it is applied in 1DV mode. Hydrodynamics from the Dutch Continental Shelf Model (DCSM) schematization are used as input. The boundary conditions were obtained from the Dutch Continental Shelf Model in Delft3D-Flow flexible mesh: DCSM DFLOW-FM (Zijl et al., 2018), run for years 2011 and 2012 at the location of the lander. We use the model to further investigate the patterns observed in the data analysis by varying parameters and observing the reaction of the fine sediments in the model. This will provide which parameters and processes are essential and will provide the sensitivity of the model to the different parameters.

1.3 Report Structure

We will begin by providing background information on relevant concepts of fine sediment dynamics, and coastal hydrodynamics (Chapter 2). Following this we will outline our approach to answering the above research questions and provide details on the available data (Chapter 3). Then we will present the results of the data analysis (Chapter 4), followed by the results of the modelling (Chapter 5). These will then be discussed (Chapter 6). We will conclude with a discussion of the relevance of our results to ongoing work, and recommendations for further research (Chapter 7).

2 THEORY

The sediment in the system we are analysing, the DCZ, consists of fines and sand. These sediments are not distributed evenly in space, or in time. This is an important aspect, as the fine sediment dynamics are in this case highly affected by the availability of sediment. In the horizontal direction, sediment is advected by currents and transported through the North Sea. In the vertical direction, sediment is resuspended and deposited depending on bed stresses. Storms erode a thicker layer of the bed than normal conditions do, as larger waves and stronger currents lead to an increase in bed shear stress. This introduces more fines into the water column as suspended particulate matter (SPM) than under normal circumstances, where only the thin layer of fines on the surface of the bed is eroded. These fines are available for some time after the storm, but for how long and how their availability decreases is not known.

2.1 THE NORTH SEA SYSTEM

The distribution of fine sediment is not homogenous throughout the Southern North Sea. Sediment is more evenly distributed in the water column, due to mixing, while in the bed the distribution varies at much smaller scales. Fines settle in the troughs of bedforms, which vary from sand bars to ripples. Concentrations over the water column are higher in south of the Southern North Sea, and there is a northward transport, advection, due to prevailing currents in this area. Advection can occur in any direction, if there is a current. In the horizontal there is long shore and cross-shore advection based on tidal currents which move longshore, and briefly cross-shore during the switch from ebb to flood and back (Rijnsburger et al., 2016). We also see vertical advection in the form of the settlement or upward movement of sediment.

The model of the North Sea from Maier-Reimer in 1977 provides an overview of the residual currents, which transport all suspended substances in the water column (Figure 3). At our research site, the yellow dot, there is a residual northward current. There are also cross shore currents, induced by the tide or a return current from waves. These currents play a large part in the sediment transport, and “mud balances” outlined by Van Alphen. Source of fines through the Dover strait, concentration decreases going northward, and decreases going further offshore of the Dutch coast (Figure 4).

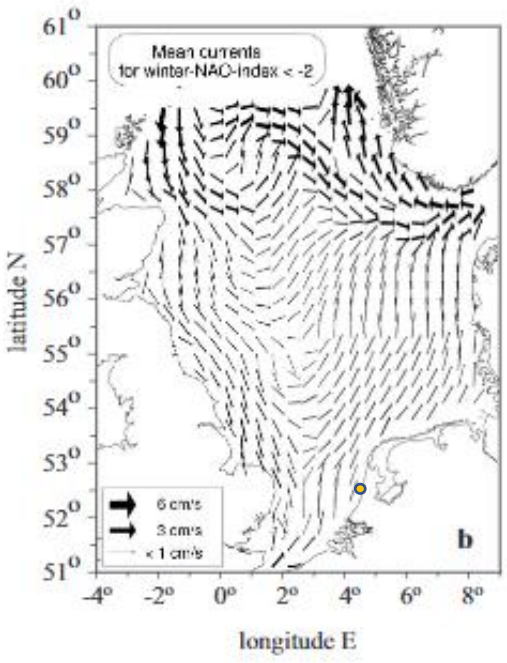

Figure 3 Mean currents from moderate winter conditions produced by a model of the North Sea, (Sündermann & Pohlmann, 2011). Yellow dot shows the approximate location of our research site, where currents run northward parallel to the coast. More severe winter conditions result in slightly stronger currents, with similar directions near the Dutch Coast.

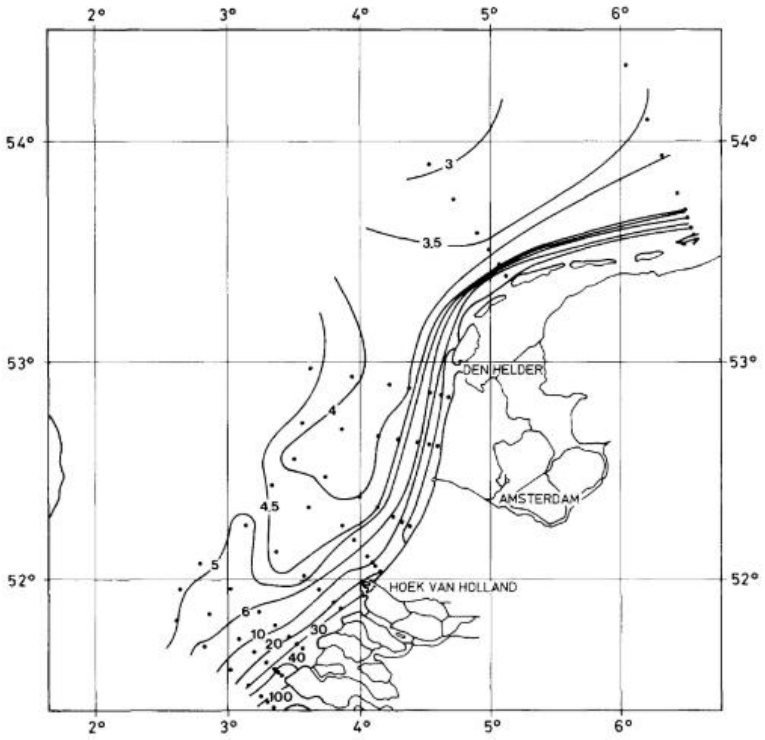

Figure 4 Concentrations of fine sediment in the water column in the DCZ. Contour lines are mg/l of suspended sediment, (van Alphen, 1990)*. The concentration of sediment is at a maximum in the south and near shore, and decreases as you move north/offshore.*

2.1.1 Coastal turbidity maximum

Along the Dutch coast, there is a coastal turbidity maximum: an area where sediment concentrations are higher than other locations in the cross shore, and it is uniform in the long shore (van der Hout et al., 2017). These high concentrations are found in the troughs of breaker bars, and at water depths of about 10 m, this is where wave stresses are less and stresses from tidal currents are also smaller than at larger depths, resulting in a calmer area where fines can settle (Hendriks et al., 2020). These concentrations vary little in the longshore but do vary in the cross shore. Sediment is therefore more likely to be advected into the area in the cross-shore direction, so potentially from the surf zone where energetic waves erode and move the bed.

Evidence from the Southern North Sea shows that this turbidity maximum is capable of moving location in the cross shore, causing changes in the overall recorded sediment concentrations depending on where the CTM is relative to the sensor (Fettweis et al., 2010).

2.2 HYDRODYNAMIC CONDITIONS

Hydrodynamic conditions are governed by an asymmetrical tide with prevailing tidal currents directed northward. The Rhine, a major river, flows out into the North Sea at Rotterdam and forms a region of freshwater influence (ROFI) which extends along the Dutch coast causing varying degrees of stratification in the water column (Flores et al., 2017; Rijnsburger et al., 2016). Due to Coriolis forces, the outflow of the Rhine turns right and flows northward along the coast. Residual currents flowing north along the coast cause a constant Northward transport of material along the coast. The climate can be described by winter and summer periods, with winters that are stormier than summers, short days and cold temperatures in winter also result in lower biological activity.

2.2.1 Tides

The tide is comprised of two main harmonic components: M2 from the lunar influence and S2 from the solar influence. The inequality in the phases of these signals causes a spring and neap cycle in the tides. At our location of interest spring tides have water level fluctuations around 1.9 m, and during neap tides 1.1 m (van der Hout

2017). Flow velocities and resulting shear stresses also vary correspondingly with higher values during spring tides than during neap tides. The asymmetry in the tides (Figure 5) is induced by the shallowness of the North Sea, which causes the tidal wave to be under the influence of bottom friction, introducing the M4 harmonic into the signal. This asymmetry results in faster flood velocities with shorter duration, and lower ebb velocities with longer duration. This causes many important behaviors, one of which is a residual northward transport of sediment caused by the larger flood than ebb velocities.

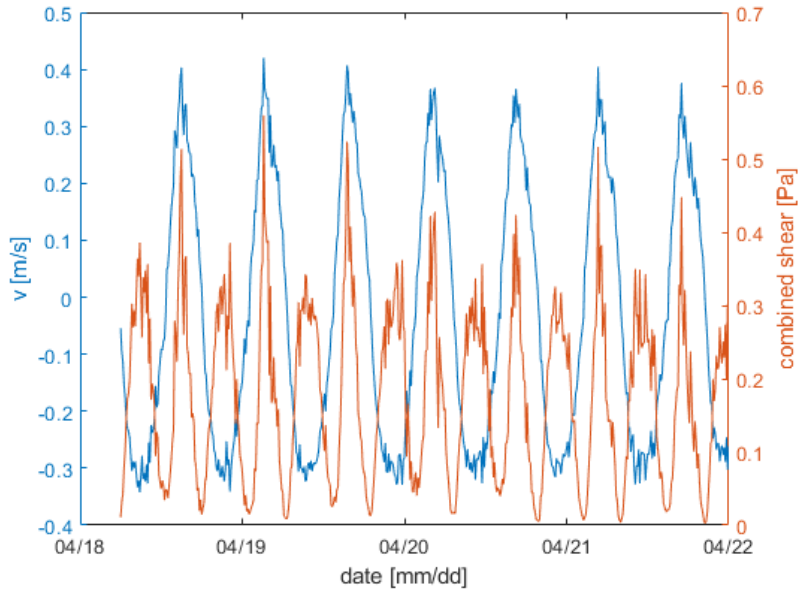

Figure 5: Near bed flow velocity and bed shear stress, showing differences in shear stress and flow velocities during flood and ebb periods. The tidal asymmetry is seen here in that the flood periods have a higher shear stress than the ebb periods and are of shorter duration.

2.2.2 Stratification

Stratification due to the Rhine is an integral part of the hydrodynamics along the Dutch coast, and in the North Sea in general. Where present, stratification determines much of the hydrodynamic behavior. Tidal currents can move in opposite directions at the bed and surface, and stratification can periodically intensify or weaken, both as an effect of tidal straining. Mixing across the interface can also be damped. This 3D behavior can make modeling and analysis of this area complicated.

At our location, there is very little stratification present, and then only during calm conditions (Nauw & van der Vegt, 2012; Rijnsburger et al., 2016). During storms, the water column generally becomes more mixed than during calm conditions. For this project, we neglect stratification on the assumption that our measurement site is sufficiently outside of the influence of the Rhine region of freshwater influence.

2.2.3 Seasonal effects

Seasonal differences in surface SPM in the Dutch coastal zone have been observed by many research projects (Fettweis et al., 2010; Suijlen & Duin, 2001; van Alphen, 1990; Van Raaphorst et al., 1998). In winter, the concentration of surface SPM is higher than in summer. One explanation for this difference is the more frequent occurrence of storms and highly energetic conditions in winter (Van Raaphorst et al., 1998; Visser et al., 1991). Wind driven currents can also contribute to seasonality, with stronger winds and currents in the winter. These may be responsible for transporting more sediment through the strait of Dover in winter (van Alphen, 1990).The previously mentioned effects of the presence of phytoplankton may also contribute to these seasonal effects.

Though since both the presence of phytoplankton and increased energetic conditions effect floc size (Fettweiss et al., 2014), which effects settling velocity, it is likely a combination of the two influences.

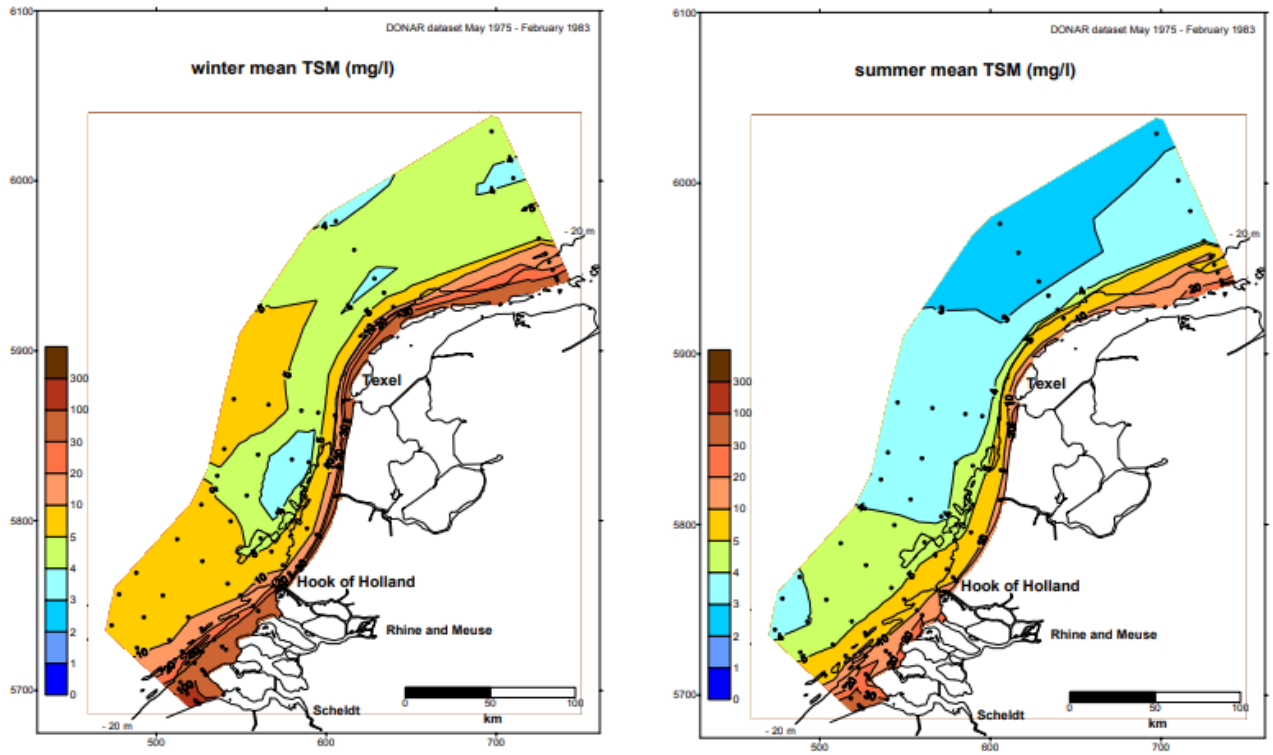

Figure 6 Mean suspended sediment near the surface during winter (left) and summer (right) from Suijlen & Duin (2001). Warmer colors indicate a higher concentration. We see higher concentrations near the coast in general, and in winter the concentrations are higher everywhere including in the coastal zone.

2.3 Interaction between sediment and hydrodynamics

The erosion and deposition of sediment depends on the hydrodynamic forcing, i.e. the bed shear stress, and the resistance of the bed as reflected through a threshold, i.e., the critical shear stress. Generally, when the shear stress exceeds this threshold parts of the bed will be eroded. For fines, this threshold is lower than for larger and denser sediments such as sand. Their deposition is also determined by setting velocity, which is lower than that of sand.

In mixed sediment systems such as the North Sea, the bed can be modeled with two layers. The bottom layer is comprised on a combination of sand and fines and called the buffer layer. Under normal conditions, this layer is stable. The top layer is comprised entirely of fines, it is generally a thin layer, but the thickness may vary. This is the fluff layer. When sediment is available in the fluff layer, this is resuspended by currents. Under calm conditions, these currents are limited to those induced by the tide and a regular pattern develops. During peak ebb/flood, the fine sediments from the upper (fluff) layer are eroded and entrained into the water column. During slack tide, when velocities are near zero, they settle out again and form the fluff layer. The supply of fines from the bed, which is determined by the fines fraction in the buffer layer and the thickness of the fluff layer, is often limited. This is referred to as supply-limited conditions (Van Kessel et al., 2011). This can happen when fines eroded from the bed do not deposit and thus remain in the water column.

Based on existing theories and the physics of fine sediment dynamics, we constructed a conceptual model which serves as our hypothesis for the behavior of the bed during and after a storm event (Figure 7). Prior to the storm, we observe normal conditions. Under these conditions with lower shear stress, only the fluff layer is eroded and deposited over the tidal cycle. During storm conditions, currents and wave conditions, and therefore shear stress, are much stronger and more of the bed is eroded. In general, waves are responsible for stirring sediment, and the currents transport it. The sediment entrained in the water column are both fines and sand. When the

sediment settles again, the sand settles first, being heavier and having higher settling velocities, and the fines which were stored in the bed settle later and become part of the fluff layer. The result is that the storm increases the available sediment. As before, the fluff layer is entrained during ebb and flood tide. However, we see that over time the mass of fine sediment in the fluff layer decreases. This happens as it again becomes buried in the bed and is stored there until the next storm event.

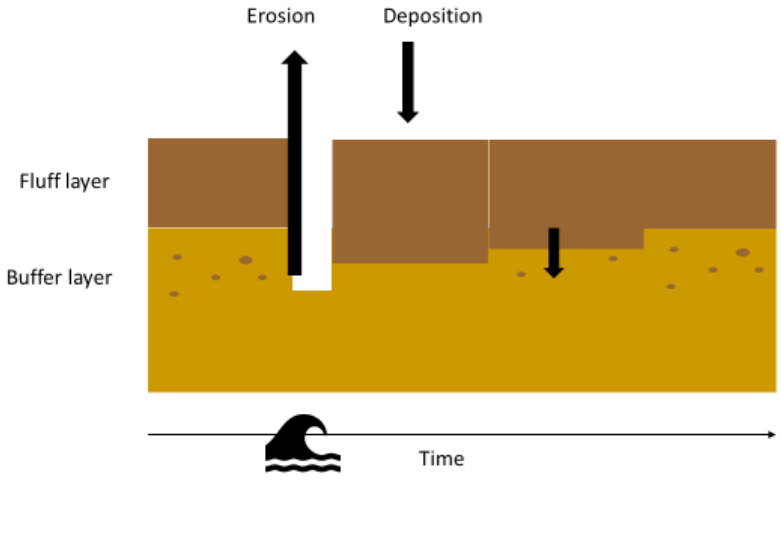

Figure 7: Idealized conceptual model of the behavior of the sea bed during and after the occurrence of a storm, dark brown indicates fine sediment, and lighter brown sand. Initially we see the buffer layer mixed, with the fluff layer on top. The occurrence of a storm erodes the fluff and part of the buffer later, this sediment then settles again and stratifies (sand on bottom, fines on top). Over time, there is a return to the pre-storm conditions.

2.4 SEDIMENTARY CONDITIONS

The sediment in the DCZ is a mixture of sand and fines. This point is important because both fractions behave differently. Fine sediment is defined as particles with a diameter smaller than 63 µm and the ability to form flocs. This behavior means that the settling velocity and density of fine sediment changes and cannot be defined by one value based on size, as it can for sand which has a predictable density. The behavior of these two sediment types, sand and fines, differs greatly. Sand generally has a larger diameter than individual particles of fine sediment. Because of this, sand has a larger volume to surface area ratio, and mass forces are therefore dominant over surface forces. The opposite is true for fine sediments, where surface forces dominate and cause interactions between sediment particles and with other small particles present in the environment such as the polymers produced as waste by algae (Deng et al., 2019), pollutants (Langston et al., 2010), and nutrients (Marinelli et al., 1998). The interaction with phytoplankton during blooms can lead to significantly different dynamics, such as an increased settling velocity (McCandliss et al., 2002). These interactions make the size and density of fine sediment flocs somewhat unpredictable.

2.4.1 Settling velocity and flocculation

The settling velocity of fine sediments does not increase with size in the same way that it does for sand, since density depends on the size of a floc due to its fractal nature. Flocs form as porous aggregates, i.e., gaps are left between particles. Flocs can form in different ways, with different densities which we are not able to measure in situ.

Flocculation of particles is caused by the attraction between oppositely charged particles. The particles of fine sediment are charged, but sea water contains ions which can surround them and cause multiple particles, even with the same charge, to stick together. Other like-charged particles behave the same way, and oppositely

charged particles also attract and bond with particles. The different types of bonds and exactly how they form is not important to understand for the project, the main takeaway is that flocculation occurs between fine sediment particles, and between fine sediment particles and other small particles.

The relationship between floc size and the presence of phytoplankton is due to the waste products produced by these organisms. As a waste product they produce Transparent Extracellular Polymer (TEPs), which aid in forming flocs (flocculant). Recent studies have investigated the effects of the presence of algae and phytoplankton on fine sediment behavior, particularly with respect to settling velocity (Deng et al., 2019; McCandliss et al., 2002). A change in floc size leads to a change in settling velocity, which is one of the main parameters determining sediment distribution and deposition out of the water column. Logically, the effect is expected to be stronger when the phytoplankton is most active, during the spring and early summer (Fettweiss et al., 2014).

Flocs do not only form, of course, they can also be broken apart. Turbulence is one of the forces which can do this. Turbulence induces mixing, causing more interaction and therefore bonding between particles. So some turbulence actually increases floc size, but more intense turbulence will break apart flocs (Figure 8). (Winterwerp, 2002). Turbulent length scales, such as the Kolmogorov microscale can be used to estimate the upper limit of floc size but does not provide further information on which floc sizes actually exist in situ (Winterwerp et al., 2002).

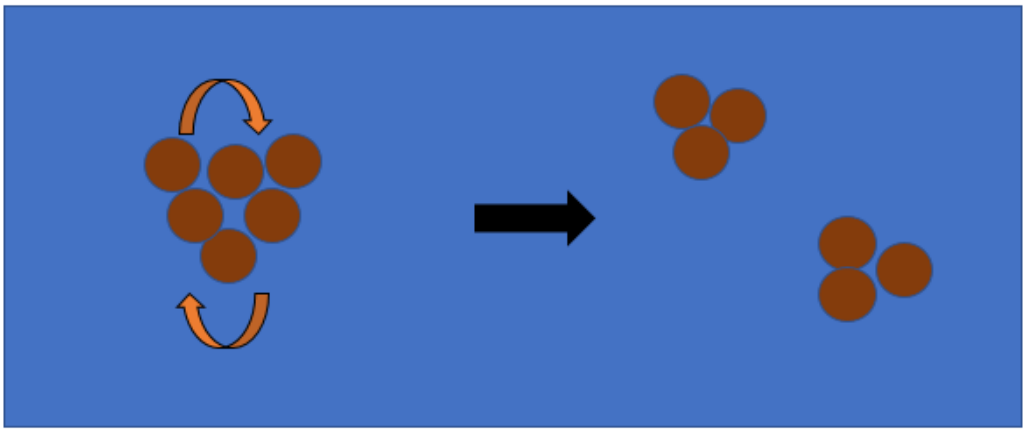

Figure 8: The breaking up of a floc due to turbulent induced eddies. The brown dots indicate very small flocs which bond and form larger flocs. The more intense the turbulence, the smaller these eddies, and the flocs will break up farther.

3 MATERIALS AND METHODS

For this study, we selected a high frequency data set spanning nearly two years. The data set consists of measured flow conditions, pressure, and turbidity in the lower part of the water column recorded near Egmond aan Zee. This data set includes several storms, making it suitable for our analysis. Due to the measuring devices being located in-situ, we obtain regular measurements during storm periods and the time surrounded them. In addition to this data set, model outcomes are supplemented where needed. The details of how we will use the data and models to answer our research questions are presented in this section.

3.1 DATA COLLECTION

Data was gathered by sensors which were mounted on a 2 m tall lander (Figure 9) that was deployed about 1 km off the coast by Egmond aan Zee (Figure 10), near the coastal turbidity maximum, from March 2011 until December 2012. Two landers were alternated every 2-6 weeks so that maintenance could be done on one at a time, and data offloaded. More details on data collection can be found in Witbaard et al. (2013).

The sensors record at several points in the lowest 2 meters of the water column. Measurements taken consisted of flow velocities, suspended particulate matter (SPM), chlorophyll-a concentration (CHL-a), temperature, salinity, and pressure from which wave conditions and water level could be derived. Sediment samples from the bed were taken every few weeks from 4 locations surrounding the lander (Figure 10). Further wave parameters such as wave period could be obtained from the nearby wave buoy at IJmuiden Munitiestortplaats. For a full list of variables, measurement locations and sensors see Table 1.

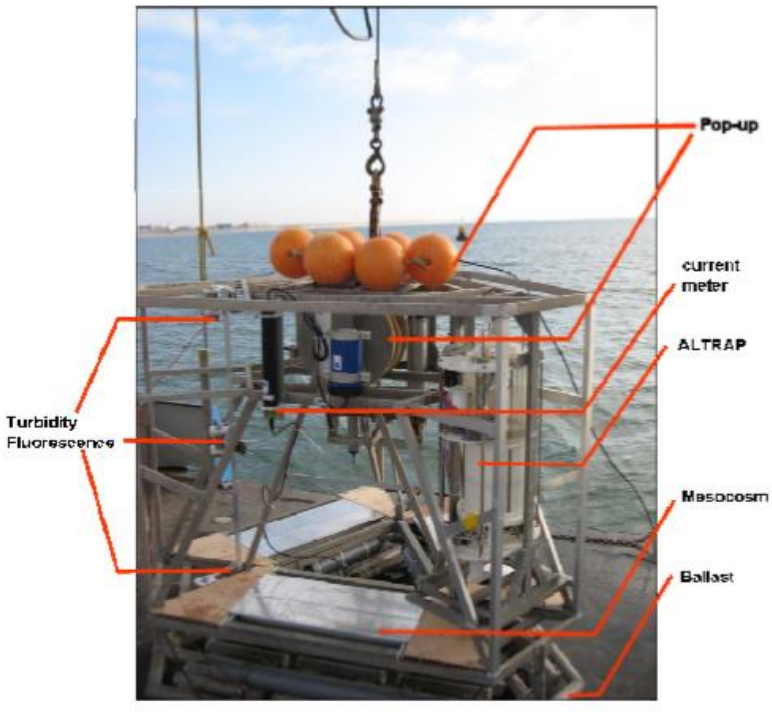

Figure 9: Image of the lander with some of the sensors, from Witbaard, (Witbaard et al., 2013). The structure is 2 m tall and equipped with sensors at several locations. The purpose of this data collection was to analyze the effect of Ensis Directus on transport of sediment within the bed, so the instruments indicated in this image are partially relevant to that.

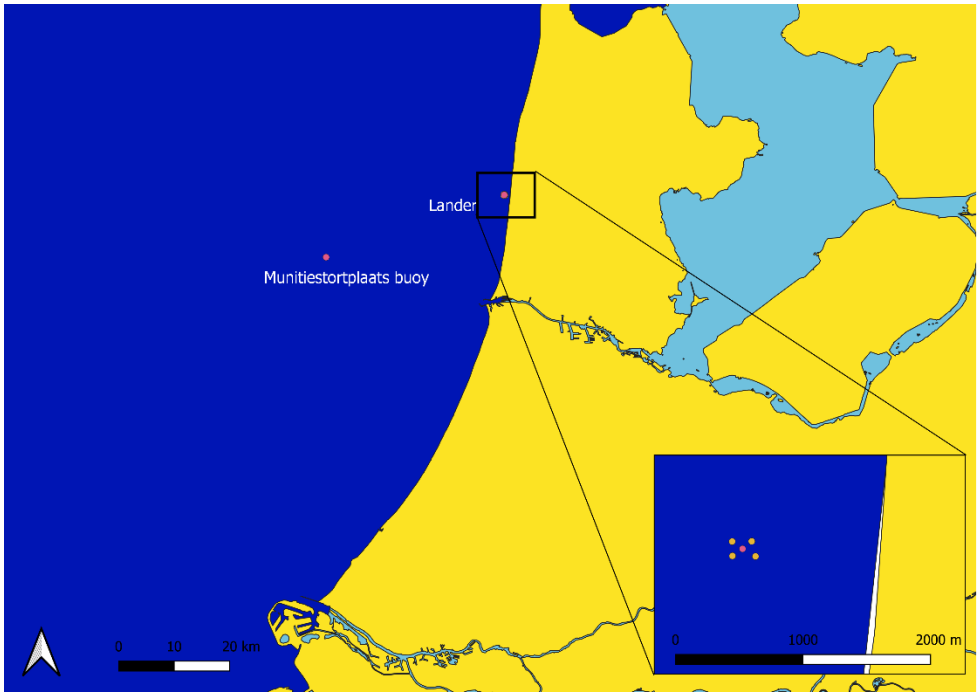

Figure 10: Locations of lander, wave buoy, and the four locations of sediment sampling in the subfigure yellow.

The sensors mounted on the lander recorded every 10 minutes, over a 2-minute burst with a sampling frequency of 1 Hz. These data were then processed to record either mean or median values over the burst. The post processed data was available from the studies by van der Hout (van der Hout et al., 2017) and Witbaard (Witbaard et al., 2013)

Table 1: Locations of data collection, height of sensor in meters above bed where applicable, sensor type, and type of data gathered from each.

Location/sensor	ADV Acoustic Doppler velocimeter	ADCP Acoustic Doppler Current Profiler	OBS Optical Backscatter Sensor	CTD Conductivity Temperature Depth	wave buoy	Box core sampler
LANDER						
0.3 mab	Velocity at 0.15 mab Distance to bed pressure	--	Suspended particulate matter, Chlorophyll-a	--	--	--
0.8 mab	--	--	SPM, CHL-a	--	--	--
1.4 mab	Velocity, pitch, roll	--	SPM, CHL-a	Temperature, pressure, salinity, density		--
2.0 mab	--	Velocity at 41 bins over water column Velocity (longshore, cross-shore, upward) Temperature Pressure	SPM, CHL-a	--	--	--
WAVE BUOY						
IJmuiden Munitiestortplaats	--	--	--	--	wave period	--

SEDIMENT SAMPLES						
Location relative to lander: NE, SE, SW, NW.						D50, percent fines

During the measurement campaign, sediment samples were taken from four stations around the lander whenever a vessel was deployed for maintenance (Figure 10). Wind data, in the form of daily mean velocity and direction, was downloaded from KNMI for the years 2011 and 2012 at the weather station IJmuiden. (http://projects.knmi.nl/klimatologie/daggegevens/selectie.cgi.).

Various sensors failed at different times over the two years, so the data sets are not continuous over the two years (Figure 11). The ADCP had the most gaps in the data, and the lowest OBS malfunctioned during the winter of 2011-2012 making this period unusable in comparison to the other storms.

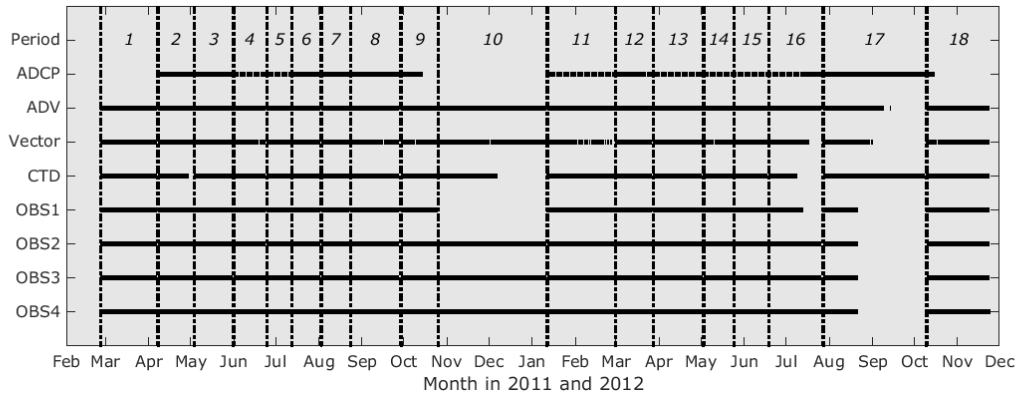

Figure 11: Time series of the sensors. Each one stopped recording at least once for some period, this figure from Carola van der Hout shows the overlap and gaps, in addition to the times a vessel retrieved the lander for maintenance and took sediment samples as vertical lines (Personal communication, 2020).

3.2 DATA PROCESSING

One of the benefits of the dataset used in this project is that it was already post-processed. Many parameters such as the SPM could be used directly from the data provided, few required either interpolation or calculation. The velocity from both the ADV and ADCP required interpolation to fill in gaps in the data. This was done using the Matlab function fillmissing to linearly interpolate. In the ADV data, the data gap comprised about 1% of the total data. For the ADCP this ratio was much higher, about 30%. Because of this gap, we rely mostly on the near bed velocity from the ADV.

To obtain the magnitude of velocity with positive values for flood and negative values for ebb, the following equation was used:

$$v = \sqrt{v_n^2 + v_e^2}\,\frac{v_n}{|v_n|} \tag{1}$$

Here, v_n is the north-south component of the velocity, and v_e the east-west component. This can also be done with ADCP data, and eventually with the model data, using the longshore and cross-shore directional velocities. Given the small angle of deviation of the coast by IJmuiden from north-south, longshore and northward are nearly the same and can be used interchangeably. Though we rely on the ADV data for most applications, the ADCP data was used to obtain a water column average. The lander interfered with the 5 bottom-most bins, so the average was found by summing over the bins above the bottom, excluding those with interference, and dividing by the number of bins for each point in time.

ADV velocities were available at 0.15 and 1.4 meters above the bed (mab). A note provided with the metadata warned that the sensor at 1.4 mab mis-identified flood and ebb periods based on the orientation. Since these were important for the analysis, the data from this sensor was not used. When referring to the ADV data throughout this project, we refer to the ADV at 0.15 mab.

3.2.1 Suspended sediment and chloropyll-a

The optical backscatter sensor (OBS) from which SPM and Chlorophyll-a concentrations were obtained do not measure these parameters directly. The device measures turbidity and fluorescence. With calibration curves, the turbidity measurements can be converted to a concentration of matter in the water column. The same can be done with fluorescence to convert the measurements to a concentration of chlorophyll-a. This was done by Witbaard during postprocessing (Witbaard et al., 2013).

Sediment samples were taken with a box core sampler, this preserved the fines content in the samples. These were then processed by cleaning and removing all organic material. During this process, flocs were also broken, and all that remained was the mineral material. This was then sieved and measured. The results of this process were provided in tables. In 2011, samples were taken from 0 to 5 cm below the water-bed interact, and in 2012 both 0-5 and 5-10 cm below the interface were sampled. For more details, refer to the report by Witbaard et al. (Witbaard et al., 2013). For each location on each day, two samples were taken for each depth. We assume the parameters do not change much between 0-5 cm and 5-10 and take the average over all samples at one location for the date of collection.

3.2.2 Wave characteristics

The wave height at the lander was calculated from the pressure sensor. This was done by using the mean difference in pressure to define wave heights (Carola van der Hout, personal communication 2020). This is different from the usual measure of wave heights, the significant wave height, which is the mean of the highest 1/3 wave heights. Thus, the median wave height is lower than the significant wave height. This will also cause the shear stress, which depends on the wave height, calculated from the field data to be lower than that from the model data.

Wave period was obtained from the wave buoy. We assume that the location is close enough, and wave period constant enough in space, that this data is representative of the wave period at the lander. To match sampling frequencies, we interpolated the hourly wave buoy data to obtain measurements every 10 minutes.

3.2.3 Shear stress calculation

The shear stress can be calculated with the depth averaged velocity, wave height, and water depth. The wave shear stress was found using the method of Van Rijn (1993) combined with that of Soulsby (1997). The current shear was found using the near bed shear velocity, u_*. These were combined to what Soulsby & Clark (2005) call the effective shear stress:

$$\tau_e = \sqrt{\tau_c^2 + \tau_w^2} \tag{2}$$

Formulas for the wave and current shear stresses used are the same as used in the Delft 3D Water Quality module (Deltares, n.d.). The expression for wave stress according to Van Rijn (1993) is:

$$\tau_w = 0.25 \rho f_w U_{orb}^2 \tag{3}$$

where ρ is the water density obtained from CTD data, U_{orb} is the maximum wave orbital velocity at the bed as obtained from linear wave theory, and f_w is the wave friction factor from Soulsby 1997:

$$f_w = 0.237 r^{-0.52} \tag{4}$$

$$r = \frac{U_{orb}}{\omega k_s} \tag{5}$$

with the wave frequency, ω, and k_s the Nikuradse roughness which is $2.5D_{50}$. From sediment sample data, the mean D_{50} is about 233 µm. The wave frequency,

$$\omega = \frac{2\pi}{T} \tag{6}$$

is obtained from the wave period, *T*, obtained from the Munitiestortplaats buoy and interpolated from hourly to 10-minute frequency. The maximum wave orbital velocity is calculated as:

$$U_{orb} = \frac{\pi H}{T sinh(kh)} \tag{7}$$

where *H* is the wave height as calculated by Witbaard from pressure data over the lander, the water depth is h obtained from the pressure measured at 1.4 mab by the CTD. The wave number is *k*, which is dependent on the wave length and can be found using the dispersion equation:

$$k = \frac{2\pi}{L} \tag{8}$$

$$\omega^2 = gktanh(kh) \tag{9}$$

h is again the water depth. This equation is solved iteratively for *k* when *ω* is known. The shear stress caused by the currents is then calculated using:

$$\tau_c = \rho u_*^2 \tag{10}$$

$$u_* = \sqrt{g}\frac{v}{C_D} \tag{11}$$

where *g* is gravity, *v* is the depth averaged current velocity, and C_D the drag coefficient.

$$C_D = 18\,log\left(12\frac{h}{k_s}\right) \tag{12}$$

The shear velocity can also be calculated from the near bed velocity:

$$u_* = \frac{u(z)\kappa}{ln\left(\frac{z}{z_0}\right)} \tag{13}$$

Where *u(z)* is the velocity at a distance *z* from the bed, *κ* is the von Karman constant, and z_0 is one twelfth of the D_{50} (Stanev et al., 2009).

3.2.4 Tidal conditions

Due to the asymmetry in the DCZ tidal signal, the magnitude of the ebb current is lower than the magnitude of the flood current. This leads to inequality in shear stress peak and duration for ebb and flood (Figure 5). Given this situation, it is useful to think of the tidal cycle in half cycles. A full cycle would include both ebb and flood tide, while a half cycle is alternatingly ebb/flood. We use the half tidal cycle is used as a temporal reference as opposed to the full tidal cycle. The benefit of this method is that one can separately analyze the flood and ebb peaks and look at tidal peaks at a higher frequency. To determine the tidal behavior, we use the velocity signal which passes through zero at slack tide. We defined the moment the signal passes through zero and recorded the index as the slack index. The maximum of the absolute velocity between two consecutive slack tides is then the peak ebb/flood moment.

Spring and neap tide moments can be defined from astronomical conditions (moon phase), but we can also obtain a continuous measure of the spring/neap cycle from the data. Tides can be observed both in the water level and velocity data. For either signal, we can take the variance as a measure of the amplitude of fluctuations around the mean. The variance was taken over 2160 minutes, which corresponds to 36 hours or about 3 full tidal cycles. Then this vector was linearly interpolated to the 10-minute frequency. This way, we obtain a good measure of the variance, while still maintaining the 10-minute frequency. During spring tide, more water is moving during ebb and flood so there are higher velocities and water levels, and a higher variance for both. The opposite is true for neap tides. Less water is moved, therefore there are lower velocities, and a correspondingly

lower variance. Included in the data set were the moments of spring and neap tide found by Carola van der Hout. These moments of peak spring and neap tide were used to validate the variance method (Figure 12). The variance of the flow velocity varies between .02 and .08 m2/s2. The variance at the full spring tide occurs when the variance is between 0.06 and 0.08 m2/s2, and neap tide between 0.02 and 0.04 m2/s2.

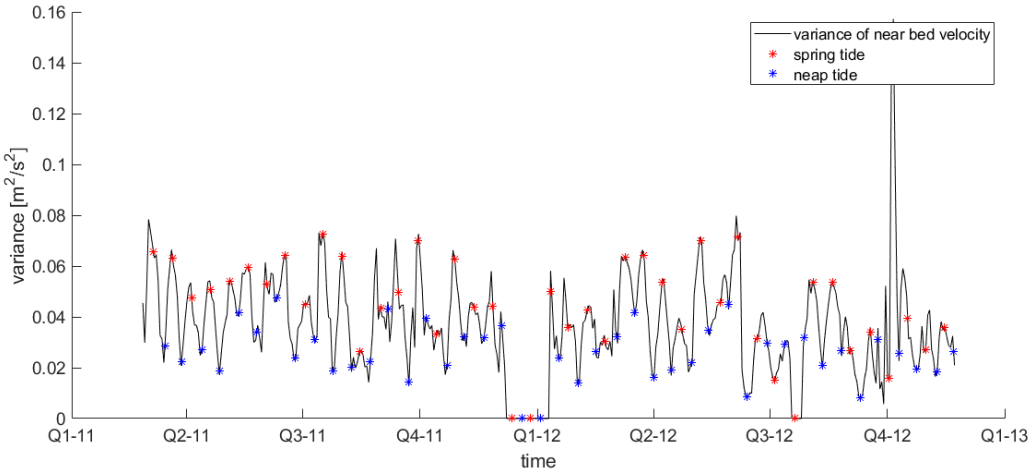

Figure 12: Validation of using variance of the velocity to define spring/neap tidal cycle by comparing the plot of the variance to the time of peak spring/neap tide as calculated Carola van der Hout and provided in the data. While some points are slightly off, the general pattern holds well enough to use the variance to define location within the spring-neap cycle.

Some of the neap/spring moments are predicted a bit sooner by the variance than the moments from the data set. Measurement error lead to some jumps such as at Q4-12 (Figure 12), and lower frequency oscillations presumably also contribute to the irregularity of the variance at spring/neap. However, it is enough to provide us with a continuous estimate of neap and spring time.

3.2.5 Bed level

The ADV located at 0.3 mab was also capable of acoustic backscatter, which records the distance below the measurement location at 0.15 mab. From this signal we obtain the distance to the bed. We use the median distance from this data to look at patterns of erosion and accretion. This provides information on the changes in bed level over time, which we can use to determine whether and when erosion/deposition took place. Even without placing this (unfiltered) time series side by side with the hydrodynamic conditions, we see that the sea bed is very dynamic (Figure 13). This confirms the presence of bed forms, ripples of varying magnitude, which change the bed height over time.

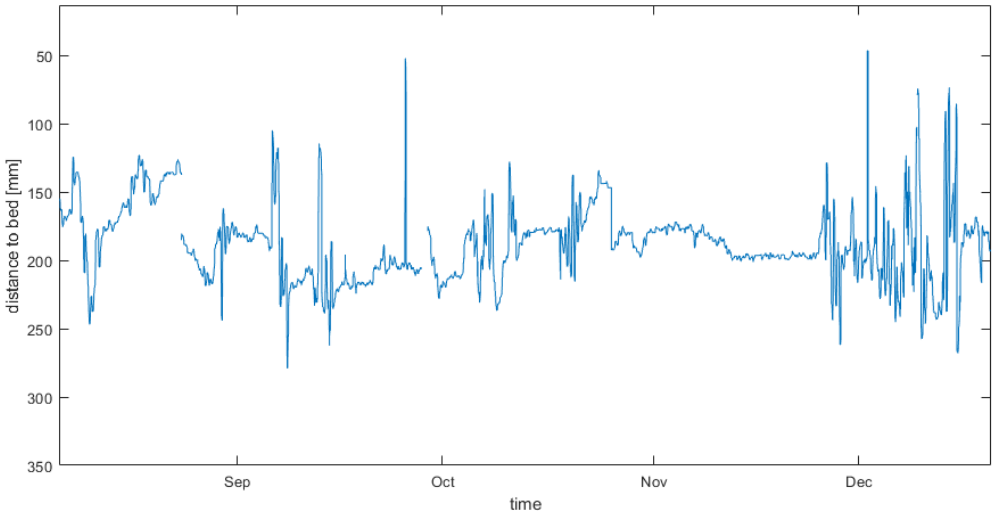

Figure 13: Sample of the median distance to bed from the ADV at 0.3 mab measuring at ~0.15 mab. Oscillations are due to ripples, bed formations caused by waves and/or currents which vary in space and time depending on the hydrodynamic conditions.

3.3 Defining periods and moments of interest

To analyze storms, we first need to define what we consider a storm. We isolate single events, and avoid periods of sustained stormy periods, or individual storm events which occur closely to other storm events. An event is a storm if the wave height exceeds 1 m, and there is a clear reaction in the suspended sediment concentrations beyond the regular tidal behavior. The hydrodynamics of storms were split into two parts: the build up to the peak, and the subsequent return to normal hydrodynamic conditions (Figure 14). A third time was defined by the behavior of the sediment. This third period extends beyond the end of the storm and is the period of storm influence. In each of these time periods, we take the peak value of parameters over a half tidal cycle and compare them in time and to each other. How exactly this is done is explained in this chapter.

3.3.1 Storm periods

Individual storms were manually identified within the data set by looking at side-by-side plots of wave height, SPM, and current velocity. Criteria for solitary storms were: wave heights above 1 m with corresponding SPM peak, no other storms occurring right before or right after the selected storm. This was determined from the SPM, ensuring that enough time had passed for the sediment fluctuations to return to the pre-storm conditions, and that pre-storm tidal SPM peaks were minimum.

The research questions concern two main phases of storm: the direct reaction, and the recovery. We also consider the season in which a storm occurs. The winter and summer seasons were defined as October to March and April to September, respectively. To analyze the reaction of the system, we consider the occurrence of peak SPM relative to the peak of the storm conditions. We can also look at changes in bed level to determine whether any erosion occurred locally. Along with the maxima over the sample period, we looked at the instantaneous reaction of the SPM to the shear stress and how the relationship changes over the course of a storm. To analyze the recovery from a storm, we assume that all the available sediment in the fluff layer is resuspended between slack tides. Meaning, the recorded peak SPM over the tide is representative of the mass of the fluff layer. Under this assumption, each tidal SPM peak was plotted to monitor the decay in available sediment.

The sample segments were split into three sections: before (beginning to storm peak), during (storm peak until end), and after (SPM peak until SPM decay of 80%) (Figure 14). The first two periods are based on the hydrodynamic conditions, while the third is based on the sedimentary conditions in the water column. This means that the third section may overlap with other sections but extends beyond the actual storm duration. The peak of a storm is defined as the moment of highest shear stress, and the beginning and end of a storm are found relative to this by setting a threshold for the wave height and moving forwards/backwards from the storm

peak to determine when the wave height drops below this threshold again. This threshold was chosen to be 0.3 m. The end of the third period is defined as the moment when the maximum sediment concentration measured during the half tide (flood or ebb) is 30% of the peak measured during the storm.

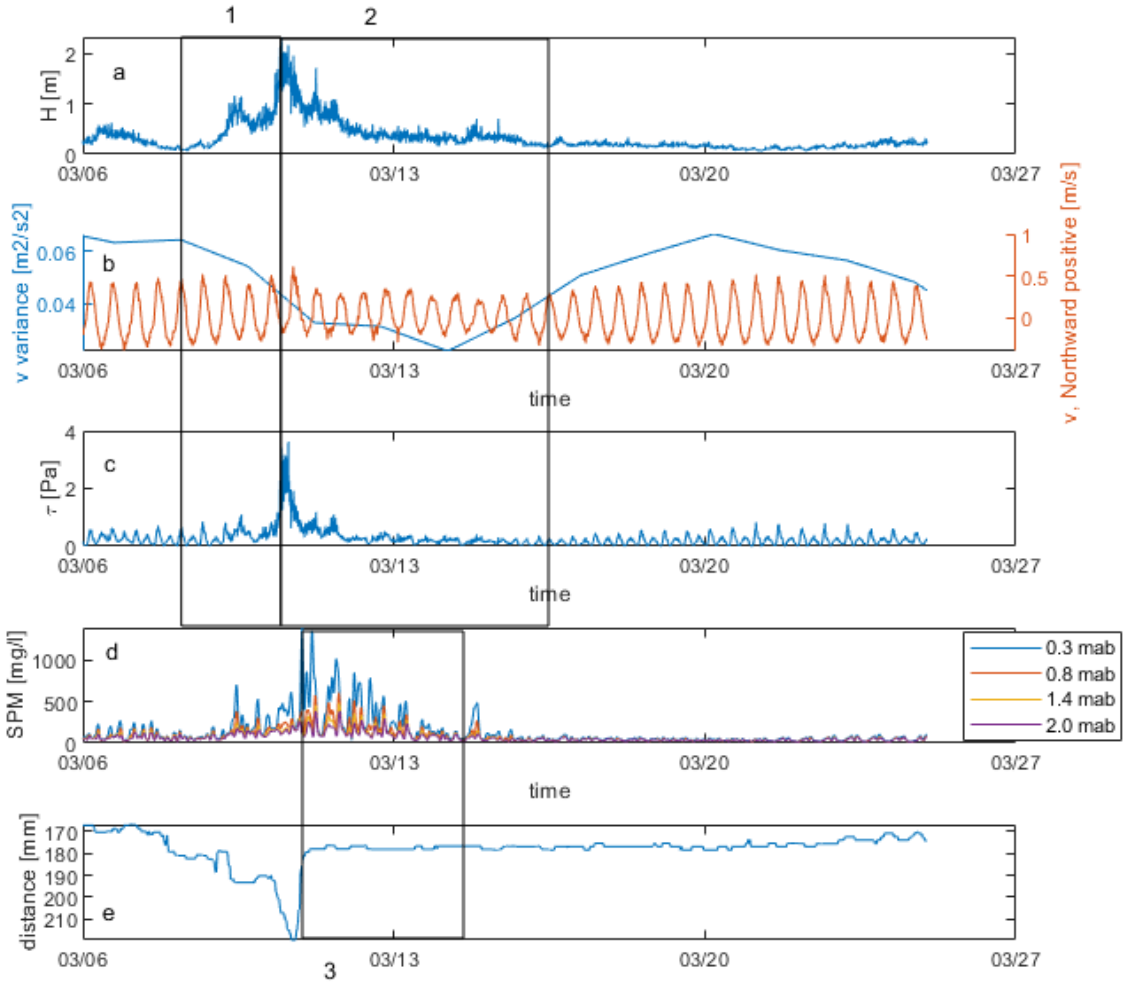

Figure 14: Time series of the fifth storm chosen for our analysis. Subplot A is the wave height. Subplot B is the near bed velocity and variance of the velocity Subpot C is the effective shear. Subplot D is the SPM at the four locations. subplot E is the bed Window 1 is the period from the start of the storm until the peak, window 2 is from the peak until the end of the storm, and window 3 is the recovery period. Window 3 and 2 can overlap, depending on where the peak in sediment lies relative to the end of the storm, which is defined by wave height.

3.3.2 Consecutive storms

In order to analyze storms occurring within the time window of influence by other storms, a different set of criteria for the selection of storms is needed. The focus was on clearly identifiable storms that occurred close together, not on periods of sustained energetic conditions. The first storm in a series was chosen to occur outside of the influence of preceding storms, and the following storm had to occur close enough to the preceding storm. Storms occurring within days of another storm are “close enough.” We look at these series to find general patterns of behavior, and whether storms close together introduce more fines into the system or if they deplete the bed. The former would mean we see higher concentrations for second storms, the latter lower concentrations.

3.4 MODELING

The data was collected in one point in space over the vertical, to duplicate this we created a 1-Dimensional Vertical (1DV) model scenario. This means we look at 1 cell in the horizontal, which has layers in the vertical. To determine the effect of horizontal gradients by omission, we define boundaries which are closed to sediment transport, and only see movement of sediment in the vertical. The exchange of sediment between the bed and the water column is modeled using the mass balance equation, which states that the change in sediment mass in the water column (*C*) is equal to the erosion (*E*) minus the deposition (*D*).

$$\frac{dC}{dt} = E - D \tag{15}$$

This is done using the water quality module of the numerical model Delft-3D (delwaq), which discretizes and solves the differential equation (15). In the following sections we describe the model domain, formulations of the sediment module, and the boundary conditions which are modeled using the flow and wave modules.

3.4.1 Domain

Numerical models solve the equations on a grid, which is user defined. As mentioned, we created a 1DV model, which is one cell. For numerical purposes we create a 3x1 grid but only observe the center cell. This cell is 10 m by 10 m in the horizontal, and the mean height in the vertical is 10.5 m. The boundaries are closed to sediment transport, meaning there is no horizontal advection, only vertical advection over 12 layers in the water column. Concentrations in the water column are determined by the balance between settling velocity and vertical turbulent mixing, and exchange with the bed is determined with the two-layer equations which are described in the following section.

While the cell is closed for the sediment model, the hydrodynamic model is a combination of a closed and open cell. With the open cell we can apply water levels and flow and solve for the shear stress on the bed. Other files are obtained from the closed cell, which are coupled with the delwaq model.

3.4.2 Sediment formulations

When looking at a one layer model, where the bed is purely fines, and assuming enough sediment is always available to erode or deposit, the Partheniades and Krone (Partheniades, 1962; R. Krone, 1962) formulations can be used to describe the erosion (E) and deposition (D)

$$E = M(\tau/\tau_{cr1} - 1) \tag{16}$$

$$D = w_S C_b \tag{17}$$

Where M is a parameter which allows for calibration of the erosion, τ is the bed shear stress, τ_{cr} is the critical shear stress for erosion, w_s is the settling velocity of the sediment fraction, and C_b is the near bed concentration. When τ is less than τ_{cr}, the erosion term becomes negative, in practice we then set it equal to zero.

These equations were expanded by van Kessel et al. (2011) to a two-layer model for mixed sediment environments (Figure 15). These adaptations were required to account for the limited amount of fine sediment available in such environments. The bed was conceptualized as having two layers, the top “fluff” layer is comprised on fines, and the bottom “buffer” layer is a mixture of fines and sand. In the equations, the subscript 1 indicates terms describing the fluff layer, and 2 the buffer layer. The top, fluff, layer is resuspended during tides, while the bottom, buffer, layer is remobilized during energetic events (i.e. strong tides or storms). The expanded equations for erosion and deposition are as followed:

$$E_1 = m_1 M_1 \left(\tau/\tau_{cr1} - 1\right) \tag{18}$$

$$D_1 = (1 - \alpha) w_S C \tag{19}$$

$$E_2 = p_2 M_2 (\tau/\tau_{cr2} - 1) \tag{20}$$

$$D_2 = \alpha w_S C \tag{21}$$

Where m_1 is the mass of fines in the fluff layer, p_2 is the fraction of sediment in the buffer layer calculated from the mass of fines in the buffer layer and bed characteristics:

$$p_2 = \frac{m_2}{(1-n)\rho_s d_2} \quad (22)$$

Where n is the porosity of the bed, $\rho_s$the density, and d_2 the layer thickness. The total deposition is distributed over the layers by parameter α. In the model the erosion term is called the resuspension, and each layer has its own value for the M parameter, which adjusts the efficiency of the resuspension. The deposition becomes active when the shear stress falls below a used defined threshold (Deltares, 2020). The mass in each layer, m_2 and p_2, is important, as the Partheniades equations do not account for amount of sediment available (they assume a full mud bed). By adapting the Partheniades in these ways, the resulting equations can we applied in mixed sediment systems (Van Kessel et al., 2011).

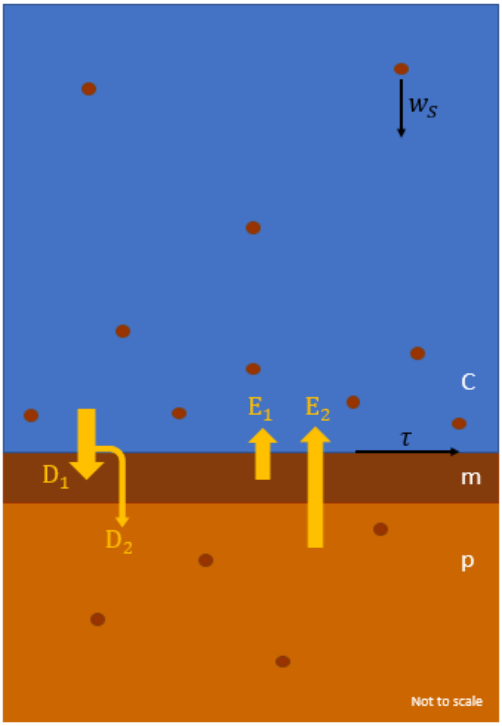

Figure 15: Schematic for the two-layer model. Dark brown indicates fine sediment, and lighter brown sand. D is the deposition term, E the erosion, w_s the settling velocity, C the concentration in the water near the bed, m the mass is the fluff layer, p the mass in the buffer layer, and τ the bed shear stress.

3.4.3 Parameters and settings

We use sediment parameters which were calibrated for the North Sea near IJmuiden using ZUNO-DD boundary conditions, (Table 2) provided by van Kessel (personal communication, 16 September 2020). This set of parameters uses 3 sediment fractions to represent the variety of fine sediment floc sizes in the North Sea. We calculate the mass in the buffer layer using equation 8 and compare with field measurements to define realistic values for the fraction of fines in the bed. We used a layer thickness of 0.3 m, a porosity of 0.4, and density of sand of 2560 kg/m^3.

Table 2: Parameters as calibrated for the North Sea model using ZUNO-DD boundary conditions. Used as the main set of parameters for this project.

Parameter	Variable	Description	Value	Units
VSedIM1	w_s	settling velocity, deposition term	10.8 [0.125]	m/d [mm/s]

VSedIM2	w_s	settling velocity, deposition term	86.4 [1]	m/d [mm/s]
VSedIM3	w_s	settling velocity, deposition term	.1 [0.0012]	m/d [mm/s]
ZResIM1/2/3	M_1	Zero order calibration erosion parameter S1	8.64E03	gDM/m^{2}d
VResIM1/2/3	M_1	First order calibration erosion parameter S1	3.0E-1	1/d
TaucRS1IM1/2/3	τ_{c1}	Critical shear for erosion S1	0.2	N/m^2
TaucRS2IM1/2/3 *	τ_{c2}	Critical shear for erosion S2	1000	N/m^2
TauShields	τ_{c2}	Critical shear for erosion S2	0.8	N/m2
FrIM1/2/3SedS2	α	Fraction of depositing sediment to layer	.15	[-]
Initial Conditions				
Parameter name	Variable equivalent	Use	Value	Units
IM1	C_{IM1}	Mass of fines 1 in water column	10	gDM/m3
IM2	C_{IM2}	Mass of fines 2 in water column	10	gDM/m3
IM3	C_{IM3}	Mass of fines 3 in water column	10	gDM/m3
IM1S1	m_{IM1}	Mass of fines 1 in fluff layer	6	gDM/m2
IM2S1	m_{IM2}	Mass of fines 2 in fluff layer	552	gDM/m2
IM3S1	m_{IM3}	Mass of fines 3 in fluff layer	0	gDM/m2
IM1S2	p_{IM1}	Mass of fines 1 in buffer layer	2760	gDM/m2
IM2S2	p_{IM2}	Mass of fines 2 in buffer layer	27978	gDM/m2
IM3S2	p_{IM3}	Mass of fines 3 in buffer layer	0	gDM/m2

*Remains unused, the variable defining the critical shear of the buffer layer is TauShields

3.4.4 Boundary conditions

Delwaq requires hydrodynamic boundary conditions to calculate the sediment balance, specifically the bed shear stress and vertical mixing. For accurate comparison of field and model data, we want the boundary conditions to be as close to the real conditions as possible. We used the DFLOW-FM (Delft3D Flow flexible mesh) model of the Dutch continental shelf (DCSM) for this reason. This is a relatively new model, and at the time of this project there are still improvements being made. However, the output of hydrodynamic conditions very closely matches the conditions observed in the field. We observed conditions at observation point in the model at the GPS coordinates of the lander, and the hydrodynamic conditions recorded for the years 2011 and 2012. These conditions were used to create a Delft-3D flow and wave model, which can easily be coupled with delwaq. We run delwaq offline, which means we run the hydrodynamic models separately once, then use these files as input for the delwaq models.

4 DATA ANALYSIS RESULTS

In this section we present the results of the data analysis. We begin broadly with yearly observations of hydrodynamic conditions and bed composition. Then we describe the individual storms, the hydrodynamic conditions of each and the resulting SPM concentrations in the water column. Then we look closer at the behavior of reaction of the fine sediment to the storm conditions, and the decay from the peak SPM concentrations. By the end of this section we have a clear idea of the timeline of sediment behavior over the course of a storm and the period after a storm.

4.1 SEABED SEDIMENT COMPOSITION

From the bed samples we analyze the percent of fines in the top 0-10 cm (Table 3). These measurements were taken every few weeks and provide insight into the variability of the fines content in the bed both in space and time. The mean fraction of fines over all stations over 2 years is 4.8%. The mean D50 over all stations sampled over the 2 years is 189 µm and varies with the varying fines content (Figure 16). The stations on the west of the lander had higher percentages of fines, which indicates this is where the turbidity maximum lies. During the first sample on 22 February 2011, one of the stations showed a significantly higher percentage of fines (14.2%) than the other three stations (3.9-5.85%). Over time, this same station varies between 3.31 and 14.2 %. The mean over the four stations for each sampling day varies between 2.89 and 7.21 %.

Table 3: Fraction of fines from box core data presented for each station, and averaged over the stations

Date of samples	Average percent fines lne	Average percent fines lse	Average percent fines lnw	Average percent fines lsw	Average percent for all stations
22-02-2011	3.90	4.89	5.85	14.21	7.21
03-05-2011	3.06	3.48	7.89	14.08	7.13
31-05-2011	2.74	6.00	2.80	5.66	4.3
24-06-2011	3.58	6.54	6.50	6.66	5.82
12-07-2011	4.46	4.40	6.57	6.21	5.41
02-08-2011	4.04	2.25	3.69	5.38	3.84
23-08-2011	3.97	2.96	3.30	3.46	3.42
28-09-2011	2.67	3.03	4.48	5.80	3.995
25-10-2011	2.16	1.33	3.30	10.14	4.23
11-01-2012	2.99	2.50	5.53	4.06	3.77
27-03-2012	5.87	3.79	4.28	3.93	4.47
29-02-2012	3.26	3.56	6.71	3.33	4.22
18-06-2012	4.12	3.84	15.41	9.40	8.19
24-05-2012	2.99	2.15	4.34	3.52	3.25
02-05-2012	2.66	2.61	2.49	3.78	2.89
26-07-2012	4.74	4.74	4.74	3.31	4.38

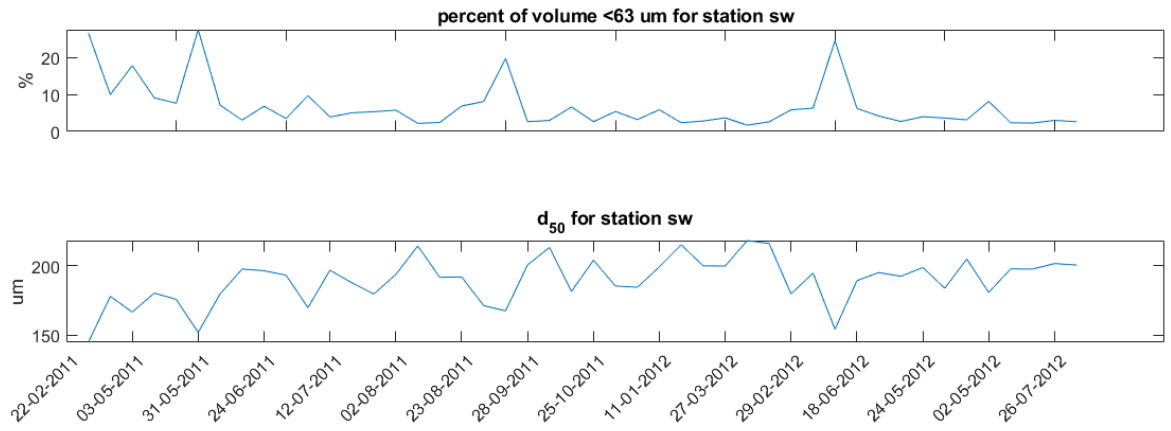

Figure 16: All recorded values of percent of fines and D50 in time over the two years for the south-west location. Values here were not averaged per day, so values higher than those which appear in the table are included in this visualization. Here we see that the percent of fines lies around 5% but has peaks which exceed 10 % and occasionally 20 %.

4.2 SEASONALITY

Along with higher SPM concentrations in winter, we observe higher wave heights, and lower concentrations of chlorophyll (Figure 17). Flow velocities vary little over the seasons, it appears the median is higher in winter than summer, though the mean value is similarly at zero. Winter winds may play a role in this higher median, through wind driven flow. Both concentrations of chlorophyll-a and hydrodynamic conditions change seasonally, both are believed to impact the seasonal sediment concentration. The waves cause sediment to be stirred up and remain in the water column, the lower chlorophyll-a measurements indicate less biological activity and thereby less biological matter for the fine sediment to flocculate with. This would result in smaller flocs which do not settle out as quickly as larger flocs.

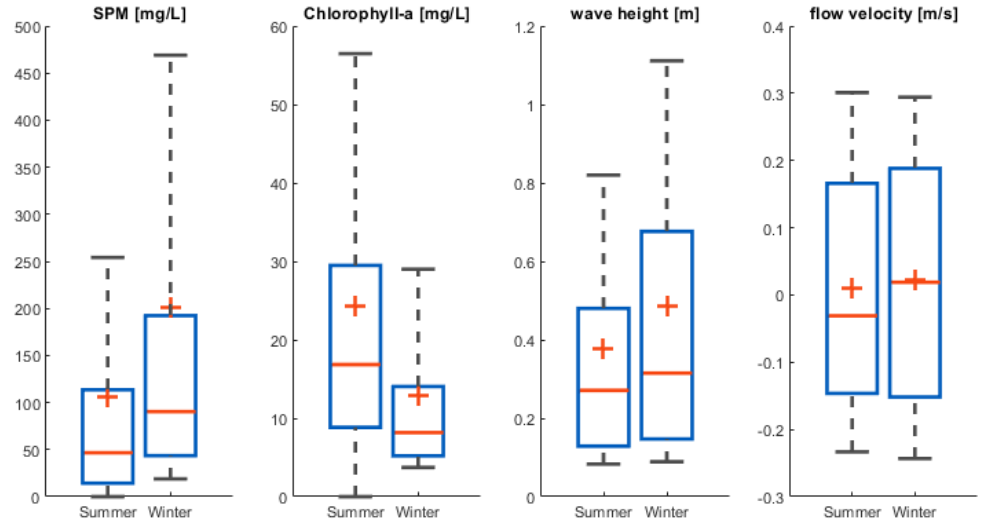

Figure 17: Box plots for summer and winter of 4 measured quantities: SPM, CHL-a, H, and v. In the box plots, the red plus symbol indicates the mean, the red line shows the median, the blue box blue box encompasses the 25% to 75% interval, and the dashed lines 9% to 91% intervals. The general pattern we observe are higher SPM concentrations, higher wave heights, and slightly higher flow velocities in winter, and higher CHL-a concentrations in summer.

4.3 STORMS: HYDRODYNAMICS

Using the criterion described in Section 3.3.1, 13 storms were identified in the dataset. Six storms occur during summer and seven during winter. Peak wave height for each storm as found from the pressure over the lander, and from the buoy at IJmuiden, are presented in the table along with storm ID and start and end dates. Wind data for the period was obtained from KNMI, this was provided at a daily frequency and interpolated in order to match the indices of the lander data. The wind speed and direction provided in Table 4 are the mean values from the start until the end of the storm.

Table 4: Storms selected for the analysis with dates, wave heights (calculated in two ways), wind speeds and direction

Storm ID	Start date	End date	Peak H IJmuiden [m]	Peak H Witbaard [m]	Mean wind speed [m/s]	Mean wind direction [deg]	Mean wind cardinal Direction*
1	7 June 2012	18 June 2012	3.95	2.916	6.4	185.60	S
2	3 March 2012	18 March 2012	2.87	1.42	8.8	347	NNW
3	11 January 2012	18 January 2012	3.75	2.105	9.0	315.60	NW
4	25 February 2011	3 March 2011	3.13	2.176	8.6	170.79	S
5	7 March 2011	18 March 2011	3.45	2.325	5.1	277.42	W
6	31 March 2011	4 April 2011	2.48	1.235	7.9	201.06	SSW
7	4 April 2011	9 April 2011	2.44	1.312	8.6	224.21	SW
8	8 June 2011	12 June 2011	2.07	1.086	4.7	246.76	WSW
9	26 August 2011	6 September 2011	3.16	2.320	8.5	277.32	W
10	4 October 2011	10 October 2011	4.15	3.890	7.0	196.38	SSW
11	17 October 2011	25 October 2011	3.63	2.842	10.7	276.35	W
12	15 May 2012	19 May 2012	2.75	2.004	8.2	307.44	NW
13	9 July 2012	14 July 2012	2.08	1.573	9.8	236.36	WSW

*Degrees to cardinal: http://snowfence.umn.edu/Components/winddirectionanddegrees.htm

The wind data from 2011 and 2012 was used to create a wind rose (Figure 18), which shows that the dominant wind direction was south-west, with strong winds coming infrequently from the north-east and north-west quadrants. Relative to the Dutch coast, winds from the south east are directed offshore (land to sea), these were weaker and occurred less frequent. The observed storms mostly had winds coming from a direction between west and south, with two having a north-west direction. The two north-west storms had the highest wind velocities.

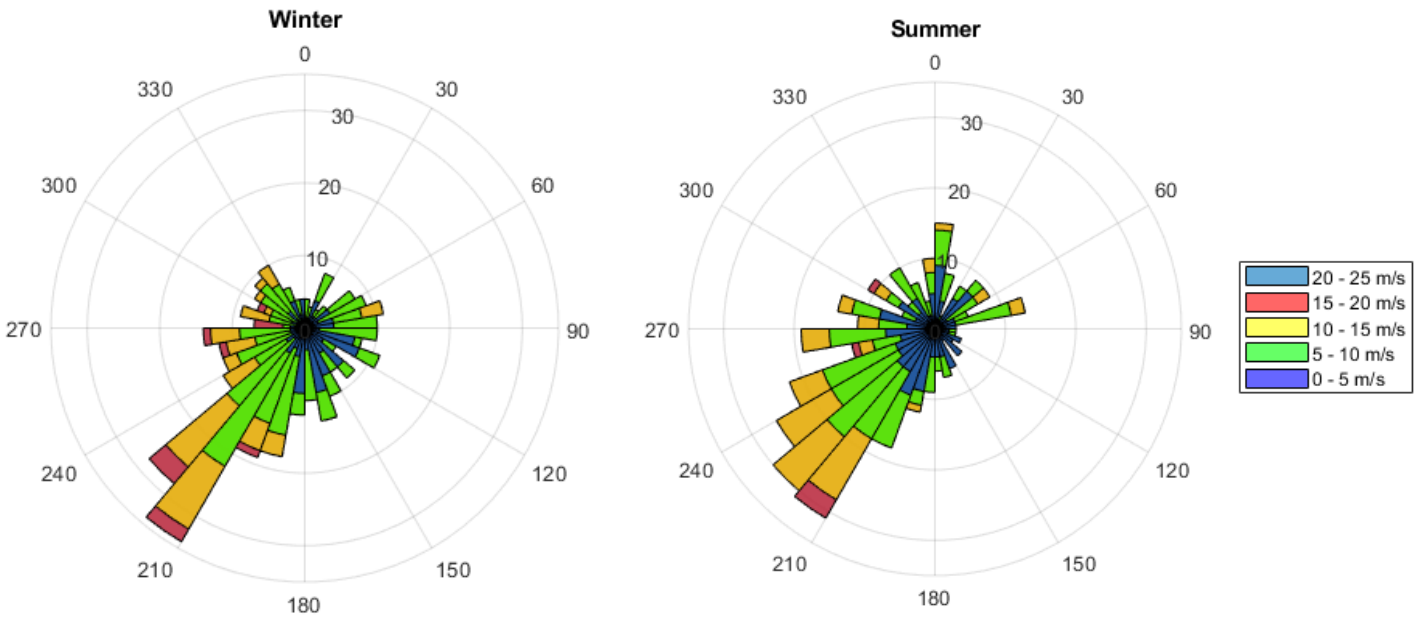

Figure 18 Winter rose for winter conditions (left) and summer conditions (right) at IJmuiden for 2011-2012. Both winter and summer have winds predominantly from the south west. Winds are stronger in the winter, and the direction is less variable than in summer.

4.4 Storms: Sediment

In the above section we identified the hydrodynamics conditions during the storms. Here we will look at the reaction of the sediment to these conditions (Table 5). We first look at two parameters: the peak SPM due to the storm at two locations in the water column, and the difference of peak concentrations between the lowest (0.3 mab) and highest sensor (2.0 mab). This last measure provides an idea of how well distributed the sediment is over the water column. The lower this difference is, the more mixed the sediment is.

Table 5: Suspended sediment concentrations for each storm

Storm ID	Peak shear [N/m2]	Peak sediment at 0.3 mab	Peak sediment at 0.8 mab	Difference between peak at 0.3 mab and 2.0 mab
1	4.8943	917.0	557.7	663.3
2	1.6157	1813.2	1183.2	630
3	2.7402	1463.3	747.9	982.1
4	2.2980	737.0	440.0	469.4
5	3.6210	1387.6	605.7	1001.9
6	0.9948	948.2	359.0	730.3
7	1.3786	1824.5	384.7	1581.3
8	0.8828	302.6	188.7	151.7
9	3.3491	776.6	288.4	560.8
10	6.9573	695.2	350.7	525.4
11	4.3109	2471.6	554.1	2199.4
12	2.4552	554.8	301.2	403.2
13	1.0562	3132.4	506.7	2893.8

We looked at each individual storm as a time series of available parameters: SPM, distance to bed, shear stress, wave height, flow velocity, and variance of the near bed velocity (Figure 19). We observed a peak in SPM which occurs slightly after the peak in shear stress and wave height and corresponds to the deposition of sediment as

we see in the distance to bed plot (Figure 19B). After this peak, we see the steady decrease in sediment resuspended over the tidal cycles. This is what we define as the decay. Not all storms are as neat as storm 5. For example, storm 10 (Figure 20). During the peak of this storm we observe very low SPM measurements. We suspect this is due to high shear stresses and mixing over the water column. This highlights how differently sediment can behave in response to different storm events. In the following sections, we will look at these in more detail and compare these behaviors for all the storms.

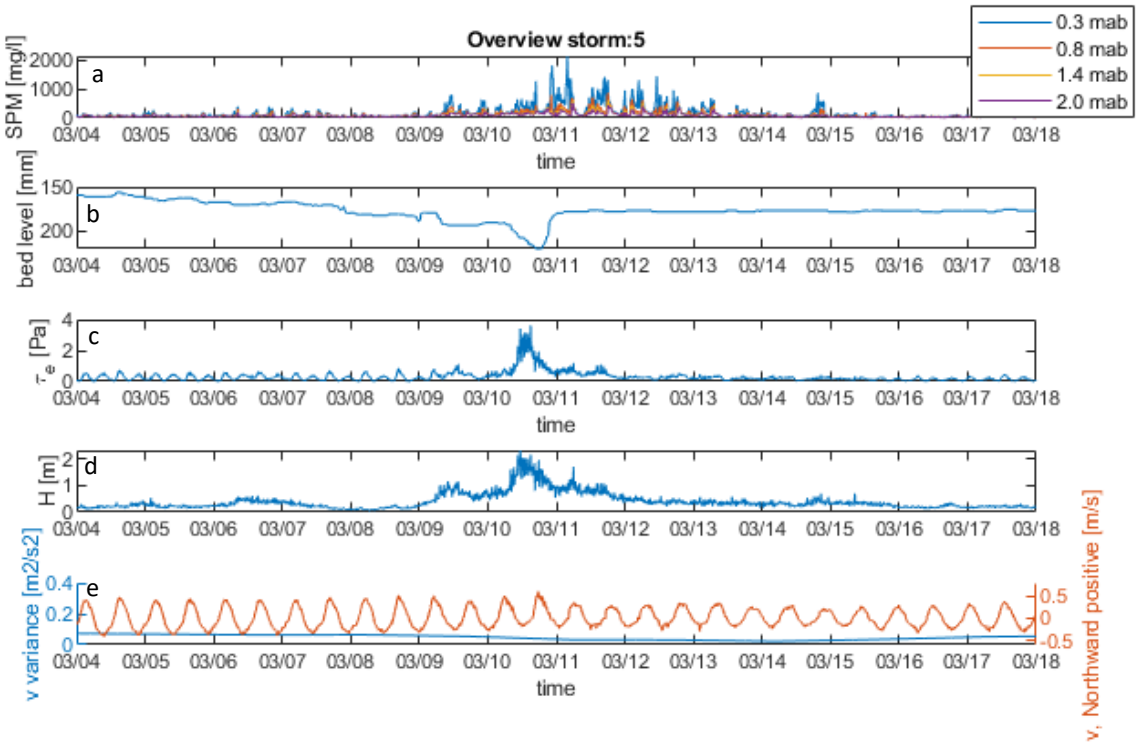

Figure 19: Time series of storm 5 from the field data. A) SPM, B) bed level, C) effective shear stress, D) Witbaard wave height, E) velocity and variance. The peak in shear stress coincided with a decrease in the bed level which indicates erosion. The SPM peaked shortly thereafter as the bed level rose again, presumably this means the sand that was eroded had settled back and only the fines were present in the water column.

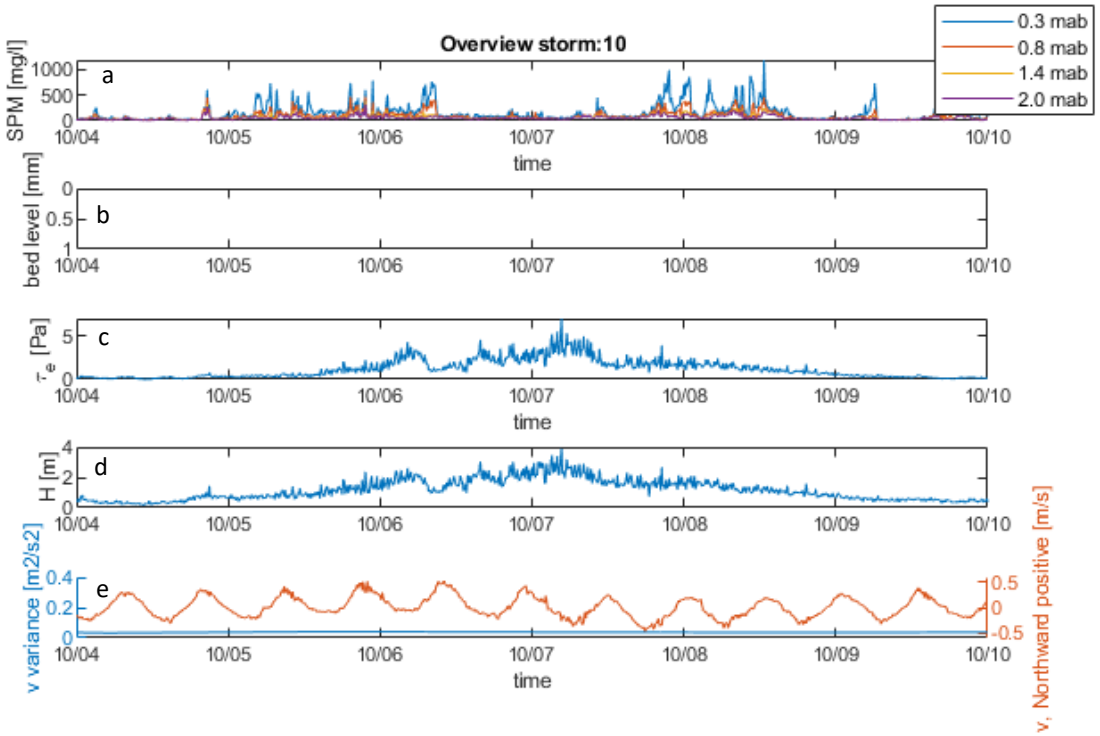

Figure 20: Time series of storm 10, which had a long duration of elevated shear. A) Suspended sediment over 4 sensors. B) bed level, which was not recorded during this period, C) effective shear stress, D) Witbaard wave height, E) flow velocity and variance. Here we see at the peak of the storm the sediment concentrations are lowest.

4.5 TIDAL VARIATION IN SPM CONCENTRATION

Even during storms, we observe tidal patterns in the SPM concentrations. Recall that sediment settles out during slack tides and is resuspended during the tide. The Dutch coast has asymmetrical tides, which are due to friction and cause short flood periods and long ebb periods. The flood then produces a higher shear stress than the ebb (Figure 5), because the same volume of water must move past in less time.

During ebb and flood currents, fines are eroded from the bed and are suspended until the currents decrease again. During slack water the sediment settles. One way to show the tidal variation of suspended sediment is by plotting the flow velocity against the SPM (Figure 21). This is referred to as a butterfly plot due to its shape and can be used to show the behavior of the sediment concentration in response to the tidal currents.

With this behavior in mind, we can create plots for periods of time which include a storm. The same pattern does exist before and after the storm (Figure 22), however after the storm we see higher sediment concentrations in the water for similar shear stresses than before the storm.

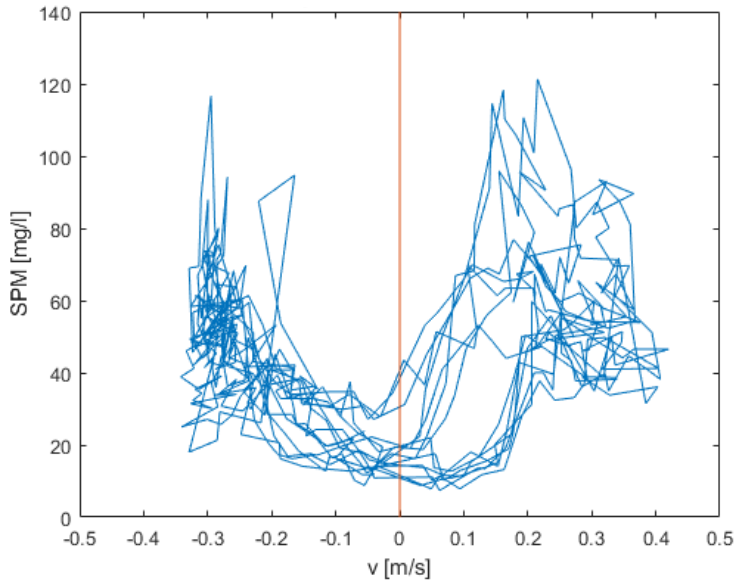

Figure 21: Butterfly plot of suspended sediment as a function of flow velocity for several tidal cycles in calm conditions. This type of plot shows the increase in suspended sediment during ebb and flood tides, and the decrease again as the fines settle during slack tide, when the velocity crosses zero.

If we apply this concept of the butterfly plot to a storm period, we can see the difference in sediment concentration before and after the storm (Figure 22). What we observe in this plot is that although the sediment concentrations are higher during ebb and flood, they still go to zero during slack. Following the storm, we see higher concentrations at ebb and flood for similar flow velocities, while concentrations still approach zero at slack tide.

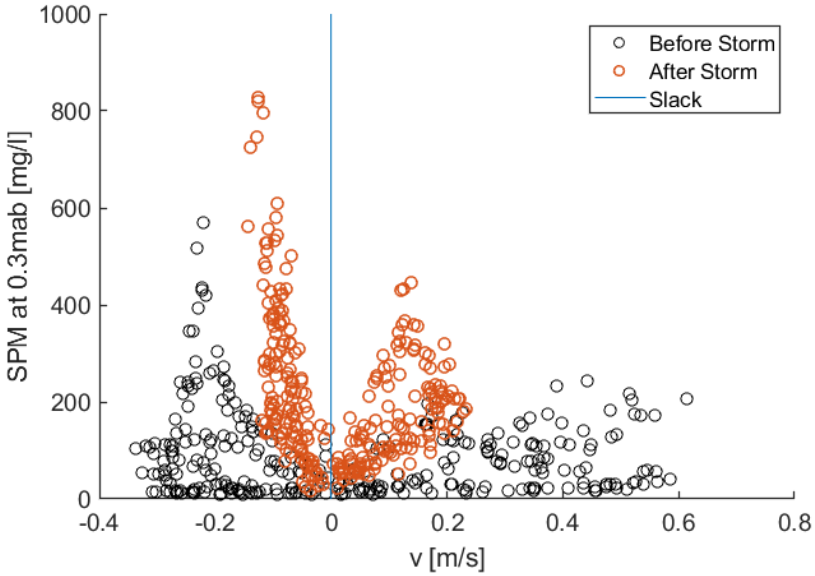

Figure 22: A scattered variation of the butterfly plot for storm 1, with two time periods (before and after storm) color coded in order to observe the difference in available sediment. In this plot we see that there are higher flood velocities than ebb, and that after the storm the sediment concentrations are higher than before the storm for the same shear stress.

4.5.1 Time lag of flow velocity and SPM

We see in Figure 22 that the lowest SPM concentration occurs around the time the velocity crosses zero, and the highest SPM concentrations occur around the highest velocity measurements. To determine whether there is a lag in the reaction time, we calculate the cross correlation. This is a method of signal analysis which shifts

one signal is relation to another and calculates the correlation at that lag. The cross correlation between consecutive slack tides of SPM at 0.3 mab and shear was found, the lag with the highest correlation factor was recorded. This was done for each half cycle for each storm, and a histogram created for the data. For most of these points, a zero lag is found (

Figure 23). This means that the peak in shear stress and SPM occur simultaneously. Several positive and negative lags are also recorded. Negative lag values indicate that the peak in SPM occurs after the peak in shear stress, while positive values mean that peak SPM occurs before peak shear stress. A negative time lag thus indicates that the peak SPM lags the peak forcing, possibly due to advection. A positive lag could mean that at some point before the peak in forcing, all available fine sediment is already suspended and even with a higher shear stress none is left to be suspended.

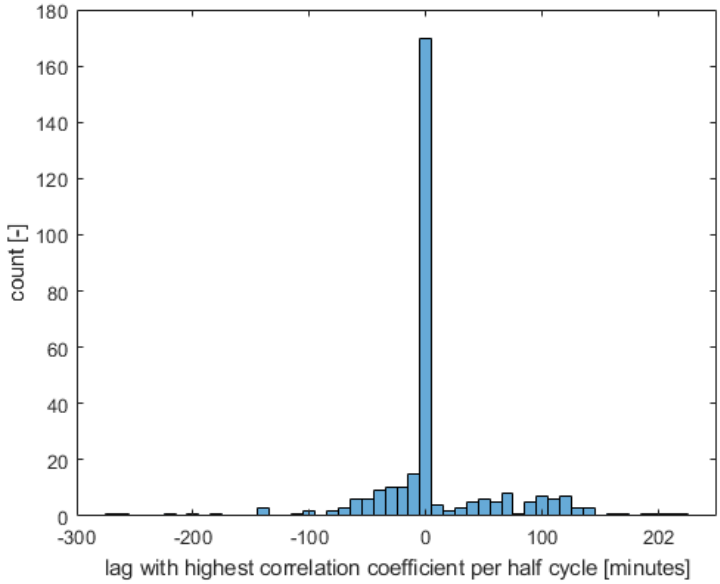

Figure 23: Histogram of the results of the cross-correlation analysis between shear stress and SPM concentration, where for each half tidal cycle the lag with the highest correlation was recorded for every storm. A positive lag indicates that the SPM peak occurs before the shear peak, and negative lag means that the shear peak occurs before the SPM peak.

4.6 Reaction

From Figure 22 we see that SPM levels are elevated following the storm, not during the period of highest shear stresses. This means more sediment is entering the bottom 2 m of the water column, where the sensors are located, either by advection or resuspension from the bed. The advection can either be horizontal due to cross or longshore currents transporting sediment, or vertical due to settling from higher in the water column. We will begin by neglecting advection in the horizontal and look at the direct relationship between shear stress and SPM (Figure 24).

We conceptually divide our storm period into three segments: before, during, and after the storm. These are split by wave height, so from the start of the segment until the wave heights exceed 0.3 m is before, then until the wave heights fall below 0.3 m again is during, and the following section until the end of the segment is after the storm. This provides us with a clearer idea of the chronology of the relationship between shear stress and SPM. What we observe in Figure 24, is that the highest shear stresses occur during the storm, and the highest sediment concentrations occur after the storm.

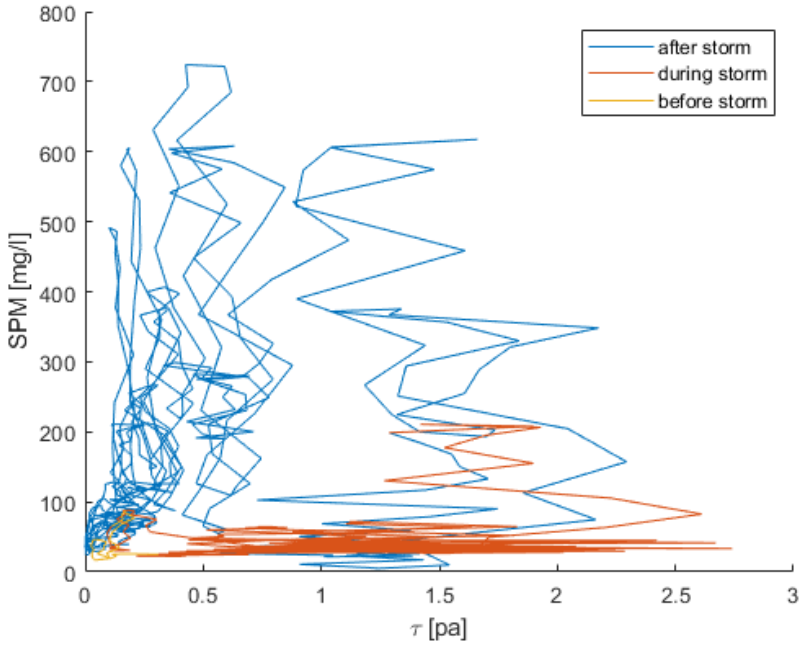

Figure 24: An adapted version of the butterfly plot for shear stress vs SPM at the 10-minute frequency, and color coded based on time relative to the storm. The shear stress presented here is the effective shear stress, which combines both waves and currents. This plot represents storm 3. During the storm we observe very little change in SPM, after the storm we see the peak SPM values.

This indicates that there are different regimes of the dependence on shear stress during the storm. We see this pattern for all the storms analyzed (Figure 26). The physical explanations behind this may be advection, or the settling of sediment once the conditions have calmed again. If the latter is the case, we should expect to see the sediment well mixed over the water column during the storm, so during the red part of the curve in Figure 24. We do not have enough information from the data on the settling velocity to calculate a Rouse number, and therefore a Rouse profile, but we can look at the distribution over the lower 2 meters with the sensors that we have (Figure 25).

What we see in these profiles is that both at the beginning and end of the period, the suspended sediment concentration is low and uniform over the bottom 2 m of the water column. The sediment increases for all stations but increases the most near the bottom causing a change in the profile (Figure 25).

A second explanation for the delay in peak SPM is a varying floc size. During the storm we have high shear stresses, which break apart larger flocs. But we also would see sediment that was formerly entrained in the bed, the floc size of which is unknown. In theory the upper boundary of the floc size is given by the Kolmogorov length scale (Winterwerp et al., 2002), which would reinforce the hypothesis that sediment exists in smaller flocs during the storm and is able to form larger flocs and settle after. Figure 26 shows the shear stress vs SPM curves for every storm, which show consistent patterns of SPM varying very little for higher shear stresses.

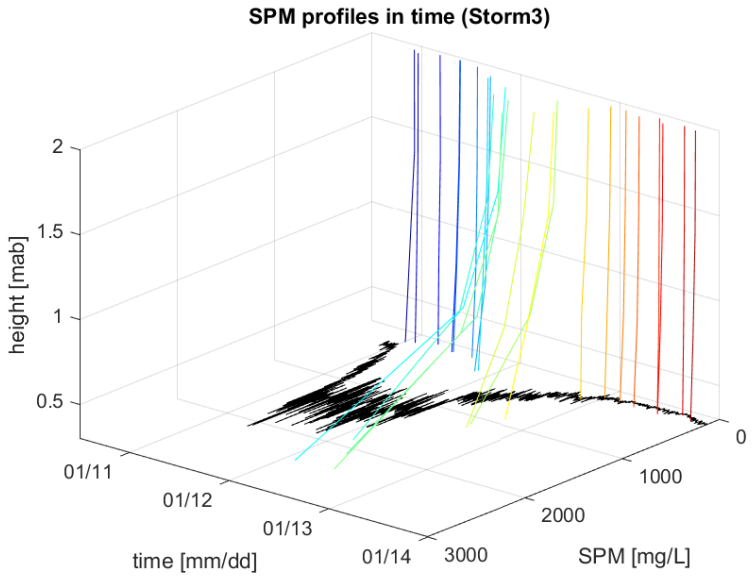

Figure 25: Profiles over the bottom 2 m of the water column in time for Storm 3, with the wave height in black scaled by 1000. These were made by connecting the measurements at the 4 points from the lander. We see that during the storm the SPM increases over the depth, and after the storm we see further increases at 2m, and larger increases near the bottom.

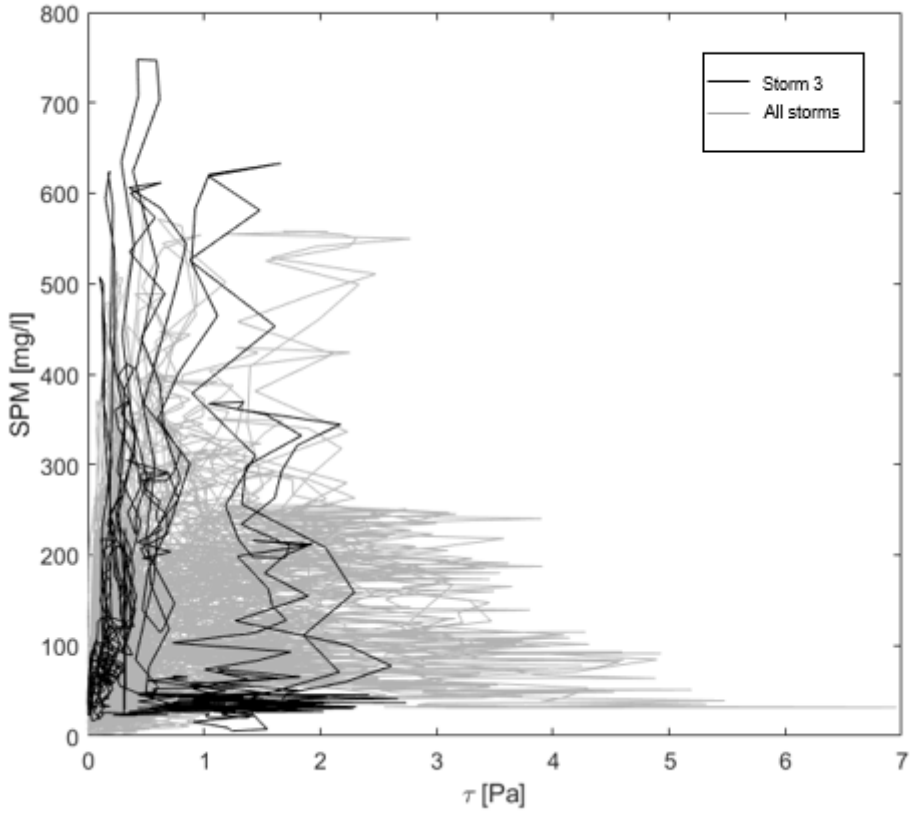

Figure 26: The adapted butterfly plot of shear vs SPM for all storms, with storm 3 highlighted for reference, from the SPM measurements taken at 0.8 mab. Here we see that all storms show the nearly independent behavior of SPM relative to shear stress and are constant at different concentrations of SPM. The highest peaks in SPM occur between 0.5 and 2 Pa.

4.7 DECAY

After the peak SPM concentration due to the storm, we observe a gradual decrease in the peaks of SPM which occur with each tide. If we normalize the SPM curves by the peak concentration, we can superimpose storm-caused SPM dynamics together by lining them up using the index of peak SPM (Figure 27). This plot shows variations, but the general pattern is a gradual decay in sediment eroded with each tide (ebb or flood) following the peak. Note that the rates at which these curves approach their steady state differs. It is useful to define a characteristic time point for the system's return to normal. With the normalized sediment curves, we define this point as the time at which the SPM has decayed to 30% of its peak value (Figure 27). This threshold is chosen based on observations, after this value the curve of SPM in time appears to stabilize for all storms.

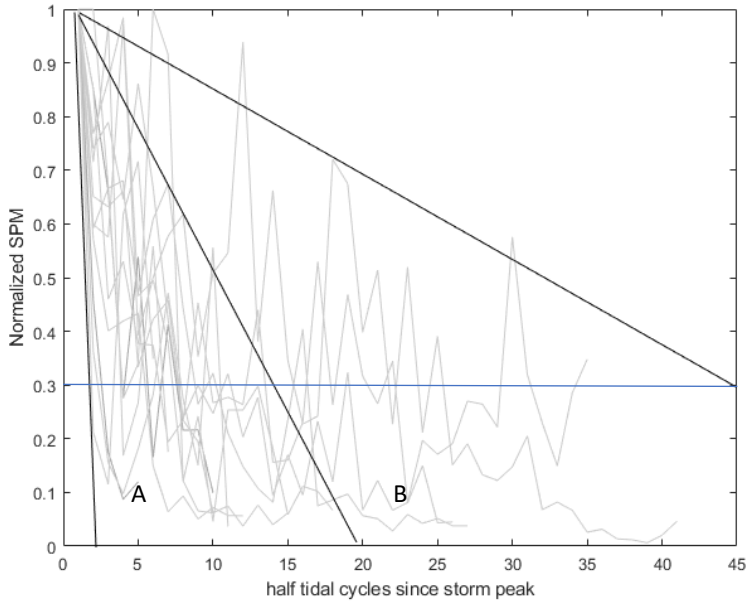

Figure 27: Normalized SPM curves for all storms overlapped, and divded into regime A and regime B. In regime A, 70% decay is reached between 2 and 17 half tides, and for regime B between 18 and 45. SPM measurements from 0.3 mab.

We look at the sensor located at 0.8 mab higher since this one is a bit less noisy, and record decay times. Half-tides can be converted to days by dividing by 4, since there are nearly 2 full tidal cycles a day. This shows we have times between 1-5 days for about 70% of the peak SPM to decay. If the signal does not fall below 0.3 and stay here, we use the lowest value that is reached by the maximum. This is usually around 0.3, but for some storms this is much higher (Figure 28). This shows that this method does not return a perfect value every time, but it is sufficient to provide an estimate of the time for recovery, using 70% decay of peak sediment near the bottom as a threshhold.

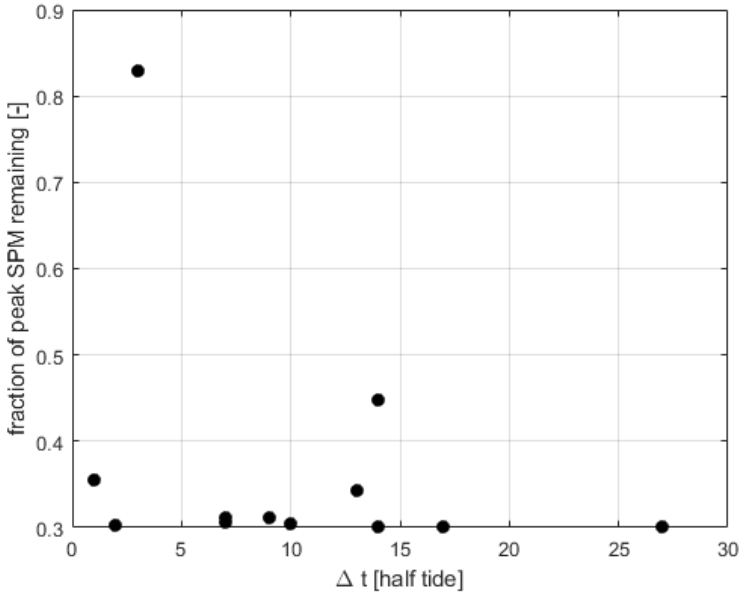

Figure 28: Result from the part-life function for each storm, which takes the normalized decay curve and finds the point at which 30%, of the next closest value, of the peak remains. The time, in half tidal cycles, between peak SPM and the sediment remaining shown on the y axis. Each point represents a different storm. We see that most storms have values close to the 70% decay, while others are slightly higher.

We can also see that perhaps a linear description of these regimes is not the best fit (Figure 27). If we follow the curves, they are more exponential in shape.

If we assume the decay is exponential, we can describe it with an exponential decay function:

$$\frac{\delta C}{\delta t} = -\lambda C \tag{23}$$

This is a function where the rate of decay of *C* depends on the actual *C*, i.e. a differential equation. The solution to this type of differential equation is:

$$C(t) = C_0 \mathrm{e}^{-\lambda \mathrm{t}} \tag{24}$$

Let us say that *C* is the peak concentration of the tidal cycle, C_0 is the storm peak from which we are measuring the decay, and *t* is the time, in our case half tides. All of these variables are known except λ, so we solve for λ at every half tide from the peak of the storm until the end of the sample period (Figure 29). Then we take the median of this value, and calculate our theoretical exponential decay curve.

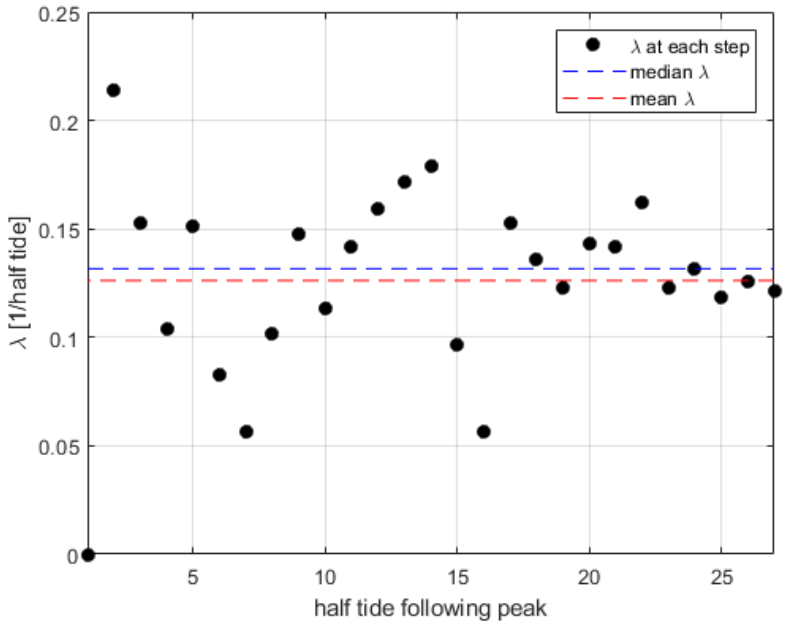

Figure 29: The decay constant calculated at each half tide for storm 5, and the median value which was taken at the single value for the storm. We take the median value to represent the value since this is more robust than the mean. Values of λ vary most right after the storm and approach a value close to the median by the end of the time series.

The storms which had more points available after the peak provided us with better fits (Figure 30), and storms with less points had a slightly worse fits (see Appendix A for full storm data sets). In general these poor fits underestimate the value of λ, meaning they show a slower decay than the observed concentrations. For the storms with better fit curves, we see a larger fluctuation of measurements around the theoretical values in the beginning and nearing the end of the sample the predicted curve and measured curve are very close.

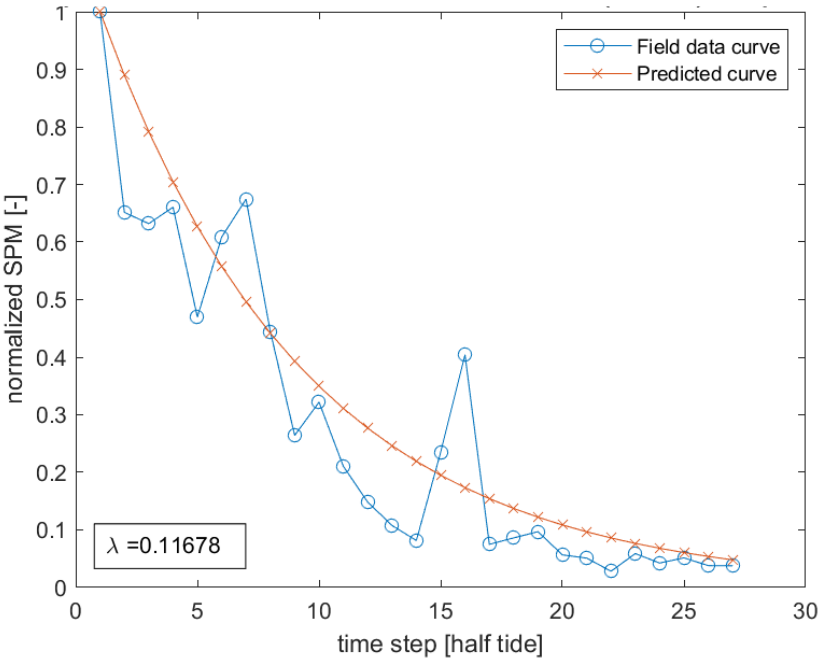

Figure 30: The decay curve of storm 5, and the predicted curve calculated using the median λ value. The predicted curve is much smoother than the field curve, but fits the general pattern of decay of the SPM.

The values for λ vary a bit, between 0.071 and 0.127 per half tide, with storm 2 having the lowest λ value and storms 6 and 7 the highest (Figure 31).

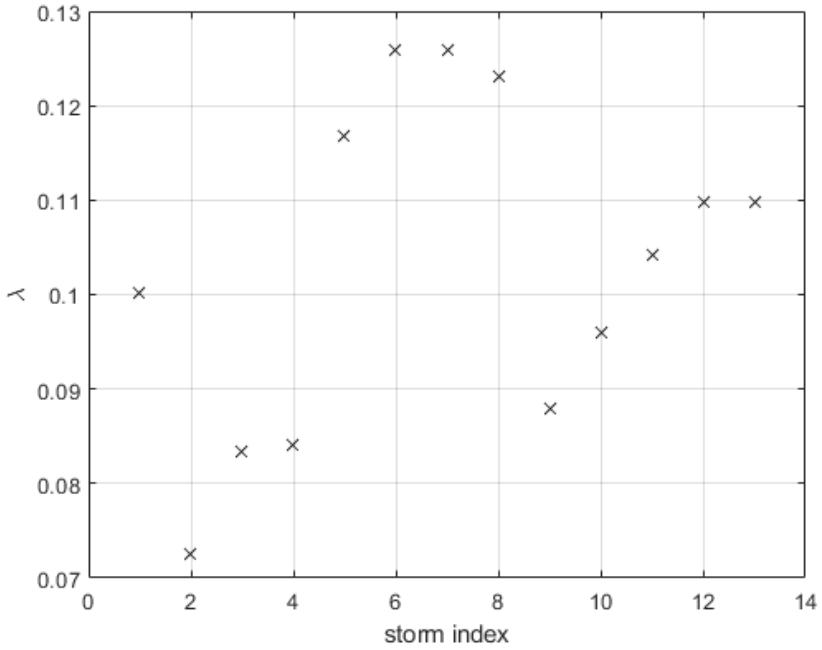

Figure 31: *The median of the λ values calculated for each storm from the normalized decay curve. For all storms these lie between about 0.071 and 0.127 per half tide.*

Recall the deposition term in the mass balance:

$$D_1 = (1 - \alpha)Cw_s \quad (25)$$

$$D_2 = \alpha Cw_s \quad (26)$$

C is the concentration, *α* the calibration parameter, and w_s the settling velocity.

If we assume the erosion and the deposition for the fluff layer are in balance, then we only see the change in time due to deposition to the buffer layer (D_2), the erosion term (E_2) is zero because we are, presumably, not exceeding the shear stress for erosion of the buffer layer. The decay is then determined by α and the concentration, assuming constant settling velocity of 1 mm/s. So, λ must be related to this process.

4.7.1 Seasonality

We also want to check if our storm recovery varies seasonally. We will do this by looking at the λ values in each season (Figure 32). We see higher λ values in the summer, which indicated that the SPM decays faster in the summer than in winter. We make this observation with only two years of data; more years of observations would be needed in order to determine if this is a consistent pattern.

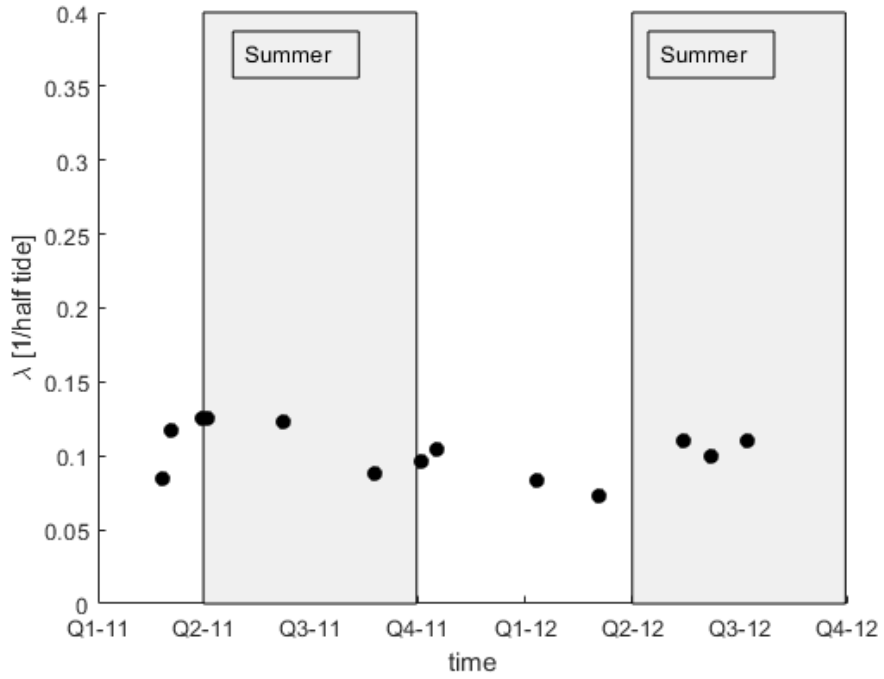

Figure 32: λ values for each storm, in time, grey areas are summer, white are winter. The values are slightly higher in summer than in winter, indicating faster decay in summer than winter. More years of data are needed to determine is this is a consistent pattern.

4.7.2 Storm conditions

The amount of sediment suspended during a storm, C_0, could also possible effect the decay. We see a large range in peak storm sediment values, and a smaller range in λ values. If we only look at the lower limit of the cloud of points, we can say that for lower SPM concentrations we see a faster recovery (Figure 33). However, considering all the points, there is too much scatter to conclusively say if there is a pattern.

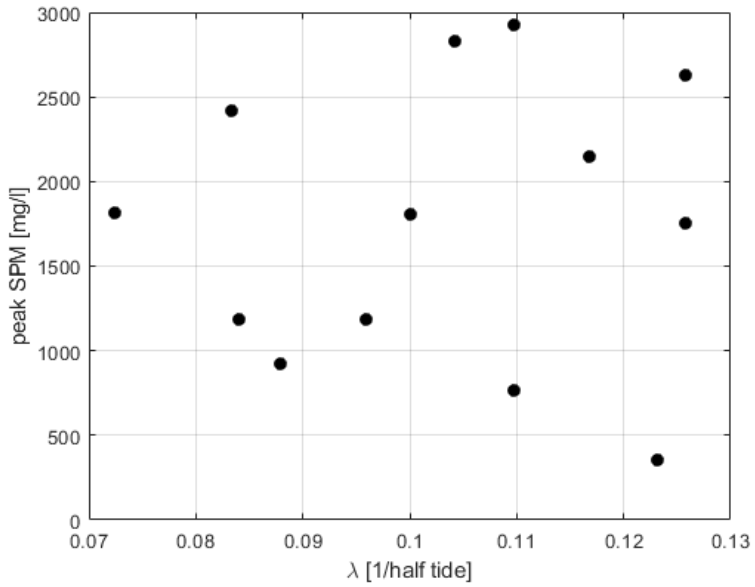

Figure 33: Values of peak SPM at 0.8 mab and λ values for each storm. We want to show if there is a dependence of λ on the peak SPM, perhaps the rate changes with the saturation of the water near the bed. There is no obvious pattern.

If the decay is only driven by buffer layer deposition and erosion then it makes sense that during spring tides, when the shear stress for erosion of the buffer layer is exceeded, the rate of changed is slowed by the addition

of eroded sediment to the water column. However, when we look at these values, there does not appear to be any sort of pattern or dependence of the decay constant on the spring-neap cycle (Figure 34).

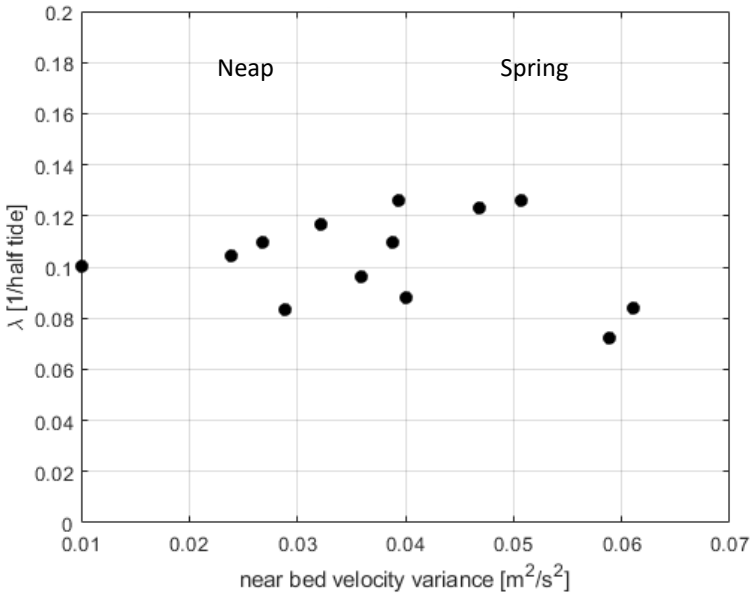

Figure 34: Post storm tidal conditions, quantified using the variance of the velocity signal, vs λ values. Neap tide 0.2-0.4, Spring tide 0.4-0.6 m²/s². We want to show if there is a dependence of the λ value of post storm conditions, but there does not appear to be a dependence.

The values of the decay constant are similar, only when we look at them in time do we observe a pattern (higher in winter, lower in summer). When we look at other dependencies such as the peak SPM or the effect of the spring-neap conditions, there is no obvious dependency.

4.8 CONSECUTIVE STORMS

We observe history effects in sediment dynamics when consecutive storms occur with short enough intervals. In the mass balance (equation 15) the current change in concentration is dependent on the sediment concentration, which depends on a previous change, and so on. But we also wish to know if the effects are present on a longer time scale, and if previous storms effect the behavior of a storm occurring closely after the first. It is hypothesized that the reaction of the fine sediment dynamics is due to the availability of sediment in the bed, which is also thought to be affected by storms.

By analyzing storms occurring is short succession, we aim to observe the changes in sediment dynamics caused by incomplete recovery between storms. We identified 4 series of consecutive storms in the data. The first series (Figure 35) showed clear SPM peaks for the first two storms. Note that the second storm occurred possibly too long after the first to be affected. The third storm produced a much smaller peak in sediment than the previous two storms, though it was accompanied by comparable shear stresses. This may indicate the sediment was depleted.

Another series of three storms showed the opposite pattern (Figure 36). There are low SPM peaks for the first two storms, and after the third storm there are very high SPM values near the bed as well as elevated levels at the others three sensors. The behavior of the SPM measurements also resemble those of the storm measured by Fettweis et al. (2010) in the Belgian Coastal Zone. This storm has higher SPM concentrations than we observe for other storms, and before the increase in SPM we see a jump in the bed level which could be measurement error but may also be the sudden introduction of sediment.

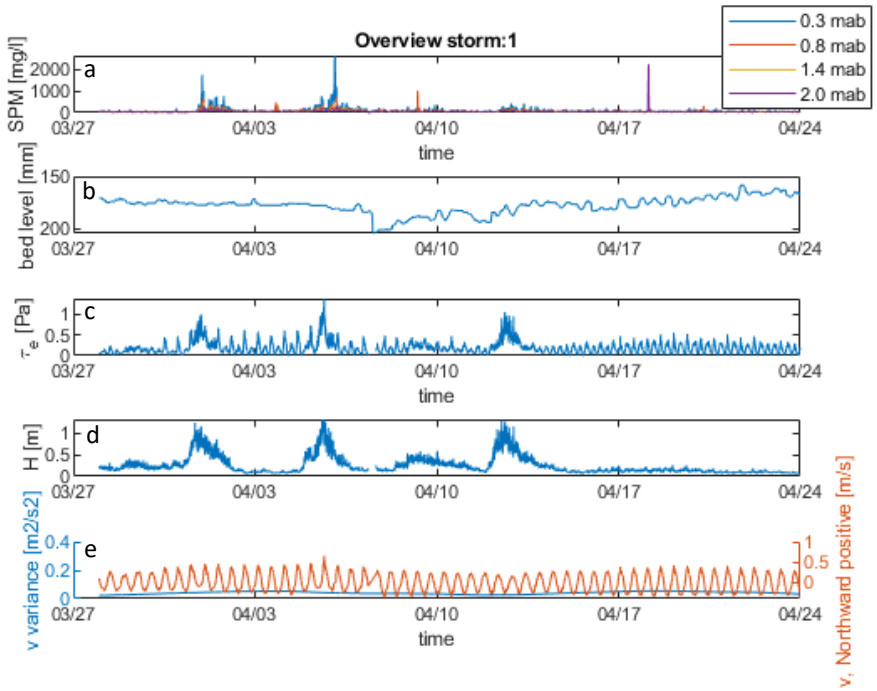

Figure 35: Time series of the parameters of the first series of storms, series 1. A) SPM. B) Bed level. C) Effective shear. D) Witbaard wave height. E) Flow velocity and variance of velocity. Note there is a small gap in the data with a jump in the bed level, due to removal for maintenance of the lander and not due to erosion/deposition of the bed. Here we see for the third storm there is no corresponding SPM peak.

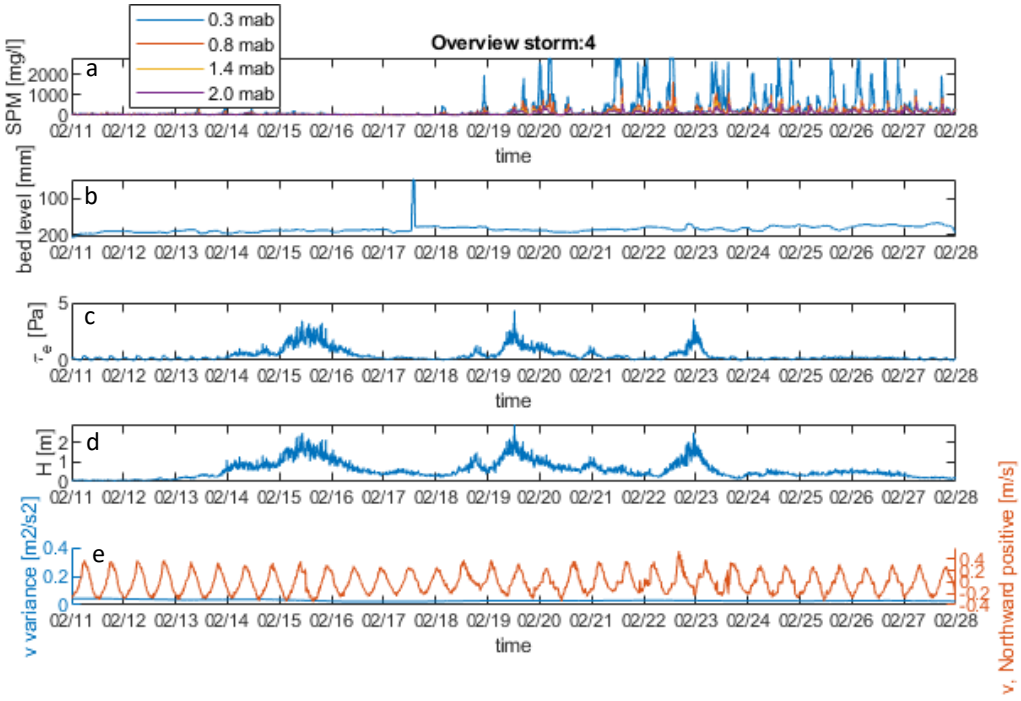

Figure 36: A) Suspended sediment over 4 sensors. B) Bed level. C) Effective shear. D) Witbaard wave height. E) Flow velocity and velocity variance. Note that the first two storms do not show any noticeable increase in SPM despite having high peak shear stresses, while the third storm is followed by a period of elevated SPM over all four sensors.

Not entirely understanding the recovery behavior before this project made it difficult to determine whether storms were fully recovered before the next storm. To properly analyze the behavior of storms in series, and times of sustained stormy conditions, it should be the main topic of a research project. The small focus on storms

in series here shows that the behavior of storms becomes more complicated when we start looking at interactions.

4.9 SUMMARY OF RESULTS

Our research questions aimed to understand the dynamics of fine sediments during and after a storm. We looked at the reaction to storm conditions and the recovery after a storm and determined the parameters that the sediment dynamics depend on. At the onset of a storm, we see increases in hydrodynamic forces (shear stress), at this point the bed is eroded. We do not yet see the increased SPM near the bed at this point, though. After the peak of the storm, when conditions start calming again, we observe a peak in SPM. This can be explained by the settling of sediment from higher in the water column once the forces keeping them suspended subside, leading to an increase in sediment near the bed.

After this initial peak, we see periodic peaks of SPM with each ebb/flood tide. The magnitude of these peaks decreases exponentially with each subsequent tide. Exponential decay parameter, λ, are similar for all storms but there is some variation which appears to have a seasonal component. We also observed that the hydrodynamic conditions varied seasonally, including wave height and flow velocity, and the biological activity as measured by chlorophyll-a concentrations. Varying recovery rates may furthermore depend on advection, which moves sediment in/out of the area and over the water column, and/or seasonal patterns in forcing.

For both the reaction and the recovery of sediment dynamics around storms, unknowns remain. We used a numerical model in order to fill some of these gaps. We could not include advection in our modeling, so we intentionally exclude it to study its effect by omission. It will be informative to expand the model in the future.

5 MODELING RESULTS

In this section we discuss how successful the model we adopted was in replicating sediment dynamics around storm events, and we perform a sensitivity analysis to determine which model parameters are essential to obtain faithful modeling. We focus on the reaction and recovery of the SPM values around storm conditions. We look at different settling velocities, vary the parameter α, critical shear stress, and varying the time over which the models are run. For instance, running segments containing storms as opposed to running the full year and selecting the storm.

The questions we aim to answer using this data analysis are:

1. What role might (horizontal) advection play?
2. How do different sediment fractions react?

The first question we address indirectly by excluding the effects of advection in the model and looking for problems with fitting the data. The second question we address by individually analyzing the sediment fractions. Answers to these questions should illuminate the strengths and weaknesses of the data and modeling and can help to direct future data collection strategies.

5.1 VALIDATION OF BOUNDARY CONDITIONS

Before we consider the output of the model, we first need to determine whether the model is representative of the real system. Important are the boundary conditions. These are the wave heights, tidal velocities, and shear stresses (Figure 37, Figure 38). What we see in the comparisons of modeling to data are higher wave heights and flow velocities, both of which result in higher shear stresses. Although the values are generally higher, the patterns are the same. This similarity in patterns is what we rely on to determine whether we see similar patterns in the reaction of the sediment. We expected higher wave heights from the model as it is using a different definition of the wave height, the significant wave height, which is higher than the median wave height from the field data. In the velocities, we see some underestimation by the modeling at the peaks of the storm, and likewise an overestimation of the tidal peak velocities during spring tides. The water levels agree quite nicely, however do not oscillate around zero in the modeling in the same way as in the field data.

We found a misalignment between the wave heights of model and field data in time, at the beginning of the year runs these are lined up (Figure 37), but 6 months into the run a lag develops (Figure 38)[1]. The years 2011 and 2012 were run separately, and then combined to a continuous two-year data set in post processing. To account for this, we shifted the dates of observation for storms affected so the general pattern of the wave heights are consistent over the period sampled. This means that the peak wave conditions occur under slightly different flow conditions, but the differences are deemed to be within the range of error of the model, since we do not see clear storm surge in the water level or flow velocities.

[1] The wave lag was due to an error in the postprocessing script of the DFLOW-FM output which combined the 6-month runs to create the 1 year runs. The issue has since been fixed, though not in time to include in this project.

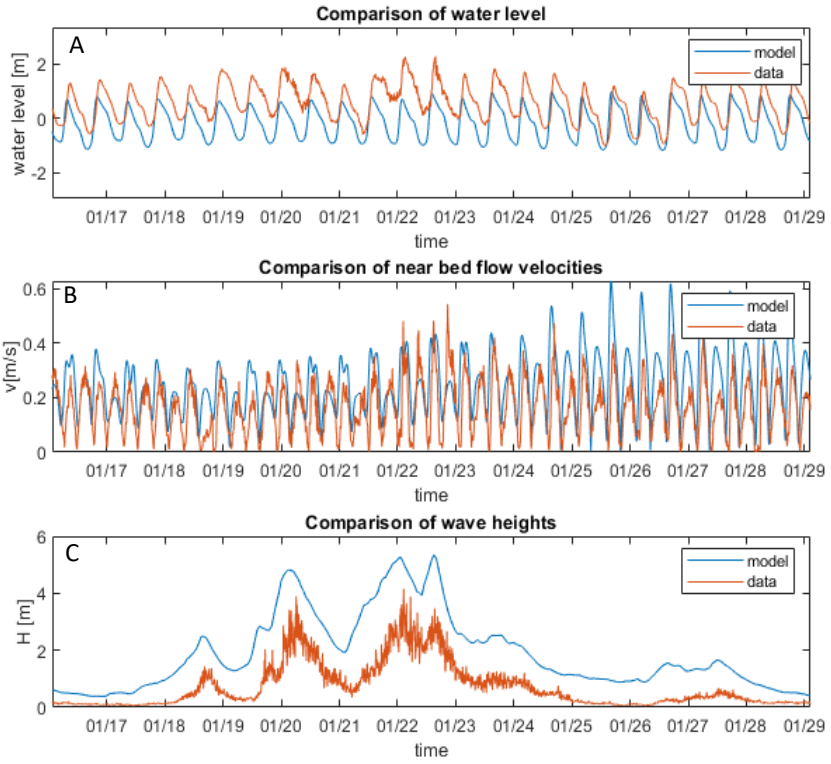

Figure 37: *Detail of the data comparison from January into February of 2012. A) Water levels. B) Flow velocities. C) Wave heights. Note how well the peaks in wave height line up. In A we can also see that storm surge is probably not included in the model, as the water level consistently oscillates around 0, while the water level from the data remains well above zero during two cycles at the peaks of the storms.*

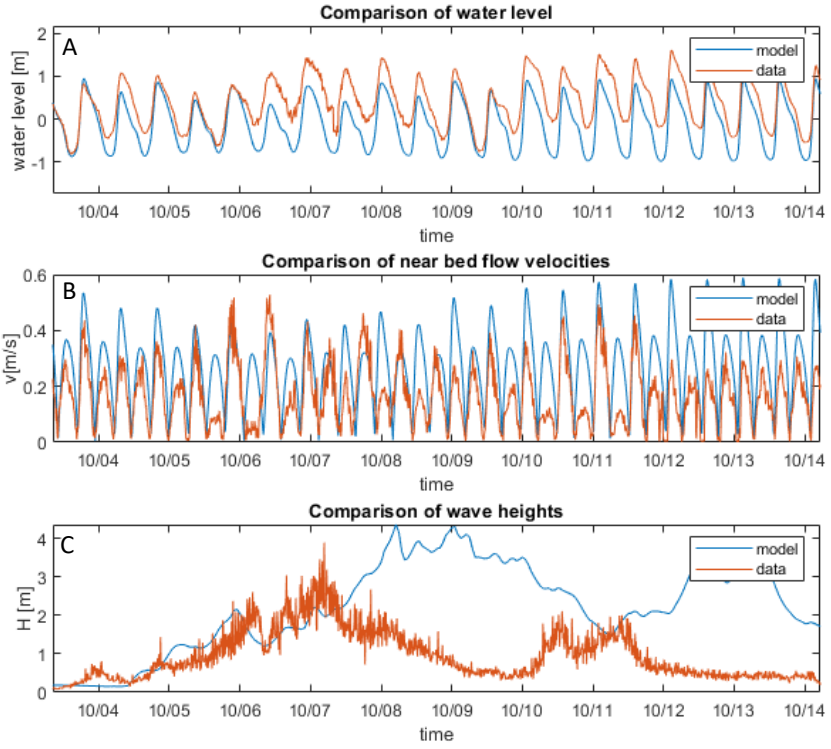

Figure 38: *Detail of comparison from October 2011. A) Water levels. B) Flow velocities. C) Wave heights. We see that the flow velocities and water levels are still in phase, however the wave conditions from the model lag those of the data.*

The differences in magnitude of wave height and flow velocities between model and field data will cause some differences in other parameters, most notably higher shear stresses than calculated from the data. But for the purpose of this project we focus on the general patterns in the sediment dynamics which are well captured by the model.

5.2 SEDIMENT CONCENTRATIONS

Concentrations in the water column were measured at 4 heights above the bed, and we analyze these measurements separately. We primarily look at the bottom two sensors, closest to the bed, as these show the most variation. Also in the model, we match the lowest measurement point (0.3 mab in the field, 0.4 mab in the model). The original calibrated data set matches conditions outside of storm periods (*Figure 39*). Peak sediment concentrations due to the storm can be matched by adjusting the critical shear stress. A lower value of critical shear stress (TauShields) will result in higher peak SPM values. But this also means that under normal conditions there are much higher SPM concentrations. The base case does match the lower limit of the SPM in the field data during the storm. After the storm, the concentrations are higher than what we see in the model. Potentially, this sediment is advected into the area.

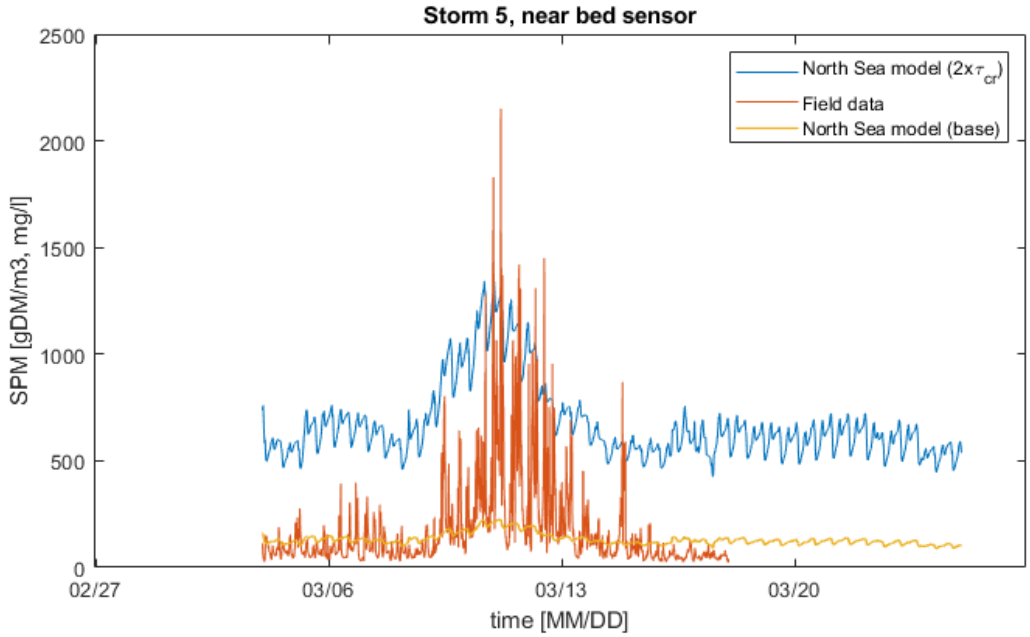

Figure 39 Near bed SPM from two model runs, and the field data for storm 5. With half the critical shear stress in the model we can match the peaks from in field data, but with the original critical shear we etter match the conditions before and after the storm. Note that the peaks are lined up, i.e. the lag in the field data is not apparent. The time on the x-axis is that of the model.

As part of the field data we also have measurements of the percent of fines in the bed at 4 locations around the lander over two years. We averaged this data over all four stations, for the two years, and obtained a value of 5% fines. In the North Sea model parameters, we used the 6% that were originally prescribed in the parameters. Because the model is closed, the total mass of sediment in the cell remains constant. In the field, in contrast, we do see changes in mass, due to horizontal advection into or out of the measurement location. We thus see a higher variability in the concentration of fines in the field than in the model (Figure 40). In the water column there is also less variability of SPM in the model than in the field. During the storm, at slack tide the minima of the field SPM are on the same order of magnitude as those from the model, but the peaks at ebb/flood are much higher than the model.

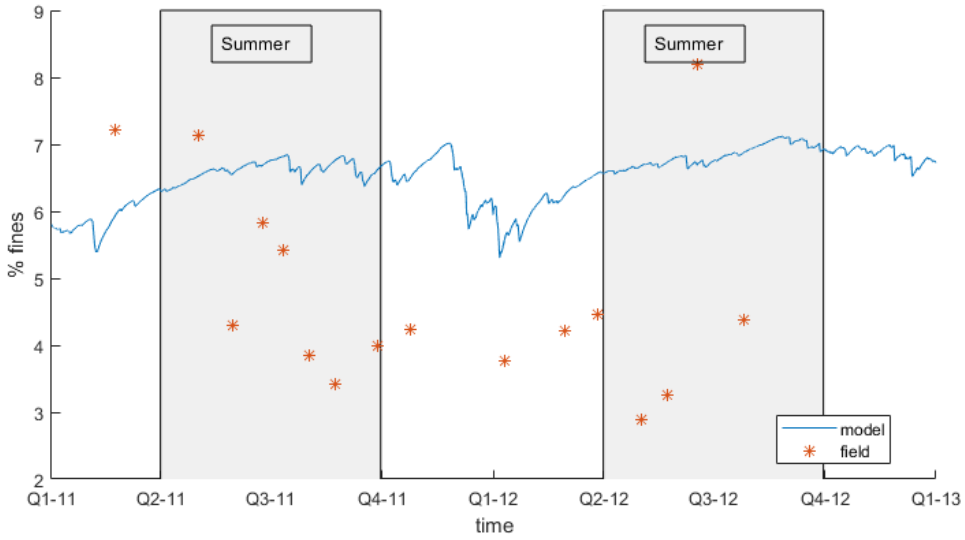

Figure 40: Fraction of fines in the bed from the model and the field data. Seasonality is modeled with available sediment in the buffer layer of the North Sea model. The model describes a closed cell, while the field is open to horizontal advection, which explains the larger range of sediment concentrations in field values.

5.3 SEASONALITY

The interaction between biology and fine sediment is not included in the model. Therefore any seasonal patterns we see in the output of the model can only be related to the hydrodynamic conditions which are included in the model. In the model output we observe a seasonal pattern in the available sediment in the buffer layer, which is lower during stormy winter periods than calm periods (Figure 40). This is exactly what we expect to see (Van Kessel et al., 2011). We also observe that the model overestimates the percentage of fines in the buffer layer, and the field data shows more variability with values from around 3% to 8%. Since the model bed is well mixed, some of this variability in the field data is due to patterns in space as well as time. We could assign lower sediment concentrations at the beginning, as this percentage is essentially given by the user through the initial concentrations. This would shift the concentration down. However, it would be more appropriate to say that the model underestimates the variability of fines in the buffer layer. This is likely related to advection, since in the model the mass of fine sediment in the cell is constant while in the field it varies depending on larger transport patterns.

5.4 Decay

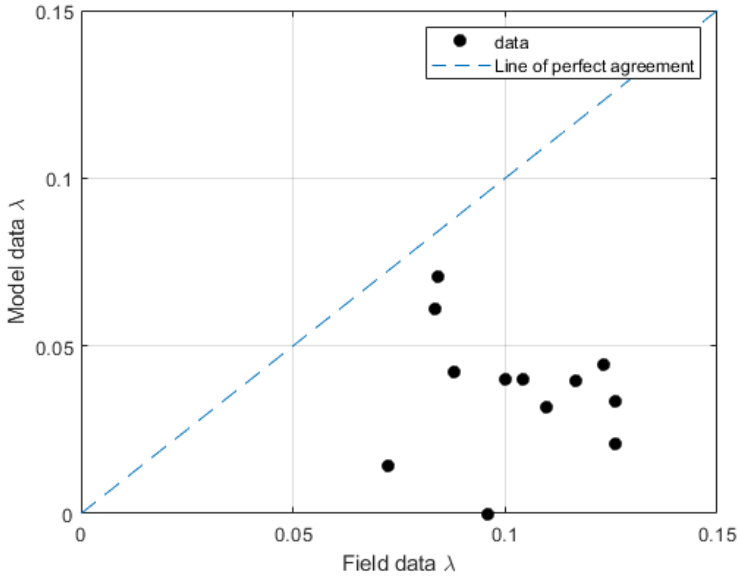

Figure 41: Comparison of field data decay constant and model data decay constant. The model has a slightly larger range of values, which are also lower than those of the field data. There is also no linear agreement between the two values, meaning the model and field scenarios decay at different rates.

A comparison of decay constant λ shows that those derived from the model are systematically lower than those observed in the field data (Figure 41). In other words, the sediment concentration in the model takes a longer time to recover than the sediment concentration in the field. Though this does not appear to be the case in the time series (Figure 39)**.** The difference between peak and regular conditions is smaller in the model results than in the field data. The peak SPM concentrations in the model results are lower than those in the field data if we calibrate to normal conditions. The critical shear stress is a crucial parameter determining how much sediment is eroded from the bed, and therefore determines the SPM concentration in the water column. If we decrease the critical shear stress to calibrate for storm conditions, then the SPM during normal conditions is much too high. The model only decreases by at most 50%, while field measurements go much lower. This discrepancy is again most likely due to advection. With the presence of currents and open boundaries in the field, the sediment remaining in the water column could be transported away. So perhaps this method of defining the decay is not the best metric with which to compare model and field decay.

5.5 Reaction

We analyzed the reaction of sediment dynamics to a storm when we visualized the field data using a shear stress vs. SPM plot which was segmented in time. We repeat this approach for the model data with some slight modifications. We look at the reaction of the three sediment classes separately, and do not color code by time. The reaction of the system to the storm in the model will not be affected by horizontal advection, leading to an underestimate of variations in SPM concentrations, i.e. a lower peak SPM (Figure 39).

In the model data we have three different sediment fractions for which we can make the shear vs SPM plots. For the two finest fractions we observe that the highest concentrations occur at lower shear stresses, and the higher stresses preceding these have lower concentrations. For the coarsest fraction however, we do see that the highest shear stresses also show the highest sediment concentrations. The two finer fractions are more representative of the behavior of the sediment during the storm, while the coarse fraction is more representative of the before and after storm conditions (Figure 24).

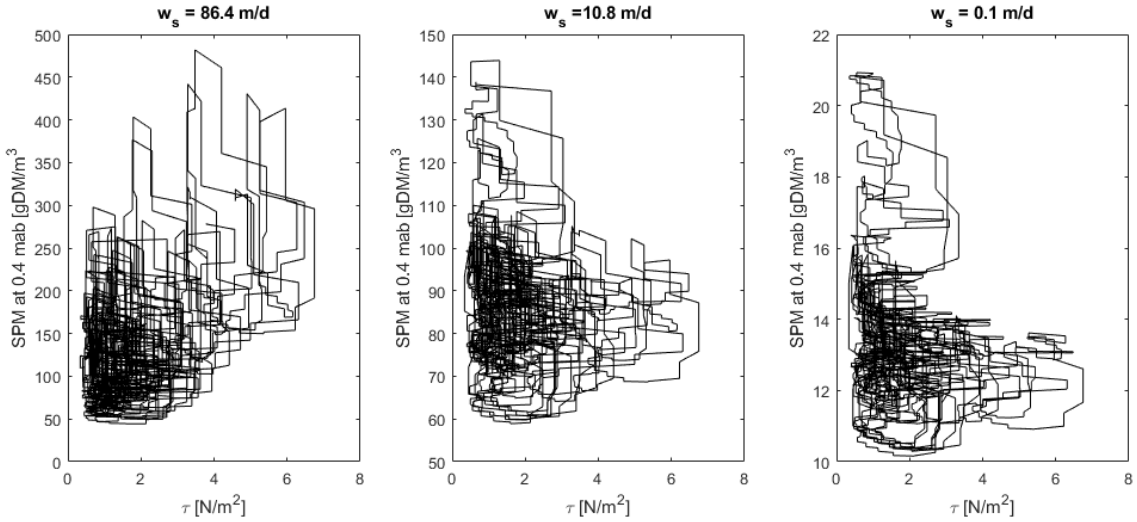

Figure 42: Reaction plots for all 3 sediment fractions in the model of storm 3. Left to right: coarse to fine. For both finer fractions we see high concentrations at lower shear stresses, while for the coarser fraction we see the opposite.

5.6 SUMMARY: MODEL RESULTS COMPARISON TO FIELD DATA

The validity of a modeling approach is determined by how consistent modeling results are with field data. We found the following discrepancies that point to deficiencies in the model we used. The model did not reproduce the lag between the hydrodynamic and the SPM peaks. Neither did it reproduce the slow/incomplete recovery of the normalized SPM signal. These differences suggest that relevant mechanisms are missing in the model. These likely are horizontal advection and time-varying parameters, such as settling velocity. We will analyze these differences further in the discussion and speculate on what these findings imply about the sediment dynamics during storms.

6 DISCUSSION

In this project we analyzed fine sediment dynamics in the lower water column before, during, and after storm events in the Dutch Coastal Zone. From our two-year dataset, we selected 13 single storms and focused on the temporal behavior of sediment dynamics around the storms. This was broken down into the reaction and recovery periods. We explored seasonal differences, and the sediment dynamics over consecutive storms by looking at 4 series of 3 storms.

6.1 STORM EVENTS

Over the 13 storms selected we observed very similar patterns in the shape of the SPM curves during and after the storm. There is a peak of suspended sediment which happens after the pea in hydrodynamic forcing, then this high concentration slowly returns to pre storm values. The decay following the peak SPM is observed in both model results and field data. The behavior of the field data can be described with an exponential decay equation, with an exponential decay parameter λ, which is the decay rate. The mean value of this parameter is 0.12 per half tide, corresponding to a decay time of about 2 days. The λ values from the field data also show seasonal variation, with higher values in summer than winter. Though more years of data are needed to conclude whether this pattern is valid.

We created a model for the same period that the data collection spanned to observe the behavior of the fine sediments during storms and identify crucial parameters. Using boundary conditions which are close to the real conditions, and a set of sediment parameters calibrated to the North Sea, our model is representative of the system with a few intentional differences. The first is the we exclude advection in the model. Since the field data does not contain information on advection, we chose this approach to indirectly asses the effect of advection on the behavior of sediment concentrations by omission. Furthermore, the parameters we define are not time varying, specifically the settling velocity is a constant parameter in the model, while it certainly varies in time in the real system. Even with these differences we observe much of the same patterns in the behavior of SPM dynamics over the storm. The discrepancies we do see are informative and point to important differences between the model and real-life conditions.

6.1.1 Reaction

In the field data, we observed that the peak sediment concentration lags the peak storm conditions. In the model using North Sea parameters, we do not see this lag. There are two possible reasons for this: horizontal advection or vertical advection. For the horizontal advection it may be that there is an area nearby which contains more fine sediment, and this is then advected into our measurement area. Vertical advection is related to the settling of particles from higher layers in the water column, above the levels the instruments measures. If during the storm the sediment is well mixed across the water whole column, the readings at the measurement points will initially be low, but will increase when the conditions are calm, and the sediment settles towards the bed.

For the analysis of the reaction to storm conditions we use shear vs. SPM plots, to analyze the magnitude and the temporal behavior of these two signals together. In these plots, we observe that the SPM peak occurs after the storm when the bed shear stress falls below ~2 Pa. During the storm, the time with highest shear stresses, we observed low SPM values which appeared to be independent of the shear stress. From the profiles over the course of the storm (Figure 25), we also see the change in profile from uniform during the storm to higher concentrations near the bed after the storm. This would indicate the suspended sediment settles after the storm (vertical advection), due to the decrease in turbulent forces which both suspended the particles and broke up larger flocs. When these forces decrease, sediment can settle, and the reformation of flocs increases the settling velocity.

We analyzed this hypothetical scenario using the model and looking at three sediment fractions, each defined by a constant settling velocity. It appears that the two finer sediment fractions represent the independent behavior during the storm, as their concentrations do not vary much over the course of the storm (Figure 43). While the coarser fraction represents the behavior that we see both before and after the storm. This explains the lag between the hydrodynamic storm peak and the SPM peak. During the storm the flocs are smaller, and

along with the higher turbulent forces the SPM is well mixed over the water column. Turbulent forces must be sufficiently low for flocs to form, and then it takes time for them to settle down towards the bottom.

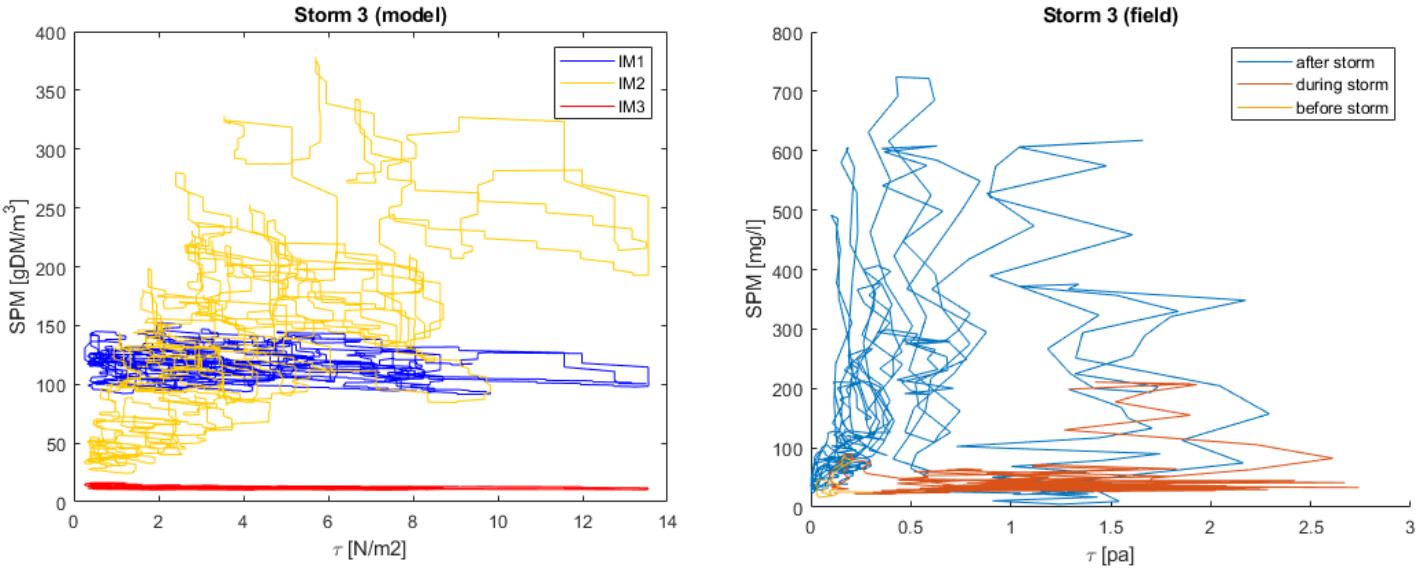

Figure 43 Three sediment fractions from the model for storm 3, left, and the measured SPM and shear stress from the field, right. Note that the colors in the left plot indicate the three different sediment fractions, and the colors on the right the period relative to the storm.

6.1.2 Decay

In addition to the lag of the peak SPM in the field data, we observe a difference in the magnitudes of the peak SPM. When calibrated to normal conditions, the model shows a much lower peak SPM and the field data (Figure 43). Note that this occurs even with the higher shear stresses present in the model, which are a result of the discrepancy in the definition of wave height and possibly shear stress formulations[2]. We can calibrate the model to match the magnitude of the SPM peaks, by decreasing the critical shear stress, though this also increases the concentrations during normal conditions. Changing this threshold is a trick to match concentrations observed in the field at a certain time, but really what we observe in the model is a decreased variability in sediment concentrations. When we eliminate advection, we remove the horizontal source/sink of material. Advection causes a higher variability, by adding/removing fine sediment to/from the location. Horizontal advection plays more of a role

We quantified the decay of SPM concentrations in two ways: we looked at how long recovery took using the part life, and at the rate using the exponential decay equation. From calculations of the part life from the field data, we determined that the system can recover 70% of the peak SPM in 1-5 days. For the model data, this measure was not applicable since the SPM does not reach the 70% decay threshold, as mentioned in section 6.1.1. The exponential decay parameter λ, which we use to fit a decay equation, represents the rate of recovery. From field measurements, the values we found correspond to a decay time of 2-4 days, which is consistent with those from the part lives of 1-5 days. These appear to vary seasonally, showing faster recovery times in summer than winter. This seasonal pattern will be further discussed in the following section (6.2). We investigated other reasons for variation, such as the magnitude of peak SPM, and the tidal conditions following the storm. The peak SPM does not appear to influence the rate of recovery (Figure 33), but does appear to influence the recovery time (Figure 44). Storms with higher peak SPM values take longer to recover this sediment, since they recover at roughly the same rate at those storms with lower peak SPM values. The timing in the spring-neap cycle also

[2] Though care was taken to match the formulations that were provided in the manual, it is not unlikely that the mismatch in magnitudes is due to slightly different formulations

does not appear to greatly influence the rate of recovery (Figure 34). There is a bit more spread in the values of λ for storms followed by spring tides, but it is unclear why.

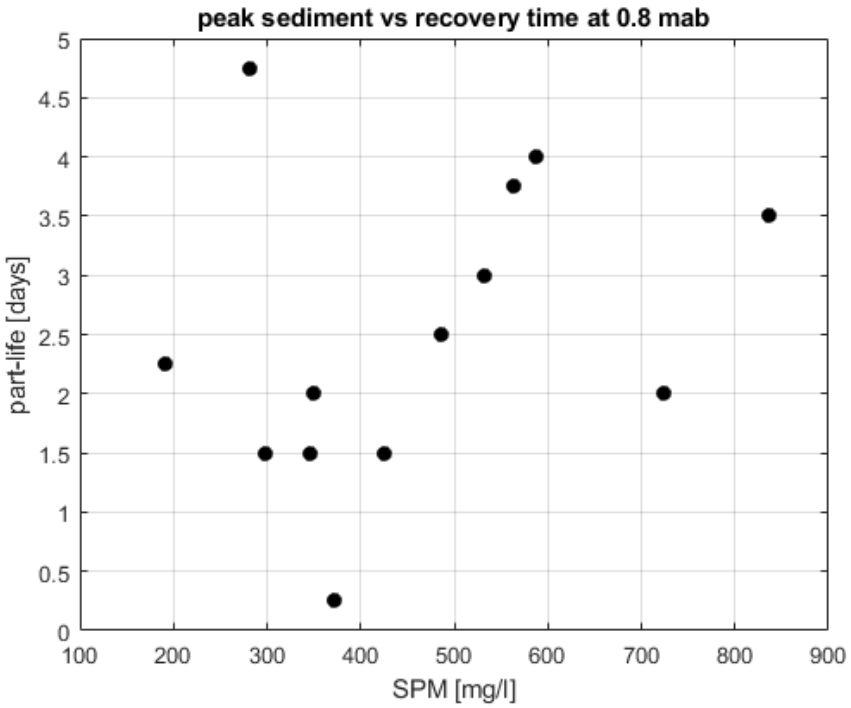

Figure 44: Peak SPM vs part life using measurements from the sensor at 0.8 mab. In general is appears storms with a higher peak SPM also had a longer recovery time.

We can use the λ values to compare recovery rates from the field with those of the model. This is a more reliable measure than the part-life, since the concentrations in the model stabilized after decaying by 5-50%, and not 70%. The form of the exponential decay equation is very similar to the deposition equation. Since the parameters in the model are constant, it was expected that the values of λ would also be constant. Interestingly, we do not observe constant λ values in the model. The values are lower and have a much smaller range than the real values (Figure 45). By doubling α in the model, we can match the range but not the values. The magnitude may also vary based on the contribution of advection, which speeds up the recovery by redistributing sediment. If this were the case, it would also mean that recovery rates vary in space. An area where sediment is advected to would take longer to recover than one where the sediment is advected from.

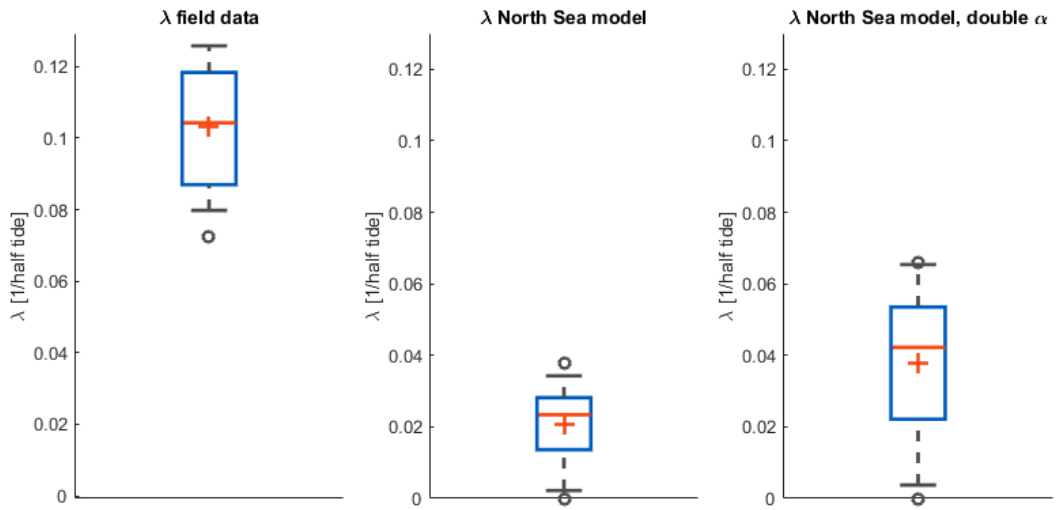

Figure 45: Side-by-side box plot of λ values from the field data, North Sea model (α=0.15), and North Sea model with a higher deposition parameter (α=0.3). The model runs with double α come closer in range to the real values from the field, while the calibrated model with lower α has a much lower range. Both model values are lower than the field.

Besides α, the parameter which determines the fraction of settling sediment that is deposited in the buffer layer, another parameter which may affect the recovery is the settling velocity. As in the reaction, we will look at λ for each of the three sediment fractions in the North Sea parameter set.

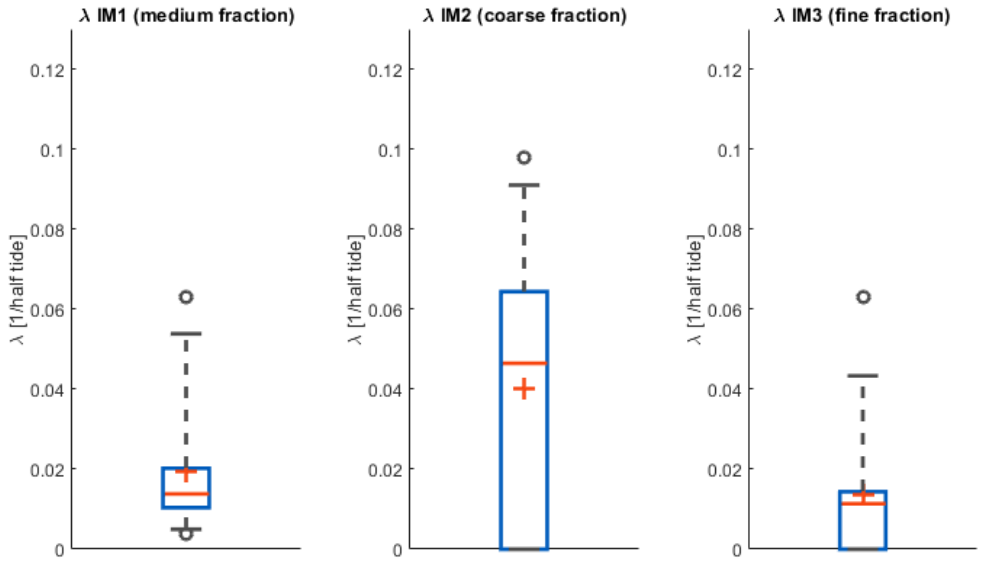

Figure 46: Comparison of λ values for the 3 sediment fractions in the North Sea model with α=0.15. The coarsest fraction has the higher range while the two smaller fractions have a smaller range. The coarse fraction, while still starting at zero, does come closer to the values from the field.

For the three sediment fractions, there are some values which are near zero. The middle sediment fraction comes closest to the field values with the higher fraction of values. This is the sediment fraction with the highest settling velocity, and the values of λ indicate faster recovery times than the other two fractions with lower settling velocity as expected. Interestingly, these two fractions show similar values of λ. This may show that the recovery is related to the settling velocity.

6.1.3 Series

We mostly analyzed single storms, and only briefly looked at storms in series. From these storm series we see that there are differences in how storms affect the sediment when they occur close together. One aspect is the depletion of the bed, when there is no sediment left to erode after a previous storm. This is complicated without detail bed measurements, but hints at the importance of sediment availability either from the bed or advected from elsewhere.

6.2 SEASONALITY

Our research questions also addressed the seasonality of fine sediment dynamics. It is generally agreed upon that there is a higher SPM concentration in winter than in summer. The reasons are debated. There is evidence that suggests floc size, or at least the strength of floc bonding, is seasonal (Fettweiss et al., 2014). Our data has confirmed that there are higher chlorophyll-a concentrations in summer but has not looked at the relation to floc size. Others suggest this difference is due to increased storm activity (Visser et al., 1991). We can confirm that there are higher wave heights in winter than in summer. Another theory points to increased advection through the Dover strait (van Alphen, 1990), which would be related to increased current velocities which we do observe to a small degree.

In our data, we observed seasonality in the exponential decay constants derived from fits to the decay of SPM concentrations following storms. Sediment concentrations recovered after storms at slower rates in winter than in summer. We can eliminate the effects of varying post-storm hydrodynamic conditions, by choosing storms that were all followed by calm periods. In this sample we found no dependence on tidal variance (spring-neap cycle). However, we cannot entirely exclude hydrodynamic conditions. Fine sediments may also be entrained into the bed by bedforms. These bedforms are formed by the hydrodynamic conditions, both past and present (Traykovski, 2007). Bedforms are complicated, and their effect on the entrainment of fine sediment doubly so. But bedforms do impact the mixing of the bed, and thereby the rate at which fines are moved from the fluff layer to the buffer layer (van Kessel et al., 2012).

Biological factors may also contribute to varying recovery rates, and we know these vary seasonally. The presence of diatoms, which produce TEPs, may indicate stronger and larger flocs (Deng et al., 2019; Fettweiss et al., 2014), which cause sediment to settle faster.

6.2.1 Floc size and settling velocity

Floc size is related to settling velocity, the larger a floc the faster it settles. Flocs form and break apart again depending on the chemical and physical properties of their environment. These are the behaviors which make fine sediment dynamics more complex than the dynamics of sand or larger sediments. Over the course of the storm it is likely that the floc size changes with the changing turbulence, and at the peak of the storm the floc size is expected to be the smallest. Research showed that the upper limit of floc size is related to turbulent length scales, and flocs are largest at slack tide, at least in the Belgian coastal zone (Fettweis et al., 2006). This is one possible explanation for the apparent independence of SPM and shear stress during the storm events. When flocs are small and turbulence is high, we expect to see sediment well mixed over the water column, and not changing much since it is not settling out quickly. After the storm, turbulence decreases and, at least in theory, flocs can grow again, which would increase the settling velocity.

We observed seasonality in λ (Figure 32). The values for winter were slightly lower than those in the summer. Something which also may be related to is the floc size. Some evidence points to a seasonal pattern in floc size, which would affect the settling velocity (Fettweiss et al., 2014). Fettweiss states that the SPM concentration is inversely correlated with chlorophyll-a concentrations, based on in situ measurements. This supports older research which used satellite imagery, mentioned in the introduction, which observes higher surface SPM concentrations in winter than in summer (Van Raaphorst et al., 1998; Visser et al., 1991). However, the conclusion of the Fettweiss et al. paper states that the seasonal variation in SPM is due to the variation in biological activity and not storm activity as previously presumed.

6.3 IMPACTS OF ADVECTION AND SPATIAL VARIATIONS

The patterns in reaction to and recovery from storms observed at the location where our data was recorded may not be the same at other locations. Both stratification and advection are expected to play a role in this, as they also vary spatially. Stratification, while also locally affecting flow patterns, may damp mixing, causing sediment to remain lower in the water column. During storms, advection transports sediment eroded from the bed. Varying patterns in flow velocities will change the rate at which sediment is advected, or if it is advected at all. Regions with sufficiently low flow velocities and/or bed shear stresses will see the local settlement of sediment.

Storms, which introduce increased concentrations of fines in the water column are an important part of the sediment balance in the DCZ. In the recovery after the storms we analyzed, we see sediment partially being entrained into the bed and likely partially being advected away. The sediment that is advected away then must be transported somewhere where conditions are calmer. Fine sediments tend to settle and collect where conditions are calmer, such as the turbidity maximum mentioned earlier which is near our measurement site, but also in dredged channels which are deeper than surrounding areas. Cross shore advection specifically may be responsible for gathering the fine sediment at the calmest location, since these gradients are more pronounced than those in the longshore and those in the vertical, if stratification is negligible.

We also evaluated changes in bed level to determine whether erosion was local. For storms 5 and 8 we did see corresponding decreases in bed level during the storm and increases after the storm when sediment settled again. For other storms this pattern is not so clear. If significant local erosion does occur, it may be immediately filled in by other advected sediments. However, the similarity in the SPM dynamics in the water column for all the storms, regardless of local bed behavior, is an indication that local bed erosion alone is not a dominant factor. With the model we further investigated the difference between an open system (field data) and closed system (model data). In the model, the sediment available in the cell is constant while in the field it is not. This explains the higher variability in the field data, as the mass of sediment at the measurement site is free to vary. What this also shows, is that there is a high variability in the concentration of fines in the bed over a longer term.

One other paper which analyzes storms in the Southern North Sea looks at a location in the Belgian coastal zone, in a coastal turbidity maxima (Fettweis et al., 2010). In the storm analyzed in this study, much higher SPM values were observed, and the recovery behavior observed in our 13 storms was not present at all (Figure 2). Following the storm, the SPM concentrations remain high. This shows that the behavior we observe is location dependent. Specifically, it depends on whether the location of interests lies inside or outside the CTM. Outside of the CTM, the sediment will be advected away following the storm, and it will be advected to the CTM since this is where conditions allow the sediment to settle. Alternatively, the sediment may settle in a channel, man-made or otherwise, and cause siltation.

7 CONCLUSIONS

Understanding storms in the North Sea will enable us to better understand the transport of fine sediment through the system. We learned that with each storm, sediment is introduced in to the water column, and following the storm decreases exponentially with each tidal cycle. This holds true near Egmond aan Zee, where the fraction of fines in the bed is between 2 and 15% on average. This new insight was gained by analysing long-term field data from the DCZ and subsequently comparing the results with those from a schematised hydrodynamic model.

We developed and aimed to answer three research questions. These enabled us to quantify the relevant behaviors of the sediment concentration in the water column and the seabed. The first two questions addressed the behavior of the sediment dynamics in time relative to the storm event. We looked at the reaction of the sediment during the storm, and when the peak SPM was reached, and then at the recovery from peak SPM back to normal conditions. The third question addresses possible seasonal effects on dynamics during and after the storms.

1. How does the system react to the occurrence of a storm?
    a. Is there a lag between the peak of the storm and the peak in suspended sediment?

We found that for all storms analyzed the peak in SPM occurred after the peak in hydrodynamic conditions (wave height, shear stress). We hypothesize that this is due to the settling of sediment from higher in the water column after the storm, which is prohibited during the storm by turbulence. This turbulence may also reduce the floc size, and thereby settling velocity, which would further aid the mixing of sediment across the water column. The measured behavior of the SPM during the storm from the field data is very similar to that of the finer sediment fractions in the model. While the behavior before and after is more like the behavior of coarser fractions. The effect of turbulence on floc size is supported theoretically and experimentally (Fettweiss et al., 2014; Winterwerp et al., 2002). These observations point to a varying floc size which impacts the reaction.

2. How does the system recover from a storm?
    a. How long does it take for the suspended sediment to return to pre-storm values?
    b. Is the recovery time consistent between storms? What does this recovery time depend on?

Following the peak in SPM concentrations, there is a gradual reduction in the SPM entrained over each tide (flood, ebb) which can be described using an exponential decay equation. The exponential decay function is fit to the data using the decay constant λ. For all storms, the values lie very close together, with a median of about 0.1 per half tide and some seasonal variation of $\pm$ 0.03 per half tide. This pattern shows that storms recover at a slower rate in winter than in summer.

We also looked at the part-life, which is a measure of the time it takes for the SPM to decrease by 70%. We found that for all storms analyzed, this takes between 1 and 5 days. This means that the sediment suspended due to the storm does not remain at the location for very long following the storm. The sediment is either advected elsewhere or entrained into the bed. The exponential decay of SPM with the tides is strong evidence that the decay involved entrainment into the bed. Modeling confirms that part of the SPM is entrained into the bed, while another part is advected away. This means the recovery times and rates will vary in space, depending on the local conditions.

3. Are there (seasonal) differences in the reaction and/or recovery of SPM?
    a. Are differences related to the presence of diatoms?

In our analysis of reaction and recovery, we observe a seasonal pattern in the decay constant of the fitted exponential decay equations. This shows there is a seasonal pattern in the recovery. We did not observe any seasonal patterns in the reaction. In the field data we observe higher wave heights and lower Chlorophyll-a concentrations along with the higher SPM concentrations in winter. So, either the generally more energetic conditions in winter or the lower biological activity could be responsible for this seasonal pattern. Since the conditions following the storms were similar for both summer and winter storms, differences in biological

activity are the likely explanation. Further measurements of floc size or settling velocity would be needed to test this hypothesis. However, based on research by Fettweiss et al (2014) from the Southern North Sea it is likely that phytoplankton contribute to the seasonal differences in sediment dynamics by affecting floc strength.

We also observe some seasonal patterns in the concentrations of sediment in the model. In the winter more sediment is stored outside of the buffer layer (fluff and water column), while during the summer more sediment is in the buffer layer. This is how the seasonality is represented in the model. However, this is not seen in the bed samples from the field data. Either because this seasonal pattern in stored sediment is not present in the field, or our one location of measurement does not show this.

We found that the model parameters used for the North Sea underestimate the variability of sediment, suggesting that advection does play a large role in the natural system and cannot be neglected. This also means that the recovery times, estimated at 1-5 days, may vary in space due to varying current patterns. We hypothesize that a time varying settling velocity may be the cause for the lag between the peak SPM and peak shear stress. While measurements are needed to confirm this, the decrease in settling velocity during the storm event is theoretically supported by the correlation between the Kolmogorov length scale and largest floc size. These findings provide more insight into the dynamics of sediment during storms in mixed sediment systems, specifically the Dutch Coastal Zone.

7.1 Recommendations

Recommendations for further research are listed here:

- In-situ measurements of floc size, or particle size distribution, to analyze how that changes over the course of a storm
    - Or even over the scale of a year for seasonal changes
- More years of similar measurements to determine if the seasonal pattern observed in λ is consistent
- Collect field data from multiple measurement locations spaced to observe advection and any potential spatial variations in the decay constant
    - Including a measuring point in the Coastal Turbidity Maximum, where sediment from surrounding locations is potentially advected to
- Comparing content of fines in the bed to the peak sediment suspended. This would require higher frequency measurements of the bed composition, which may not be feasible with current technology and measurement techniques.
- Allow for time varying settling velocity in the model and determine what difference this makes
- Expand modeling to include advection to see if this makes the difference in the recovery

Not all these recommendations are feasible with current technology, but technology will certainly advance, and the suggested measurements will become possible.

BIBLIOGRAPHY

Bijker, W. E. (1980). Sedimentation in channels and trenches. *IN: PROC. SEVENTEENTH COASTAL ENGNG. CONF.,*. https://doi.org/10.1061/9780872622647.104

de Nijs, M. A. J., Winterwerp, J. C., & Pietrzak, J. D. (2009). On harbour siltation in the fresh-salt water mixing region. *Continental Shelf Research*. https://doi.org/10.1016/j.csr.2008.01.019

Deltares. (n.d.). *Delft 3D flexible mesh suite: D-Water Quality*.

Deltares. (2020). D-Water Quality Processes Library Description. In *Deltares* (Vol. 5, Issue 1).

Deng, Z., He, Q., Safar, Z., & Chassagne, C. (2019). The role of algae in fine sediment flocculation: In-situ and laboratory measurements. *Marine Geology*, *413*(January 2018), 71–84. https://doi.org/10.1016/j.margeo.2019.02.003

Fettweis, M., Francken, F., Pison, V., & Van den Eynde, D. (2006). Suspended particulate matter dynamics and aggregate sizes in a high turbidity area. *Marine Geology*. https://doi.org/10.1016/j.margeo.2006.10.005

Fettweis, M., Francken, F., Van den Eynde, D., Verwaest, T., Janssens, J., & Van Lancker, V. (2010). Storm influence on SPM concentrations in a coastal turbidity maximum area with high anthropogenic impact (southern North Sea). *Continental Shelf Research*, *30*(13), 1417–1427. https://doi.org/10.1016/j.csr.2010.05.001

Fettweiss, M., Baeye, M., Van der Zande, D., Van den Eynde, D., & Joon Lee, B. (2014). Seasonality of floc strength in the southern North Sea. *Journal of Geophysical Research : Oceans*, 1911–1926. https://doi.org/10.1002/2013JC009563

Flores, R. P., Rijnsburger, S., Horner-Devine, A. R., Souza, A. J., & Pietrzak, J. D. (2017). The impact of storms and stratification on sediment transport in the Rhine region of freshwater influence. *Journal of Geophysical Research: Oceans*, *122*(5), 4456–4477. https://doi.org/10.1002/2016JC012362

Hendriks, H. C. M., van Prooijen, B. C., Aarninkhof, S. G. J., & Winterwerp, J. C. (2020). How human activities affect the fine sediment distribution in the Dutch Coastal Zone seabed. *Geomorphology*. https://doi.org/10.1016/j.geomorph.2020.107314

Lummer, E. M., Auerswald, K., & Geist, J. (2016). Fine sediment as environmental stressor affecting freshwater mussel behavior and ecosystem services. *Science of the Total Environment*. https://doi.org/10.1016/j.scitotenv.2016.07.027

Marinelli, R. L., Jahnke, R. A., Craven, D. B., Nelson, J. R., & Eckman, J. R. (1998). Sediment nutrient dynamics on the South Atlantic Bight contiental shelf. *The American Society of Limnology and Oceanography*, *43*(6), 1305–1320.

McCandliss, R. R., Jones, S. E., Hearn, M., Latter, R., & Jago, C. F. (2002). Dynamics of suspended particles in coastal waters (southern North Sea) during a spring bloom. *Journal of Sea Research*, *47*(3–4), 285–302. https://doi.org/10.1016/S1385-1101(02)00123-5

Nauw, J. J., & van der Vegt, M. (2012). *Hydrodynamics of the Rhine ROFI near IJmuiden*. *1*(1). https://doi.org/10.3990/2.191

Partheniades, E. (1962). *A study of erosion and deposition of cohesive soils in salt water*. University of California Berkeley.

R. Krone. (1962). *Flume studies of transport of sediment in estuarial shoaling processes (Final report)*.

Rijnsburger, S., van der Hout, C. M., van Tongeren, O., de Boer, G. J., van Prooijen, B. C., Borst, W. G., & Pietrzak, J. D. (2016). Simultaneous measurements of tidal straining and advection at two parallel transects far downstream in the Rhine ROFI. *Ocean Dynamics*. https://doi.org/10.1007/s10236-016-0947-x

Stanev, E. V., Dobrynin, M., Pleskachevsky, A., Grayek, S., & Günther, H. (2009). Bed shear stress in the

southern North Sea as an important driver for suspended sediment dynamics. *Ocean Dynamics*, *59*(2), 183–194. https://doi.org/10.1007/s10236-008-0171-4

Suijlen, J. M., & Duin, R. N. M. (2001). *Variability of near-surface total suspended matter concentrations in the Dutch coastal zone of the North Sea*. *December*, 86.

Sündermann, J., & Pohlmann, T. (2011). A brief analysis of North Sea physics. In *Oceanologia*. https://doi.org/10.5697/oc.53-3.663

Traykovski, P. (2007). Observations of wave orbital scale ripples and a nonequilibrium time-dependent model. *Journal of Geophysical Research: Oceans*, *112*(6), 1–19. https://doi.org/10.1029/2006JC003811

van Alphen, J. S. L. J. (1990). A mud balance for Belgian-Dutch coastal waters between 1969 and 1986. *Netherlands Journal of Sea Research*, *25*(1–2), 19–30. https://doi.org/10.1016/0077-7579(90)90005-2

van der Hout, C. M., Witbaard, R., Bergman, M. J. N., Duineveld, G. C. A., Rozemeijer, M. J. C., & Gerkema, T. (2017). The dynamics of suspended particulate matter (SPM) and chlorophyll-a from intratidal to annual time scales in a coastal turbidity maximum. *Journal of Sea Research*, *127*(March), 105–118. https://doi.org/10.1016/j.seares.2017.04.011

van Kessel, T., Spruyt-de Boer, A., Van der Werf, J., Sittoni, L., van Prooijen, B., & Winterwerp, H. (2012). *Bed Module for sand-mud mixtures*. Deltares.

Van Kessel, T., Winterwerp, H., Van Prooijen, B., Van Ledden, M., & Borst, W. (2011). Modelling the seasonal dynamics of SPM with a simple algorithm for the buffering of fines in a sandy seabed. *Continental Shelf Research*, *31*(10 SUPPL.), S124–S134. https://doi.org/10.1016/j.csr.2010.04.008

Van Raaphorst, W., Philippart, C. J. M., Smit, J. P. C., Dijkstra, F. J., & Malschaert, J. F. P. (1998). Distribution of suspended particulate matter in the North Sea as inferred from NOAA/AVHRR reflectance images and in situ observations. *Journal of Sea Research*, *39*(3–4), 197–215. https://doi.org/10.1016/S1385-1101(98)00006-9

Visser, M., de Ruijter, W. P. M., & Postma, L. (1991). The Distribution of Suspended Matter In the Dutch Coastal Zone. *Netherlands Journal of Sea Research*, *27*(2), 127–143.

Winterwerp, J. C. (2002). On the flocculation and settling velocity of estuarine mud. *Continental Shelf Research*. https://doi.org/10.1016/S0278-4343(02)00010-9

Winterwerp, J. C., Bale, A. J., Christie, M. C., Dyer, K. R., Jones, S., Lintern, D. G., Manning, A. J., & Roberts, W. (2002). Flocculation and settling velocity of fine sediment. *Proceedings in Marine Science*, *5*, 25–40.

Witbaard, R., Duineveld, G., & Bergman, M. J. N. (2013). *The final report on the growth and dynamics of Enis directus in the near coastal zone off Egmond, in relation to environmental conditions in 2011-2012*. 79.

Zijl, F., Veenstra, J., & Groenenboom, J. (2018). *The 3D Dutch Continental Shelf Model - Flexible Mesh (3D DCSM-FM): Setup and validation*.

APPENDIX A: DATA ANALYSIS SCRIPTS

Data processing scripts

To analyze the data, we created multiple scripts and functions. The most important first steps include defining moments of interest and defining the tidal maxima values, and matching indices for the variables with different frequencies. We apply the same approaches outlined in this section to analyze the model data, using modified scripts to account for differences in format.

General approach

The main input required is a vector containing the identification numbers of the storms, any combination of integers from 1 to 13. The for loop then iterates the process over every storm. In the first iteration the data is opened. Then for each iteration, the start and end date of the storm are found based on the value of N input into the function stormdates. The indices corresponding to these start and end dates are found using dateindex. The indices of slack tide are found between the start and end index using findslack2 and are used as input to find the maximum SPM per half cycle, and the maximum velocities, wave heights or shear stress with findtide. The maximum SPM per half cycle is then normalized by the peak value.

Matching indices for data from the buoy Munitiestortplaats, which was recorded at a different frequency, were found with the built in function find() and indices a and b found from Dateindex():

```
[aij,startij]=find(indexIJ==a);

[bij,endingij]=find(indexIJ==b);
```

where indexIJ is the vector provided in the data which contains the corresponding index of the 10-minute data. The same procedure is used to find the indices for the wind data.

For the analysis of the sediment decay, the SPM curve was normalized using the peak value in order to compare the decay rates following the peak. The decay rate, and half-life, could be found from the normalized curve. The function to find the half-life also can calculate other percentages of decay. If we want to look at the return to pre-storm conditions, or to calm conditions, we can look at the decay by 70 or 80%.

The dates of storm samples, once being manually identified, were listed in a Matlab function to be called upon in turn in the for loop of the main script. These main scripts, master scripts, were essentially a for loop which calculated certain parameters for each storm and recorded them in a table or created a plot. The flow chart of this approach is shown in Figure 47 and Figure 48.

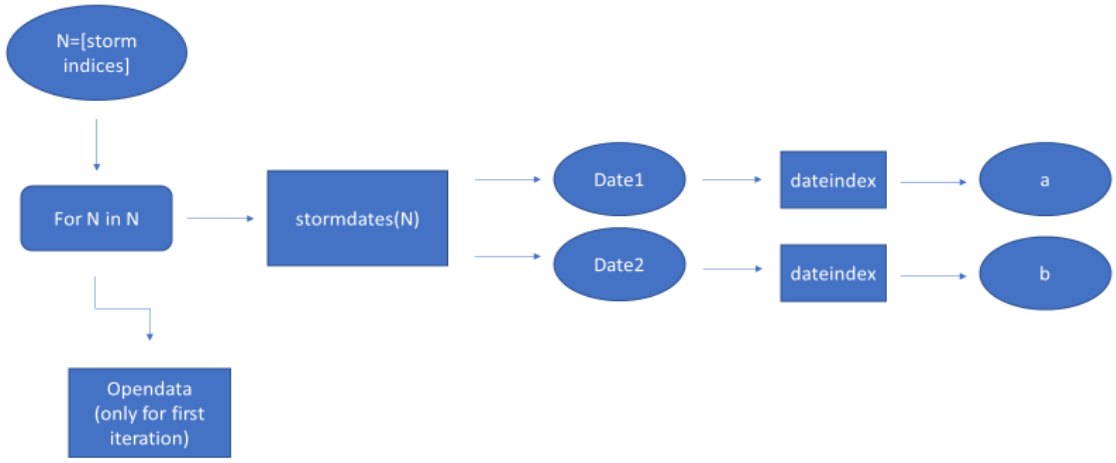

Figure 47: Steps of the script from the input, a vector including the ID of the storms you wish to look at, until determination of the starting (a) and ending (b) index of the period of interest.

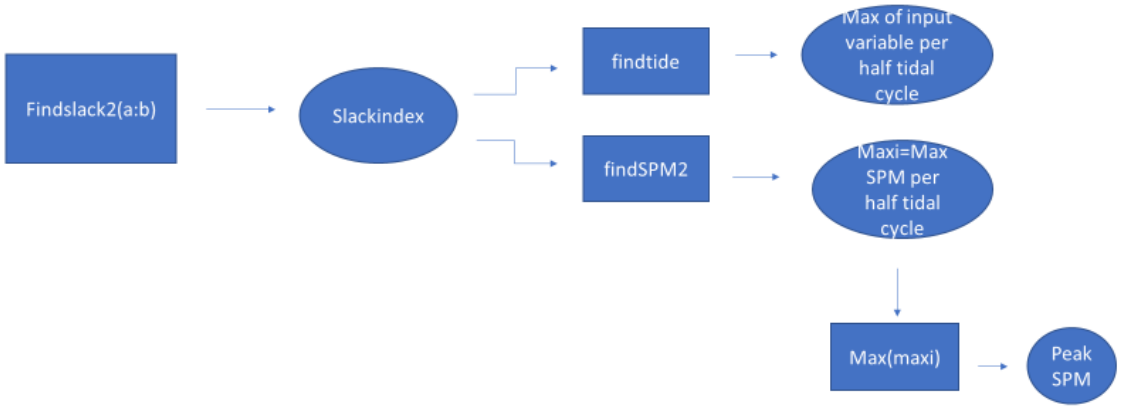

Figure 48: steps of the script using the starting and ending index as found in the previous steps to identify the indices of slack tide over the period, as well as maximum SPM, shear stress, velocity, and/or wave height.

Functions

All functions which are used to analyze the data are briefly described here:

Stormdates

[date1,date2]=stormdates(N)

The above list of dates is contained in the function stormdates, which takes as input the index of the storm (1:13) and gives as output the start and end date.

Dateindex/DateindexModel

[index, check_date]=DateIndex(date)

This function takes as input the date of interest, either starting or ending, and returns the index of this time in the larger dataset and the date of that index as verification. The start index is called “a” and the ending index “b”. The rest of the analysis is then done storm by storm by performing all functions on the data from a:b.

Opendata

[time,SPM,CHL,waves,wavesIJ,indexIJ,v_cycle,T,v_ls,v_cs,t,wlev]=opendata()

This function contains all the commands to open the data, as well as any calculations performed on the data, and gives as output the data vectors.

Findslack2

[slackindex]=findslack2(v_cycle)

Using the velocity signal as calculated in equation 1, this function finds the index closest to the zero crossing. This is done by recording the index i for which the product of v_cycle(i) and v_cycle(i+1) is negative. The recorded index is I, meaning the slack index is the index preceding the zero crossing. Slack tide happens within the 10 minutes following this index.

Findtide

[tidev,tideindex]=findtide(v,slackindex)

Returns the max value and index of max value between two successive slack tides. The input variable is v, but any signal except SPM/CHL can be input into this function to find the maximum value over the half tidal cycle.

findSPM2

[maxindex maxi]=findSPM2(SPM,slackindex)

Finds the maximum SPM concentration between two successive slack tides. It was determine from looking at the data that the maximum SPM concentration occurs consistently between the two slack tides, and that the minimum occurs right around slack tide (Figure 49). This function is different from findtide in that the natural log of the input signal is taken, and the maximum of that resulting signal is recorded. This was found to produce more consistent results than finding the maximum of the direct signal.

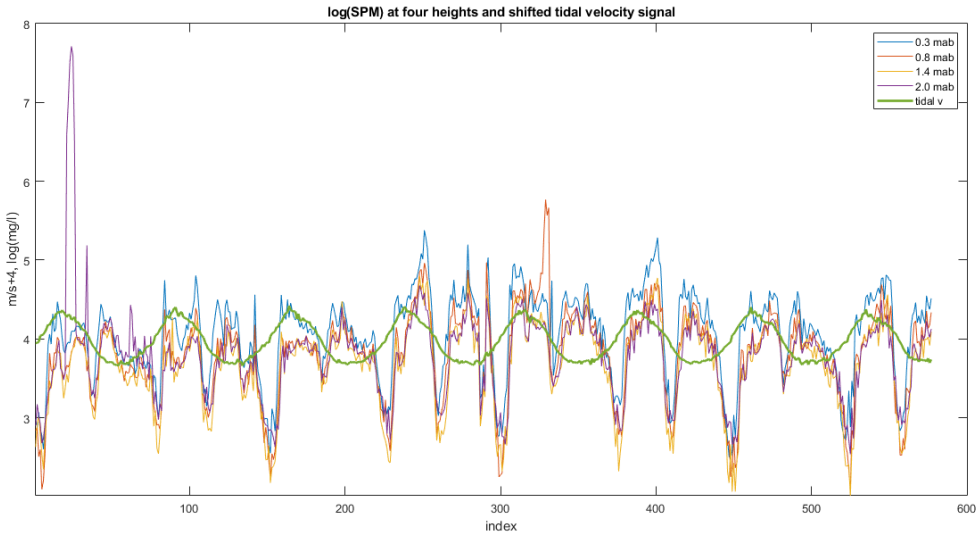

Figure 49: SPM concentration at four sensors overlaid with the velocity signal> note that this fluctuation between positive and negative values and crosses zero between crest and trough.

Partlife

[val, t_life]=partlife(normsignal,fraction)

To quantify the decay of the sediment concentration following a storm, this function was created to determine the index at which the sediment concentration falls below some percentage of its maxima during a storm sample. The input SPM must already be processed by findSPM2 and normalized by its peak value before use as input in this function. The function then returns the index and value of the minima of the normalized signal minus the fraction. For the half-life, fraction = 0.5. For a decay of 80% fraction = 0.2. The resulting index (t_life) is relative to the peak, and in half tidal cycles. So, a value of 10 would indicate 10 half tidal cycles (ebb or flood), or 5 full tidal cycles (ebb and flood). The decay by 80% is used in this report and is referred to as the part-life.

ExpDecay/ExpDecayModel

Takes the SPM signal from the peak of sediment to the end of the segment, calculates a constant that describes the decay function.

APPENDIX B: DATA OVERVIEW PER STORM

STORM 1

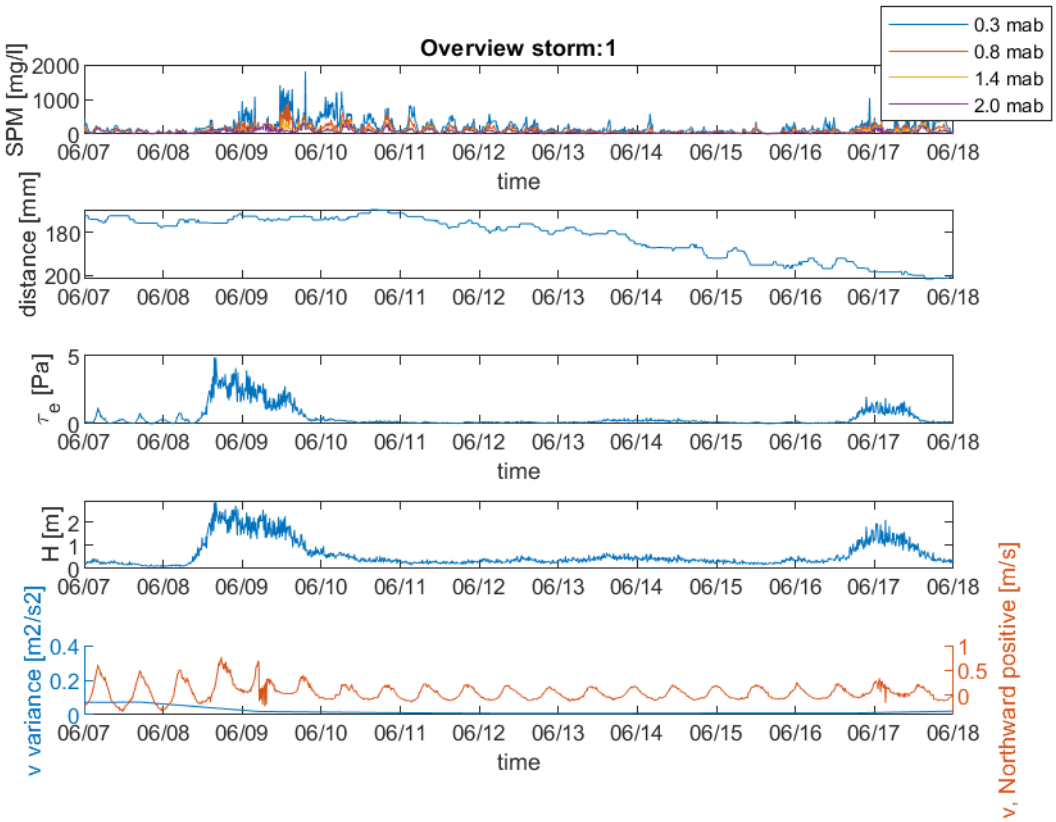

Figure 50 Storm overview. From top to bottom: suspended sediment concentration, distance to bed, shear stress, median wave height, near bed velocity, and velocity variance

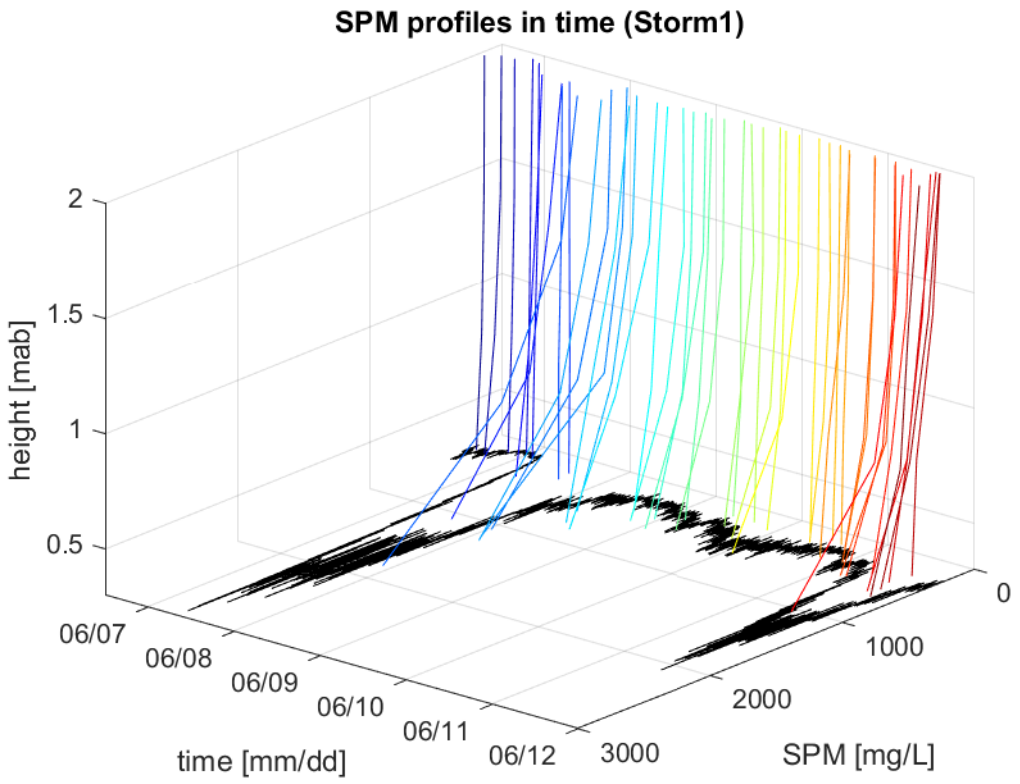

Figure 51: Sediment concentration profiles from the peak of each tide (ebb/flood) in rainbow, and the wave height scaled by 1000 in black

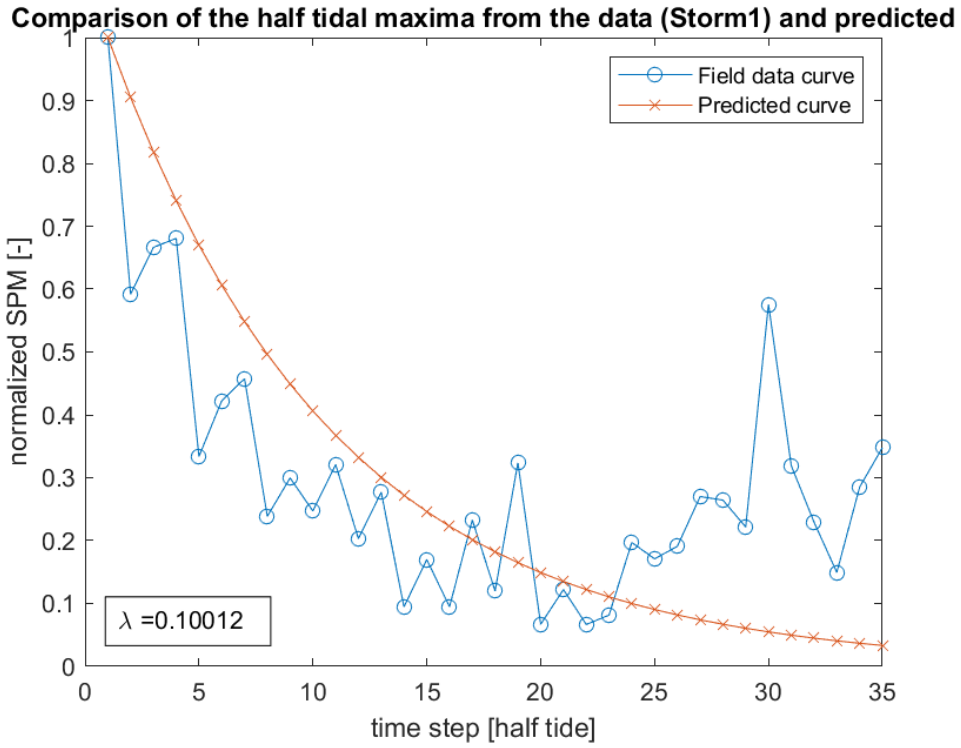

Figure 52: Predicted decay curve calculated with λ as shown in the figure, and data decay points. Each point represents the maximum SPM per tide (ebb/flood) normalized by the SPM peak due to the storm

STORM 2

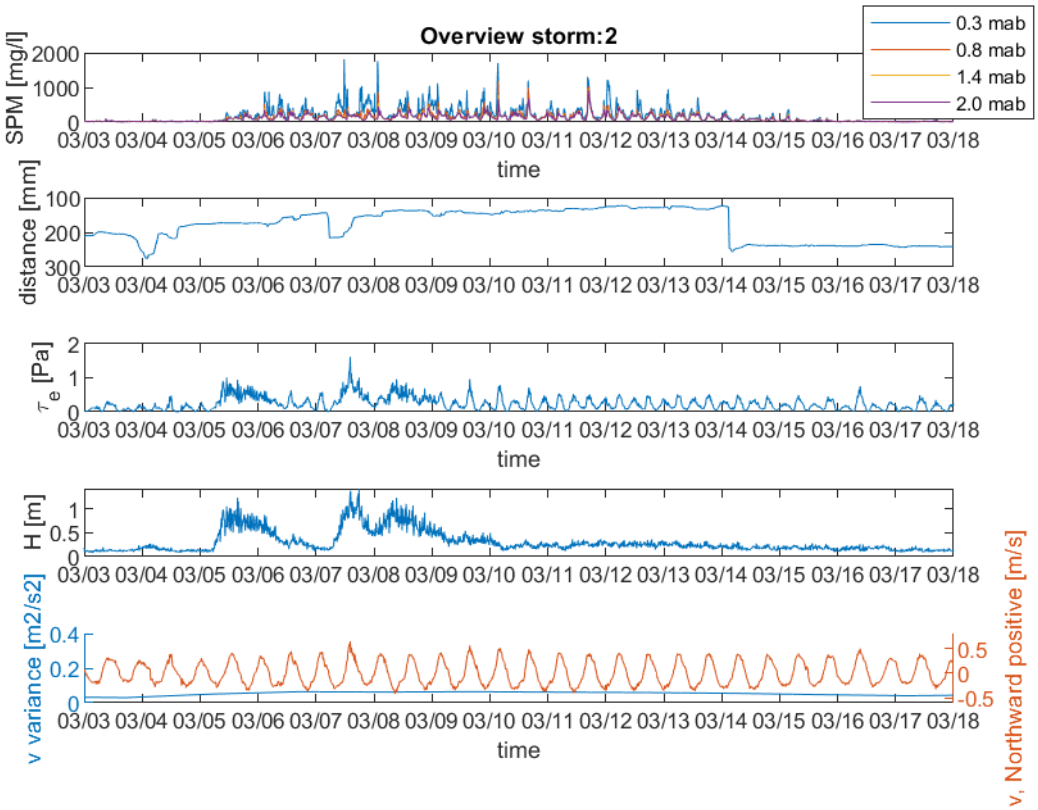

Figure 53: Storm overview. From top to bottom: suspended sediment concentration, distance to bed, shear stress, median wave height, near bed velocity, and velocity variance

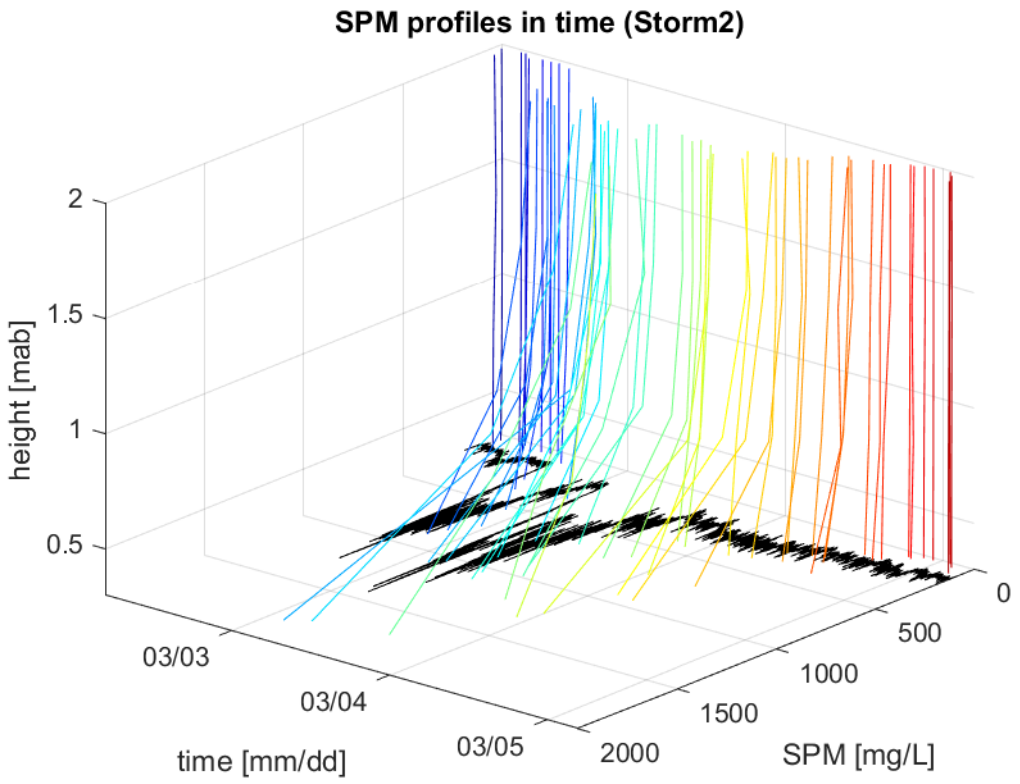

Figure 54: Sediment concentration profiles from the peak of each tide (ebb/flood) in rainbow, and the wave height scaled by 1000 in black

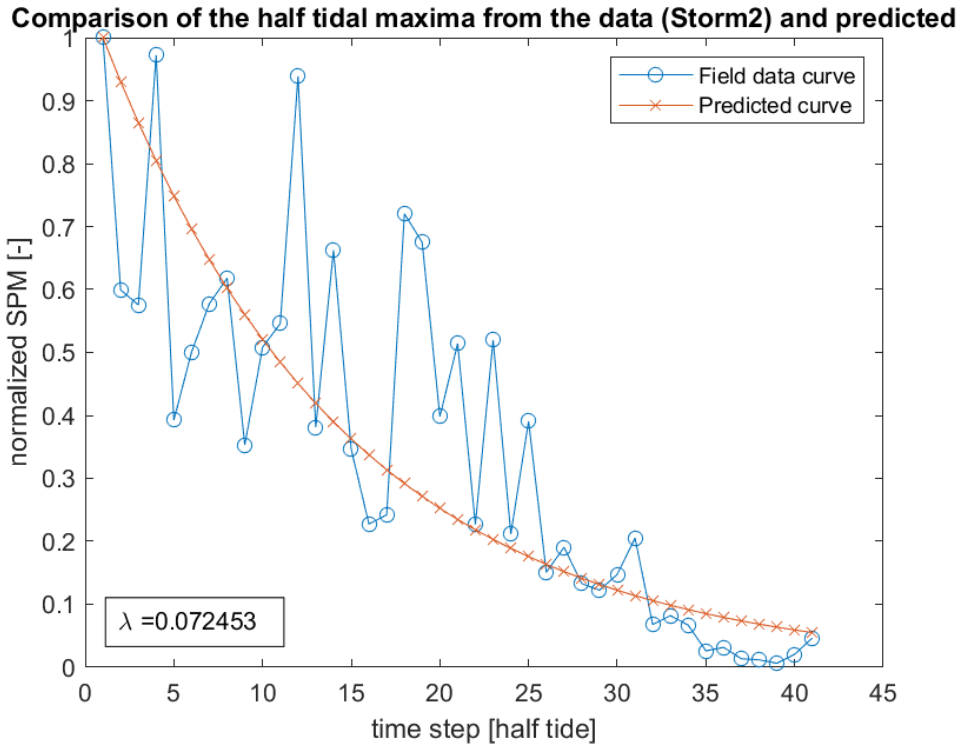

Figure 55: Predicted decay curve calculated with λ as shown in the figure, and data decay points. Each point represents the maximum SPM per tide (ebb/flood) normalized by the SPM peak due to the storm

STORM 3

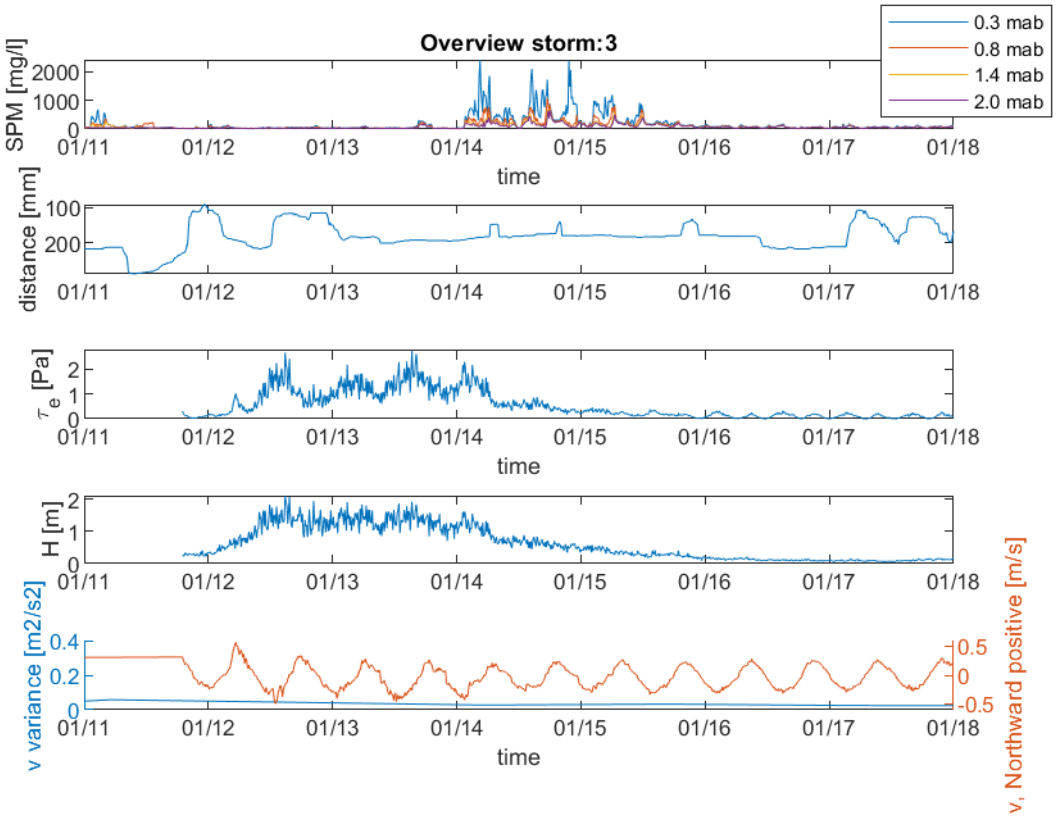

Figure 56: Storm overview. From top to bottom: suspended sediment concentration, distance to bed, shear stress, median wave height, near bed velocity, and velocity variance

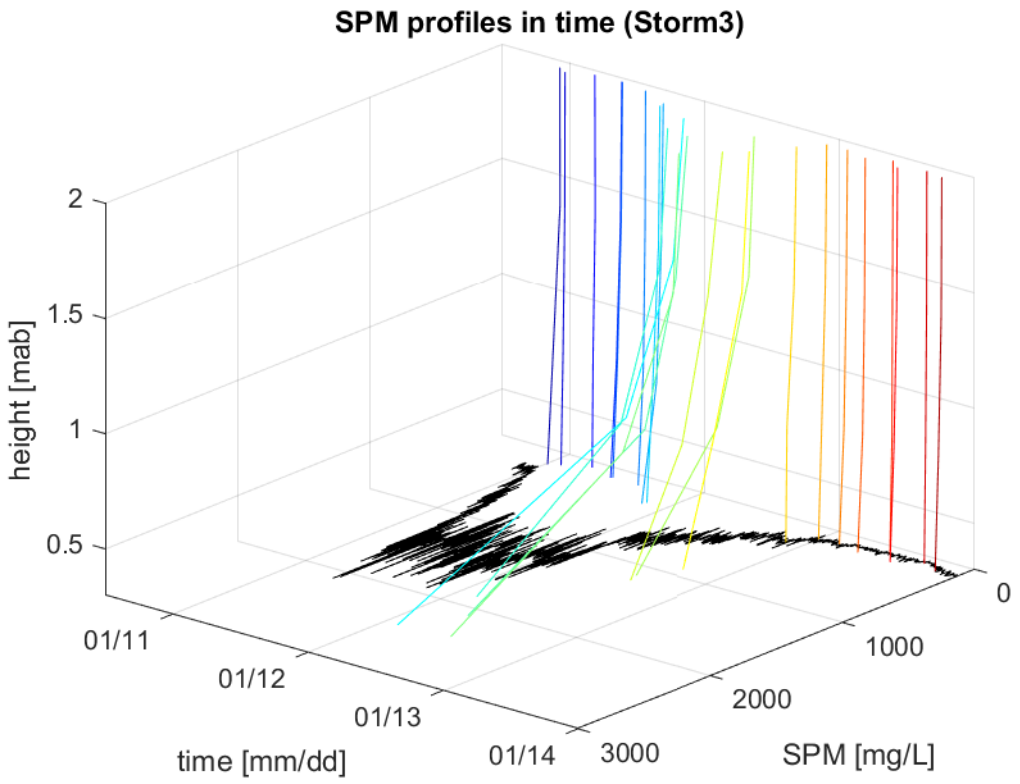

Figure 57: Sediment concentration profiles from the peak of each tide (ebb/flood) in rainbow, and the wave height scaled by 1000 in black

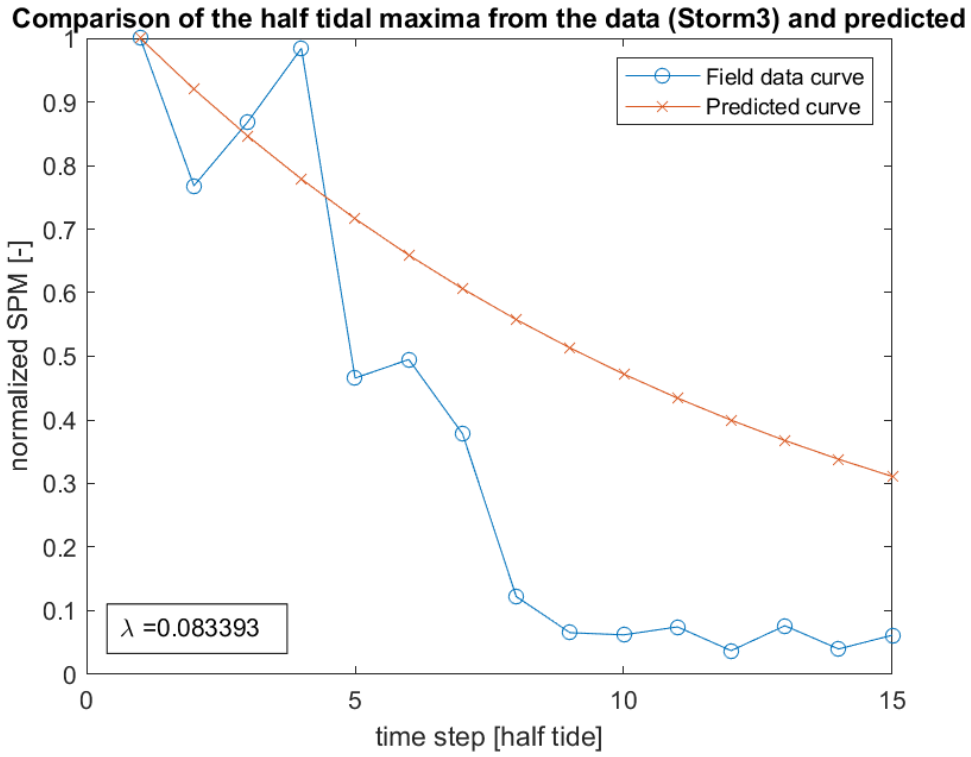

Figure 58: Predicted decay curve calculated with λ as shown in the figure, and data decay points. Each point represents the maximum SPM per tide (ebb/flood) normalized by the SPM peak due to the storm

STORM 4

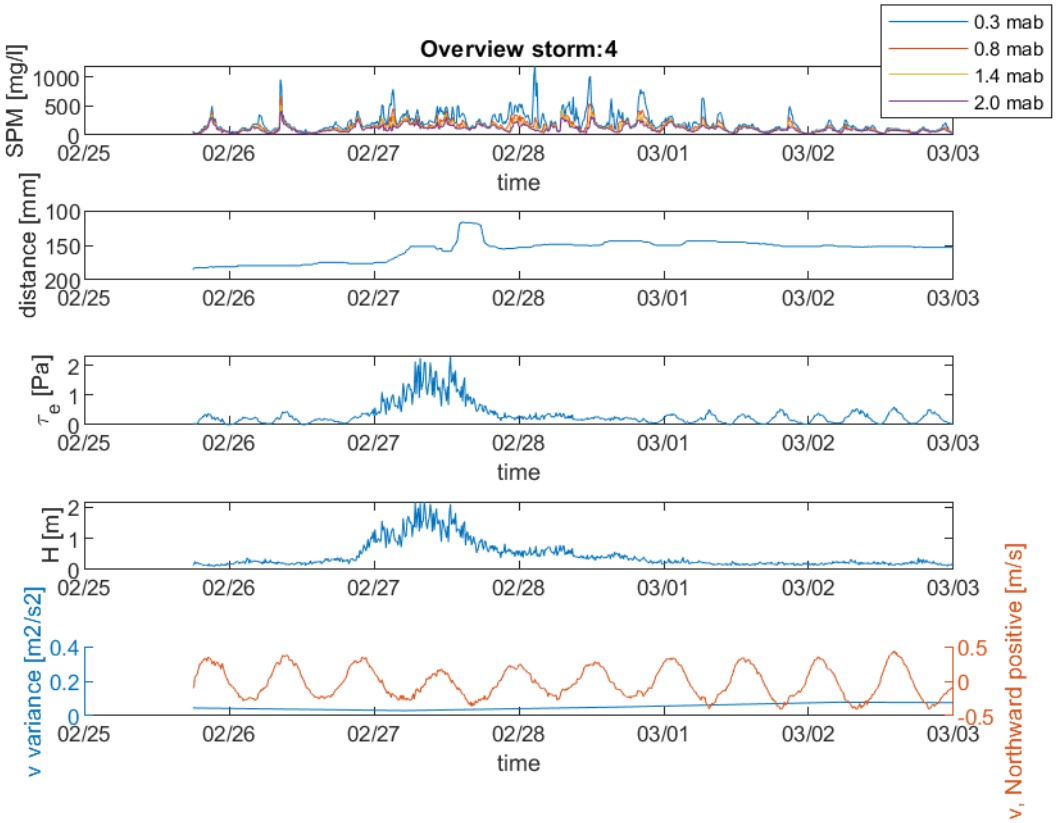

Figure 59: Storm overview. From top to bottom: suspended sediment concentration, distance to bed, shear stress, median wave height, near bed velocity, and velocity variance

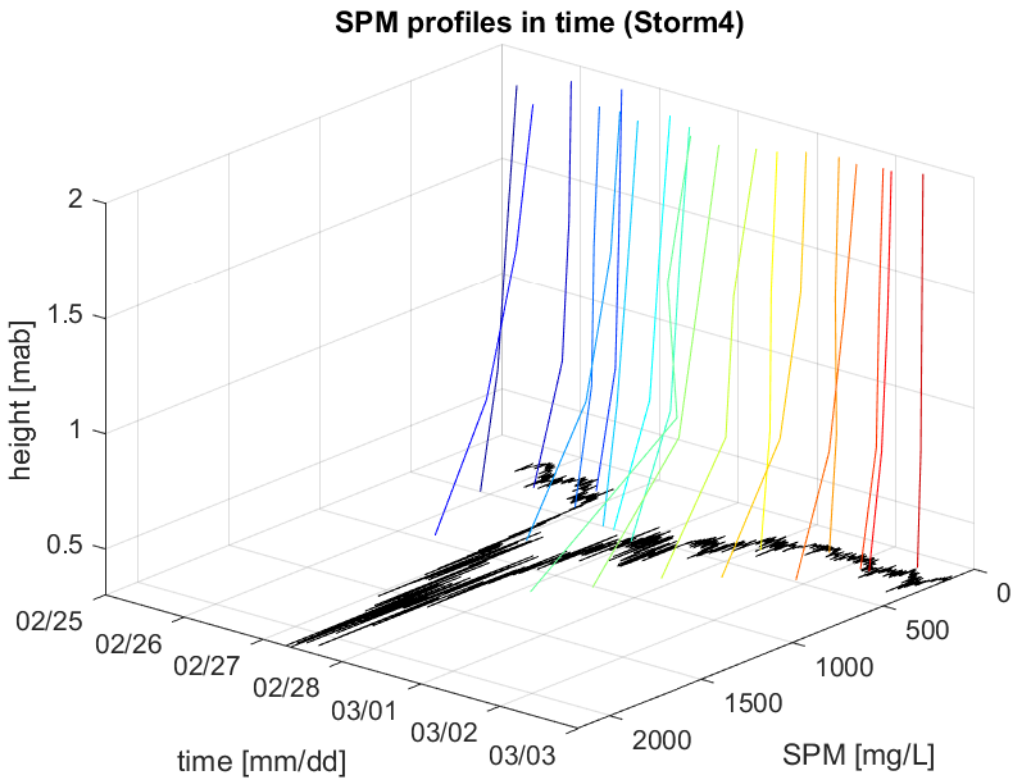

Figure 60: Sediment concentration profiles from the peak of each tide (ebb/flood) in rainbow, and the wave height scaled by 1000 in black

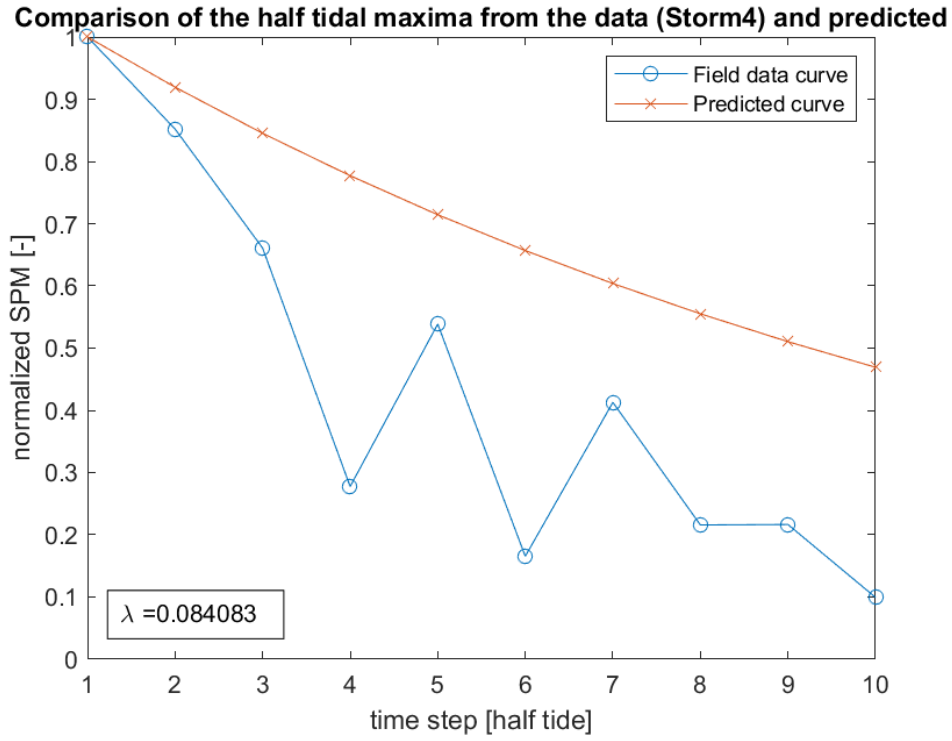

Figure 61: Predicted decay curve calculated with λ as shown in the figure, and data decay points. Each point represents the maximum SPM per tide (ebb/flood) normalized by the SPM peak due to the storm

STORM 5

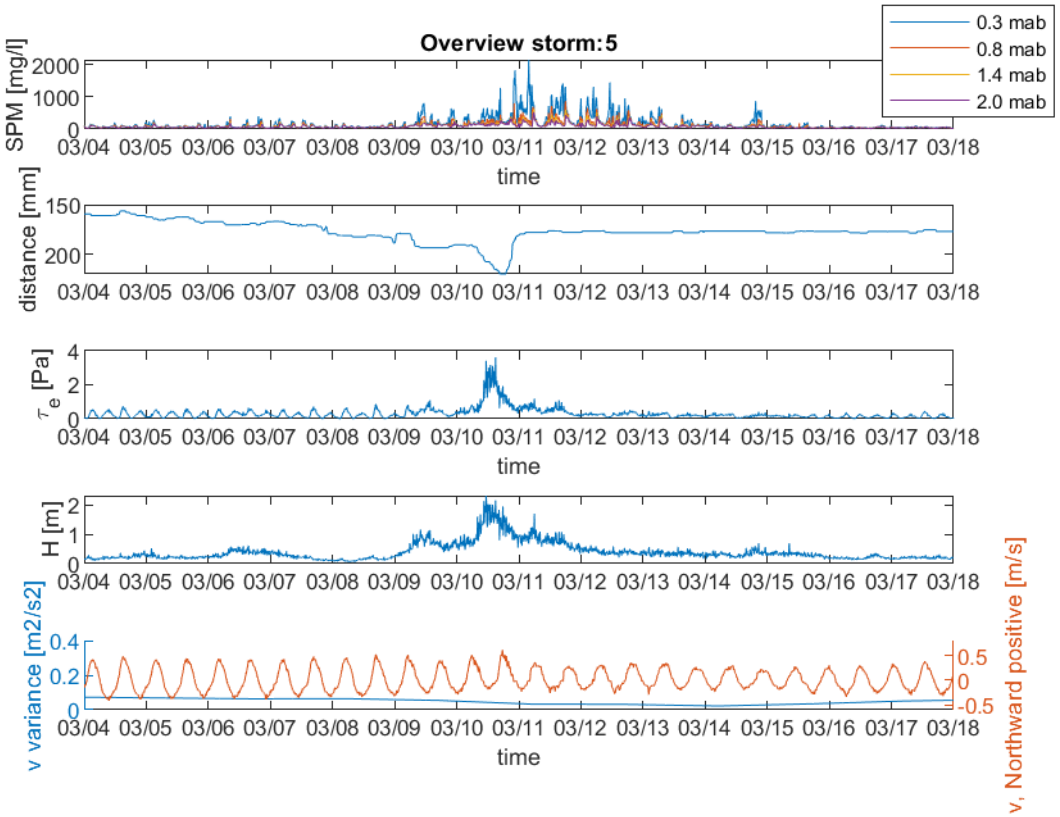

Figure 62: Storm overview. From top to bottom: suspended sediment concentration, distance to bed, shear stress, median wave height, near bed velocity, and velocity variance

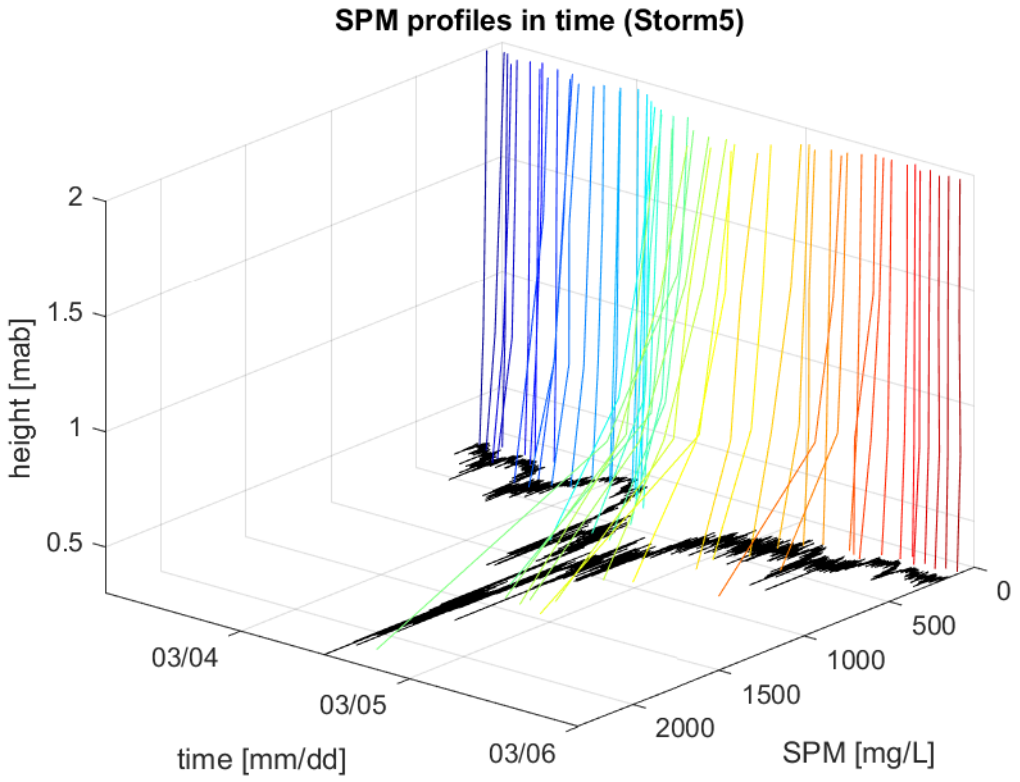

Figure 63: Sediment concentration profiles from the peak of each tide (ebb/flood) in rainbow, and the wave height scaled by 1000 in black

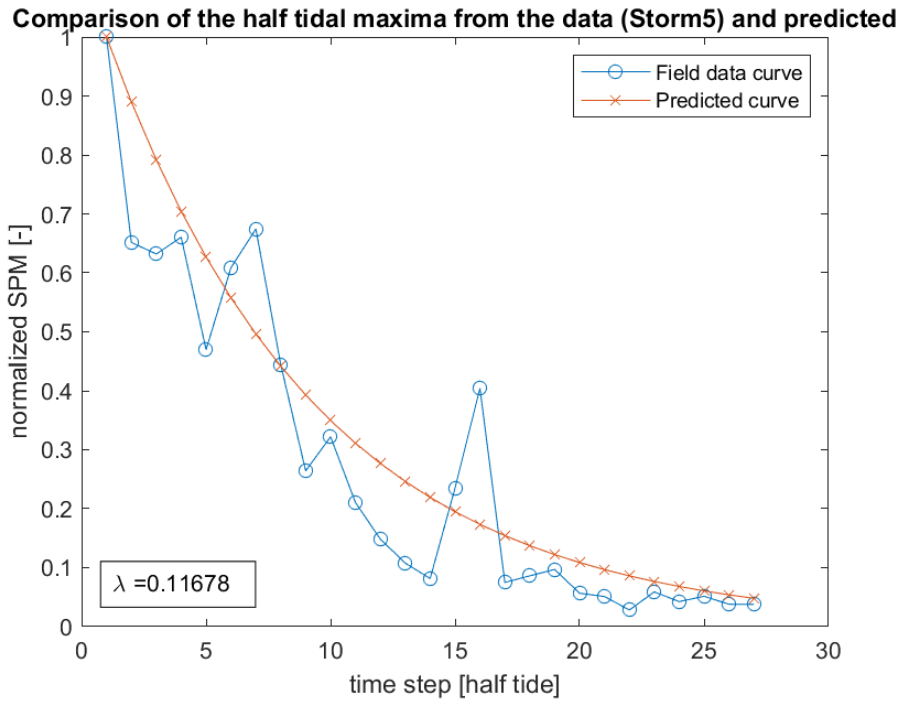

Figure 64: Predicted decay curve calculated with λ as shown in the figure, and data decay points. Each point represents the maximum SPM per tide (ebb/flood) normalized by the SPM peak due to the storm

STORM 6

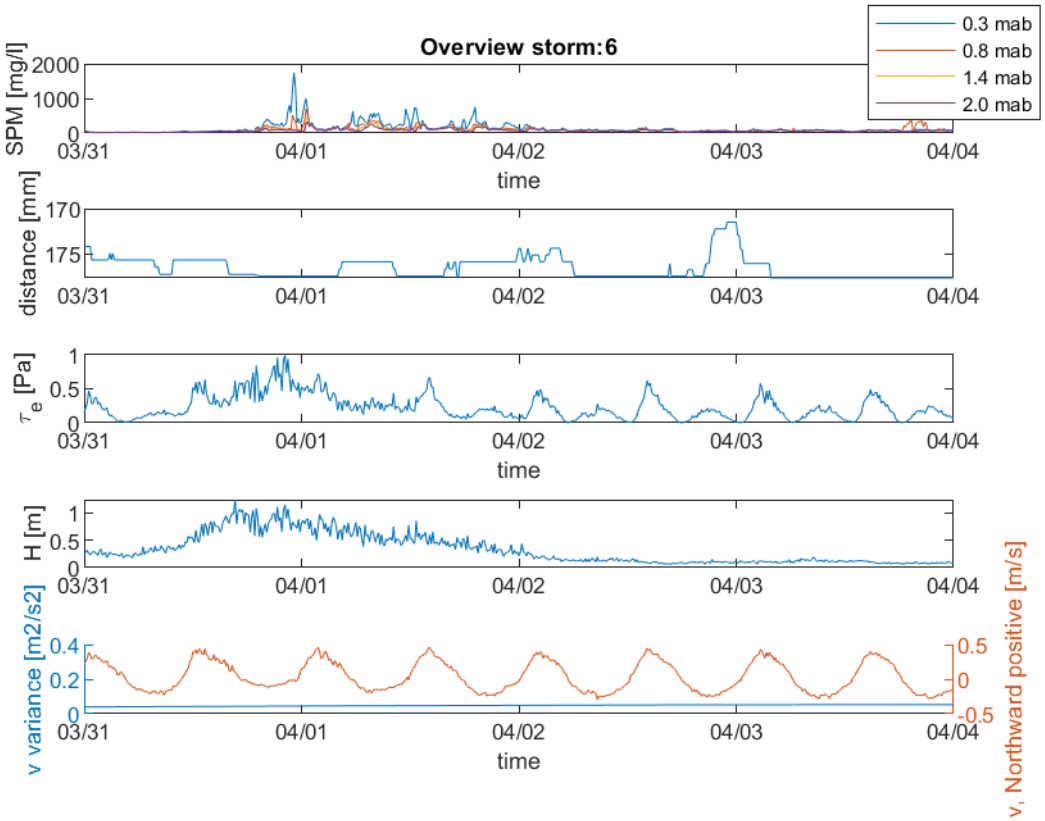

Figure 65: Storm overview. From top to bottom: suspended sediment concentration, distance to bed, shear stress, median wave height, near bed velocity, and velocity variance

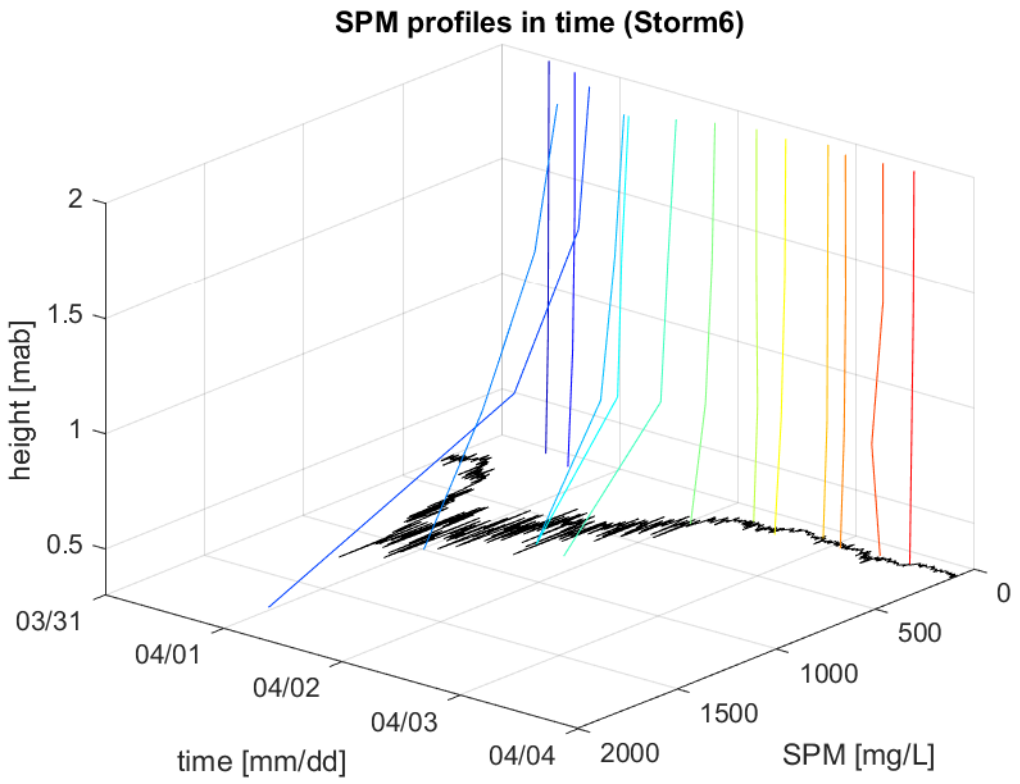

Figure 66: Sediment concentration profiles from the peak of each tide (ebb/flood) in rainbow, and the wave height scaled by 1000 in black

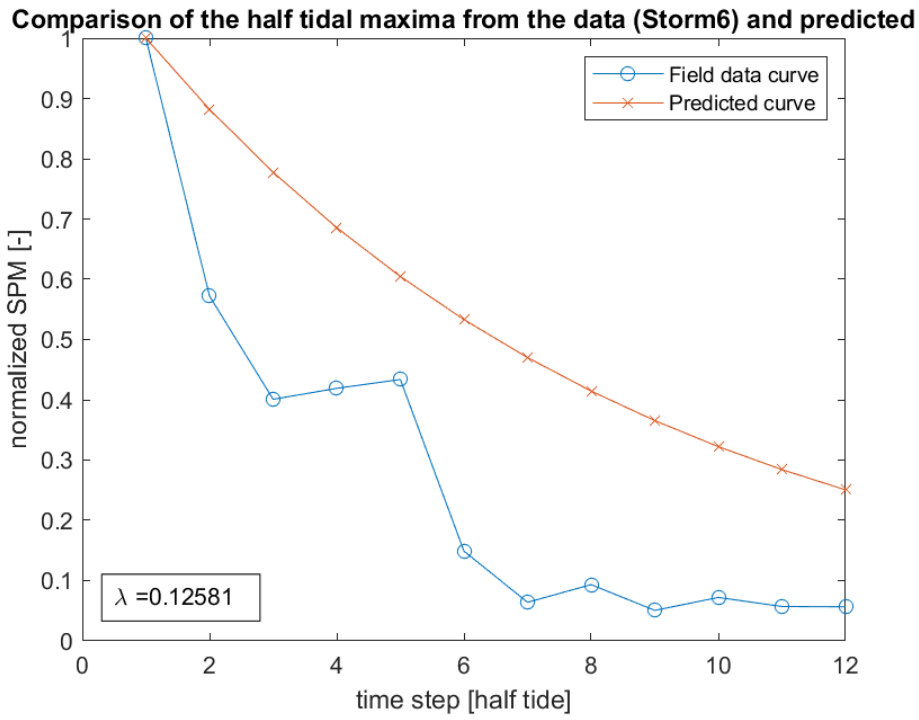

Figure 67: Predicted decay curve calculated with λ as shown in the figure, and data decay points. Each point represents the maximum SPM per tide (ebb/flood) normalized by the SPM peak due to the storm

STORM 7

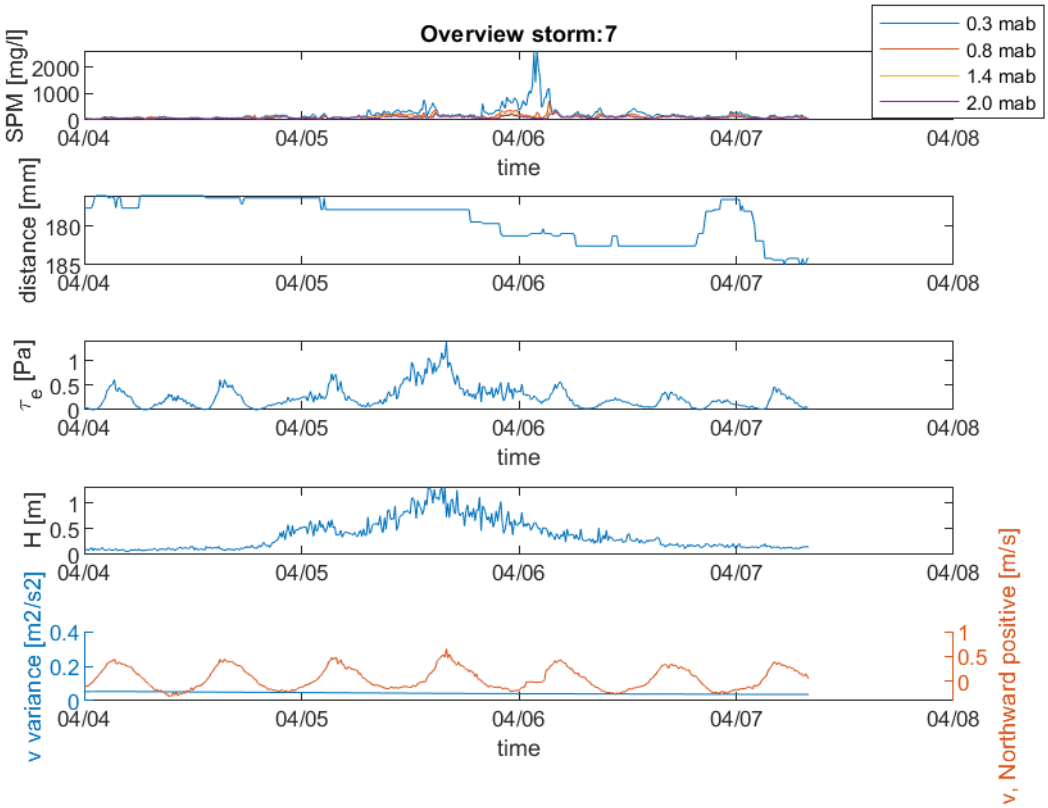

Figure 68: Storm overview. From top to bottom: suspended sediment concentration, distance to bed, shear stress, median wave height, near bed velocity, and velocity variance

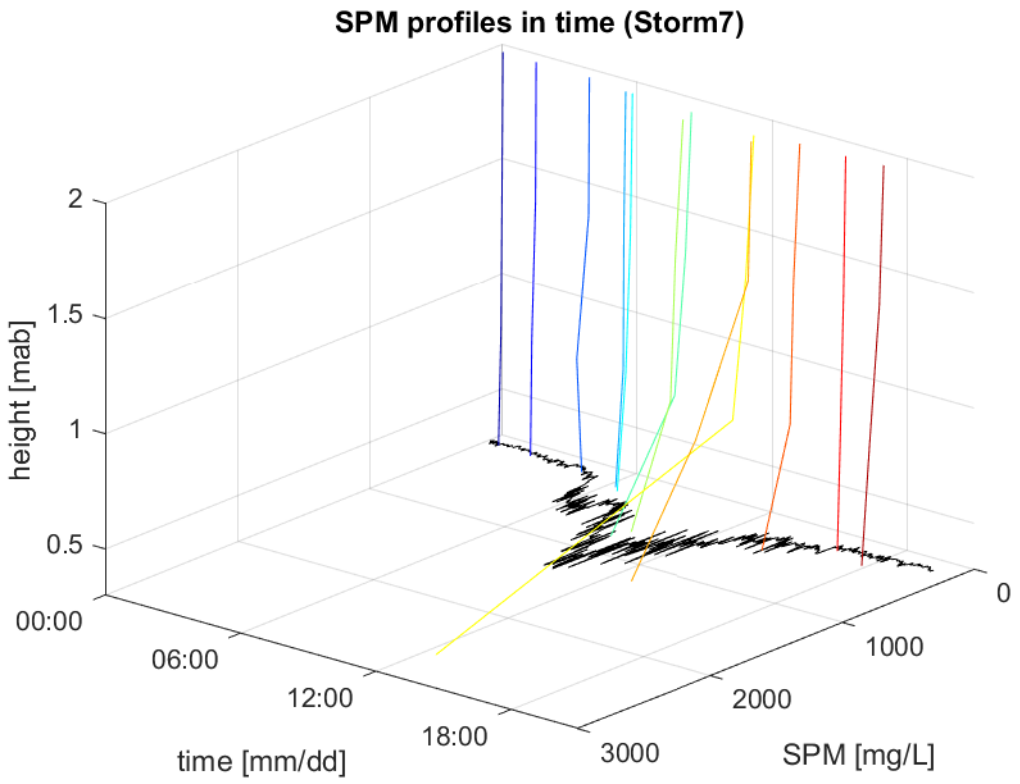

Figure 69: Sediment concentration profiles from the peak of each tide (ebb/flood) in rainbow, and the wave height scaled by 1000 in black

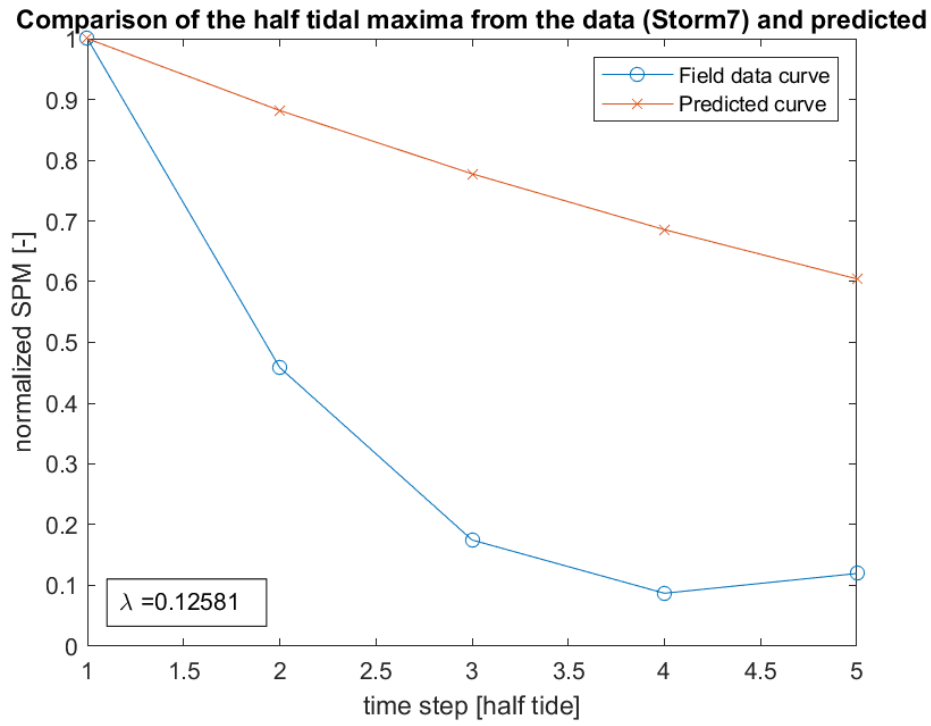

Figure 70: Predicted decay curve calculated with λ as shown in the figure, and data decay points. Each point represents the maximum SPM per tide (ebb/flood) normalized by the SPM peak due to the storm

STORM 8

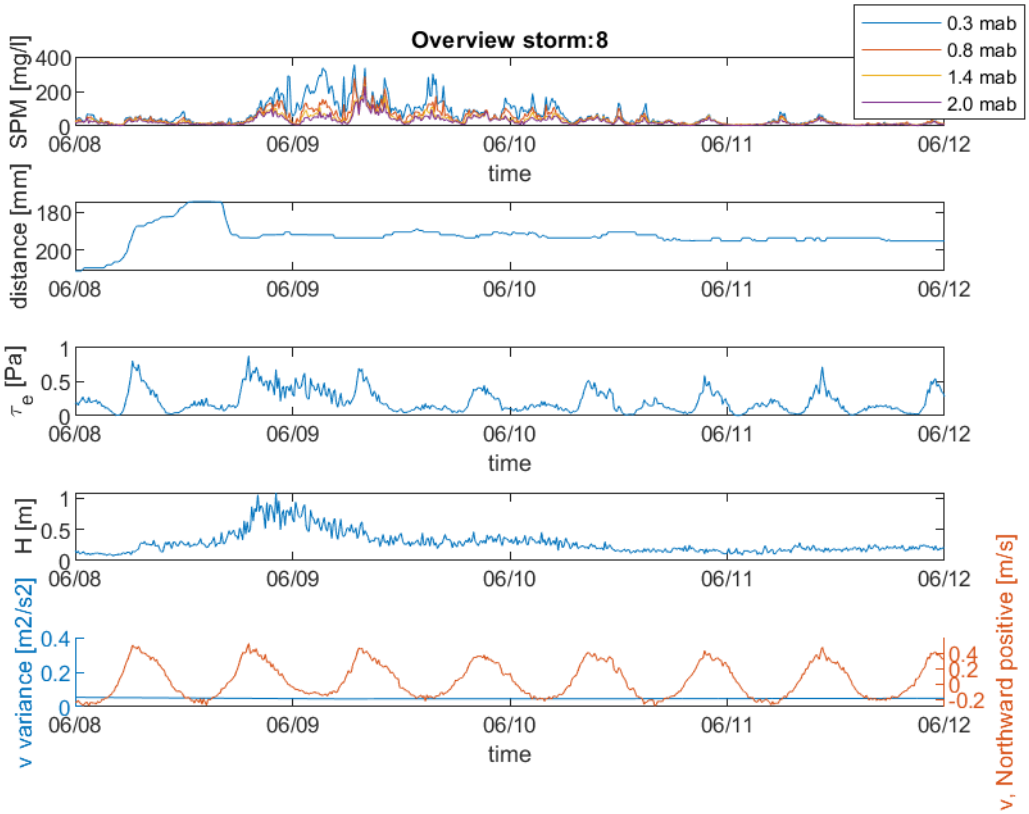

Figure 71: Storm overview. From top to bottom: suspended sediment concentration, distance to bed, shear stress, median wave height, near bed velocity, and velocity variance

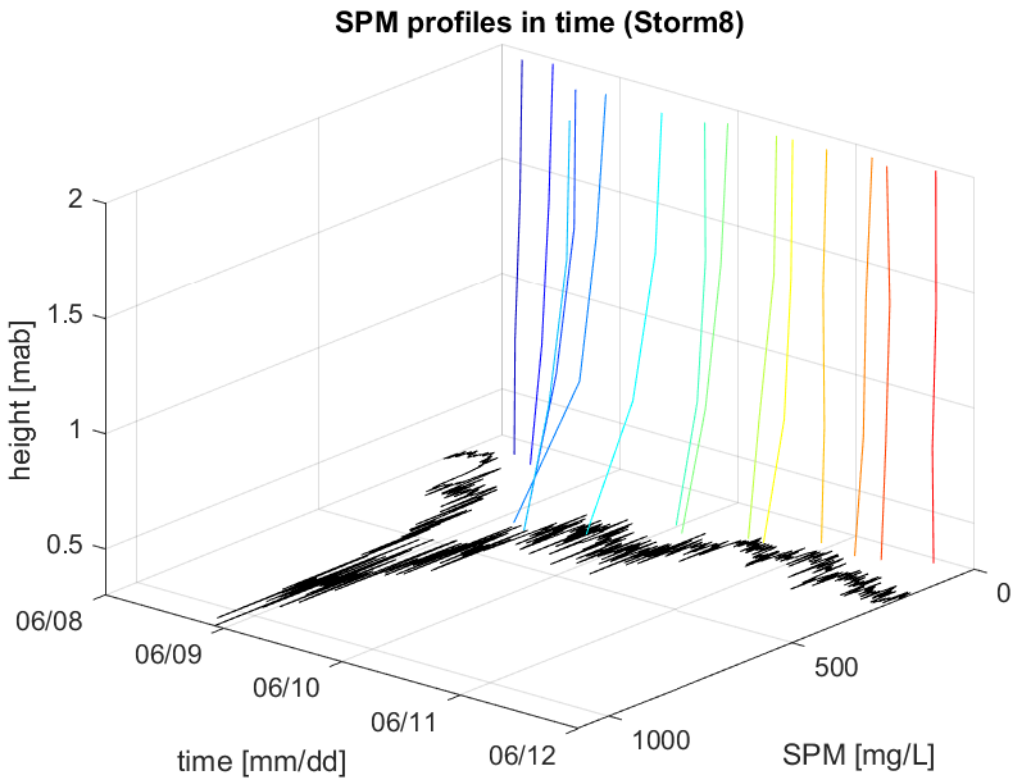

Figure 72: Sediment concentration profiles from the peak of each tide (ebb/flood) in rainbow, and the wave height scaled by 1000 in black

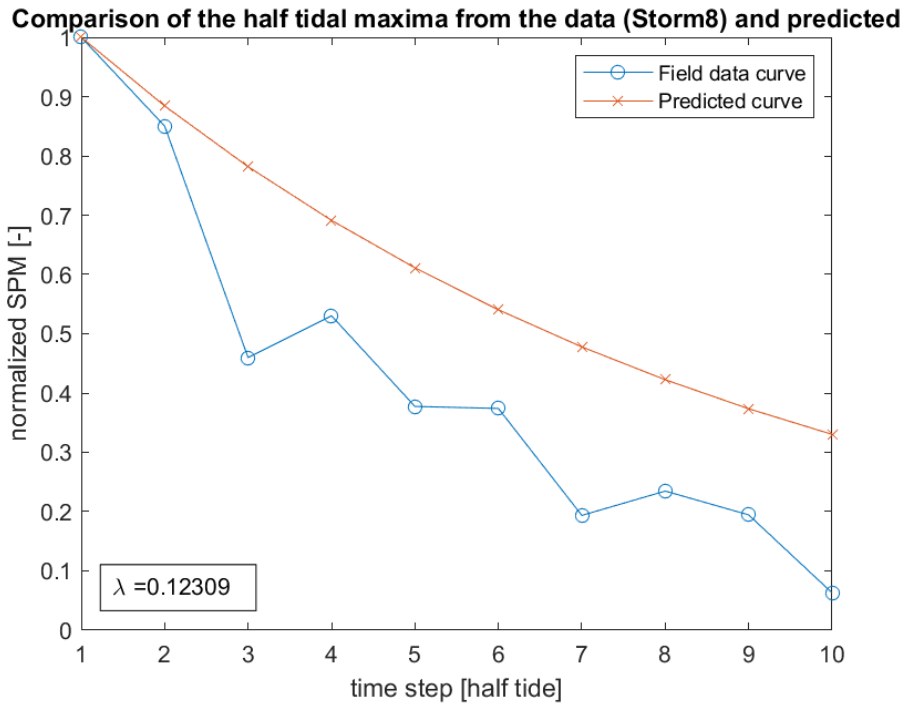

Figure 73: Predicted decay curve calculated with λ as shown in the figure, and data decay points. Each point represents the maximum SPM per tide (ebb/flood) normalized by the SPM peak due to the storm

STORM 9

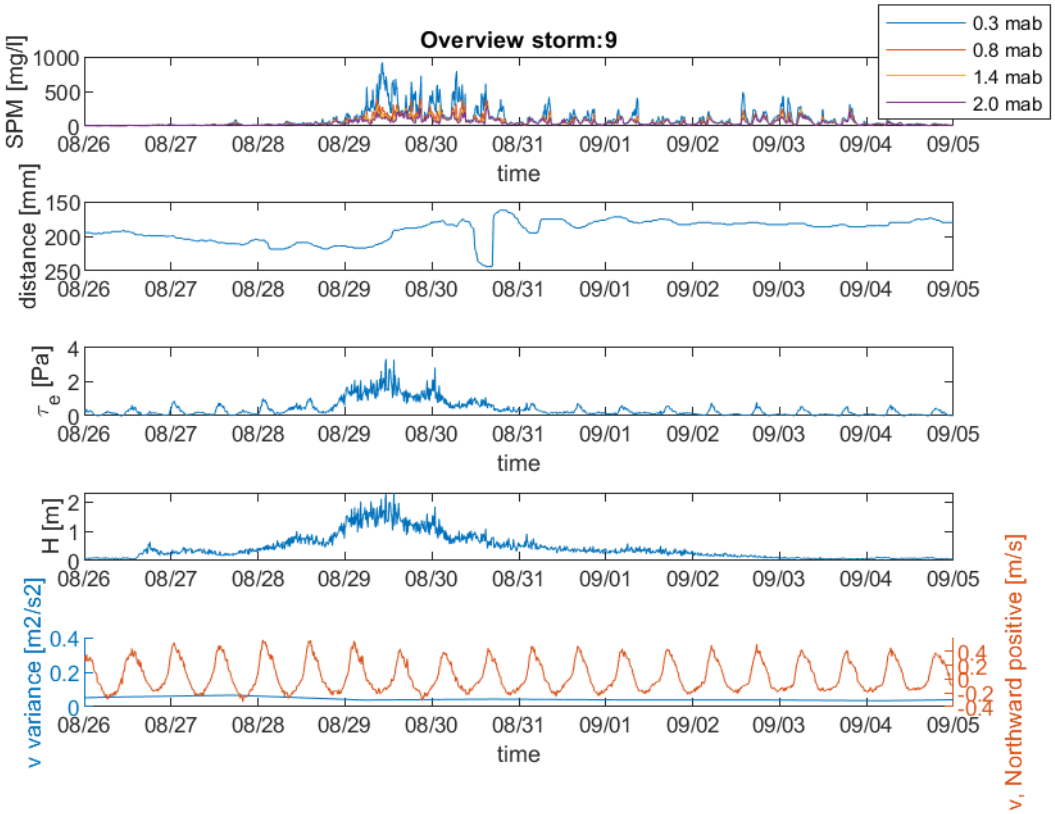

Figure 74: Storm overview. From top to bottom: suspended sediment concentration, distance to bed, shear stress, median wave height, near bed velocity, and velocity variance

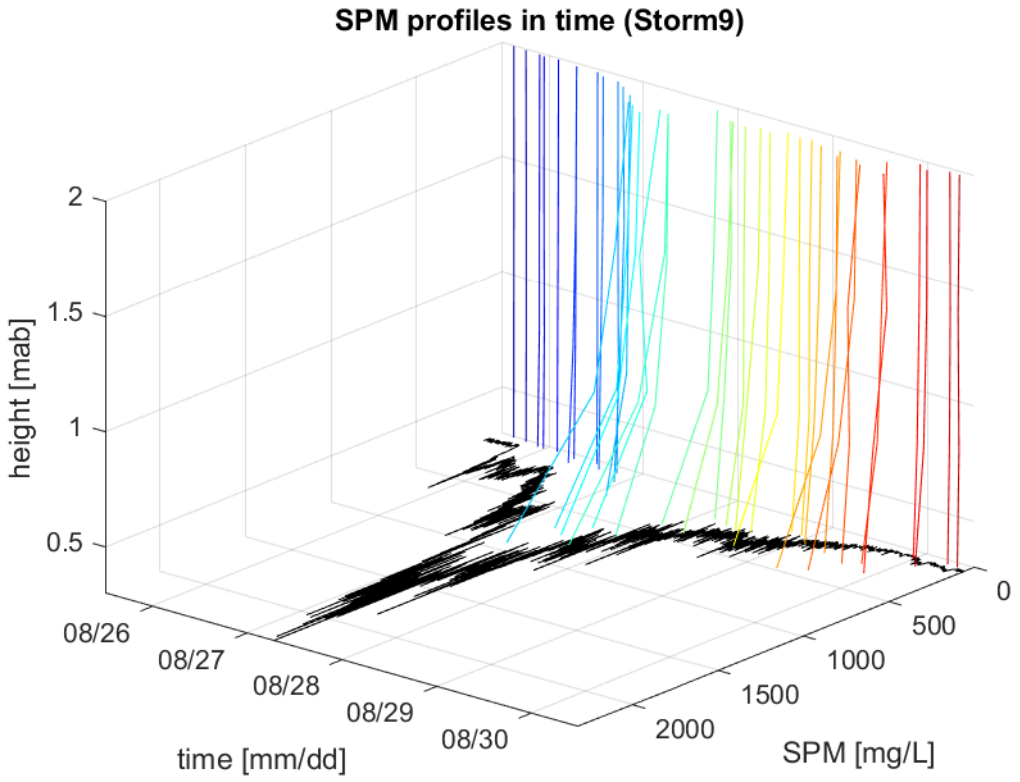

Figure 75: Sediment concentration profiles from the peak of each tide (ebb/flood) in rainbow, and the wave height scaled by 1000 in black

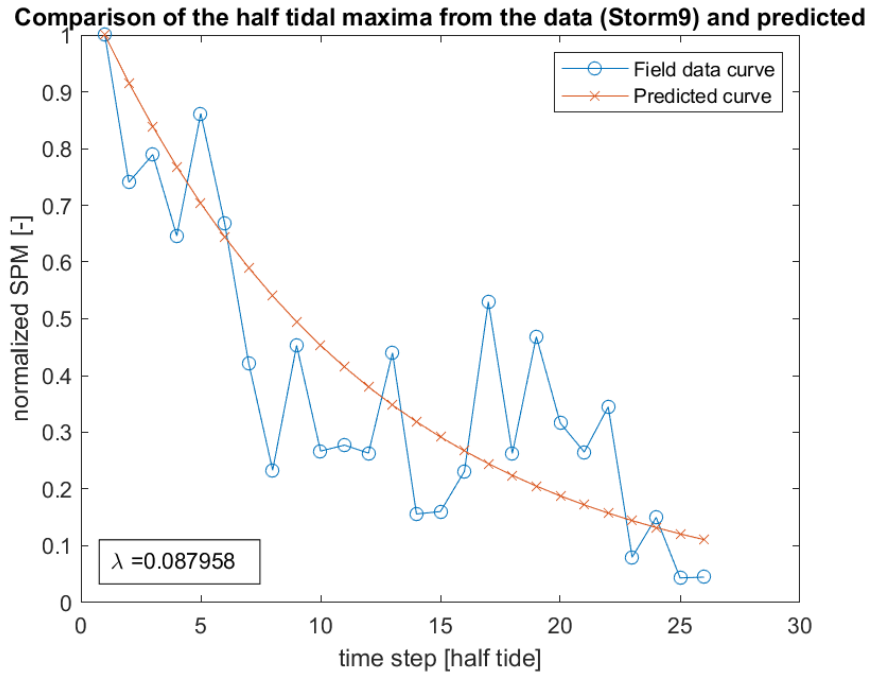

Figure 76: Predicted decay curve calculated with λ as shown in the figure, and data decay points. Each point represents the maximum SPM per tide (ebb/flood) normalized by the SPM peak due to the storm

STORM 10

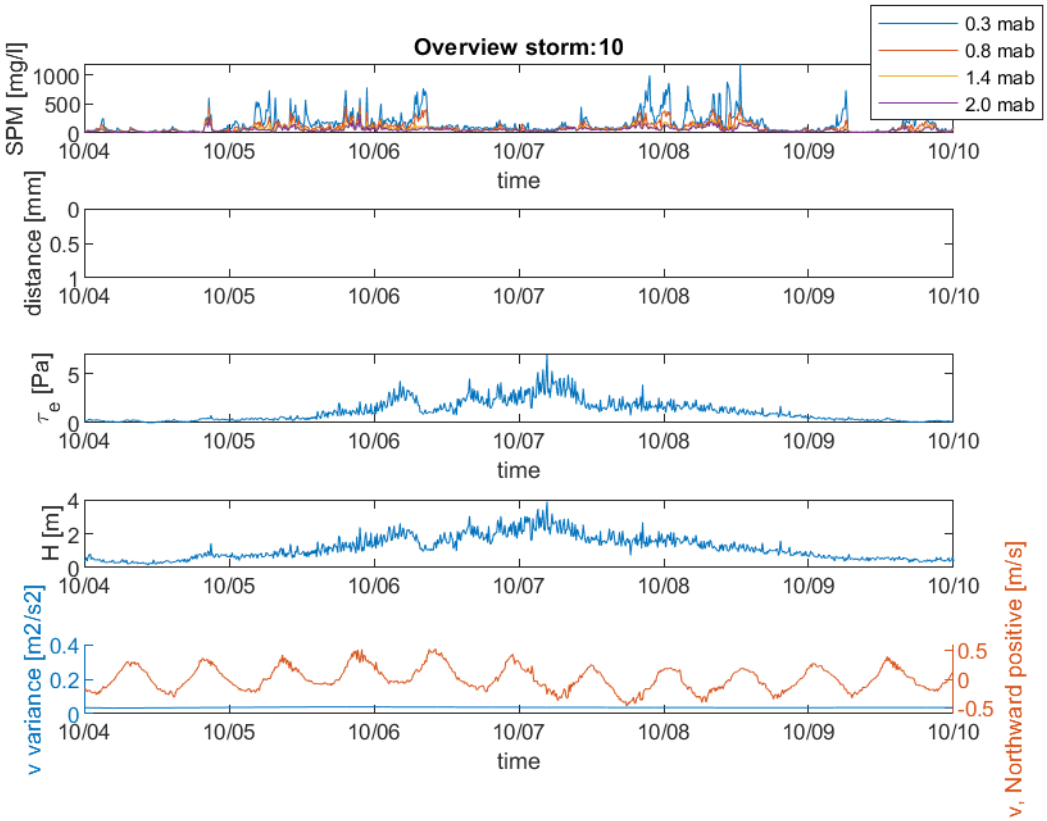

Figure 77: Storm overview. From top to bottom: suspended sediment concentration, distance to bed, shear stress, median wave height, near bed velocity, and velocity variance

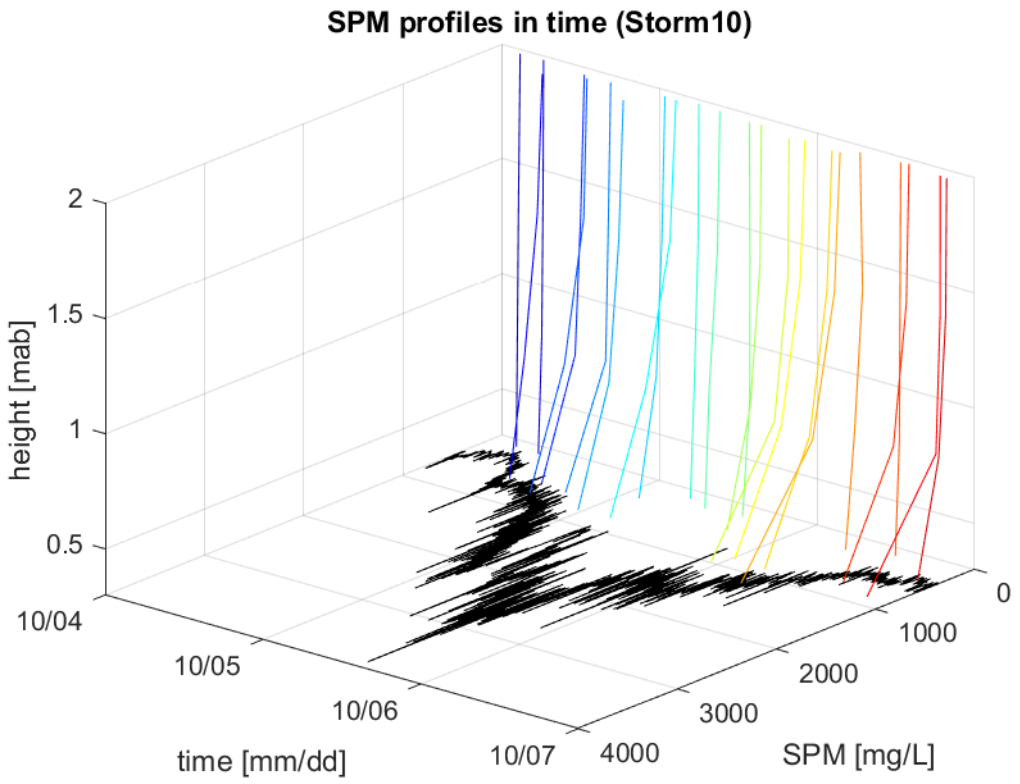

Figure 78: Sediment concentration profiles from the peak of each tide (ebb/flood) in rainbow, and the wave height scaled by 1000 in black

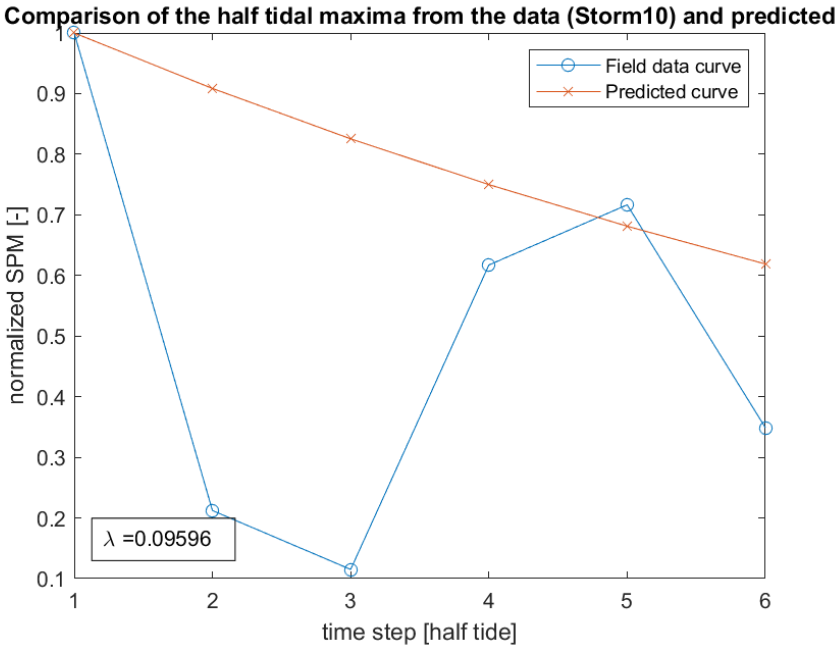

Figure 79: Predicted decay curve calculated with λ as shown in the figure, and data decay points. Each point represents the maximum SPM per tide (ebb/flood) normalized by the SPM peak due to the storm

STORM 11

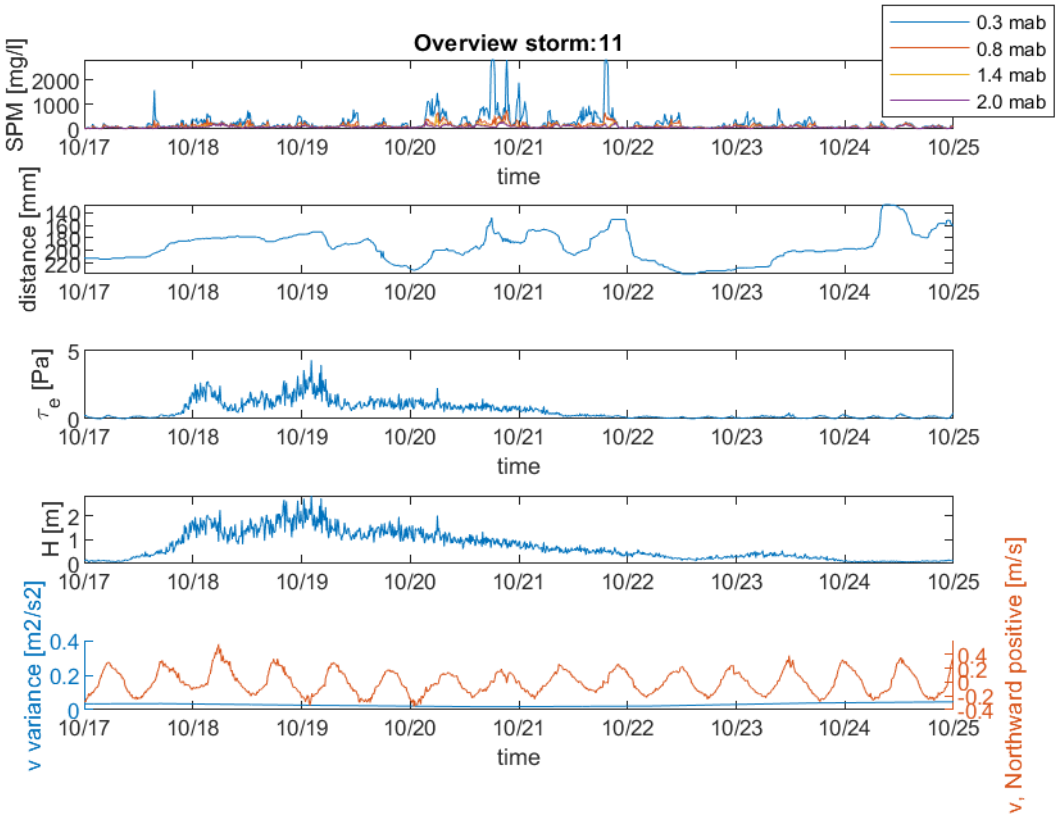

Figure 80: Storm overview. From top to bottom: suspended sediment concentration, distance to bed, shear stress, median wave height, near bed velocity, and velocity variance

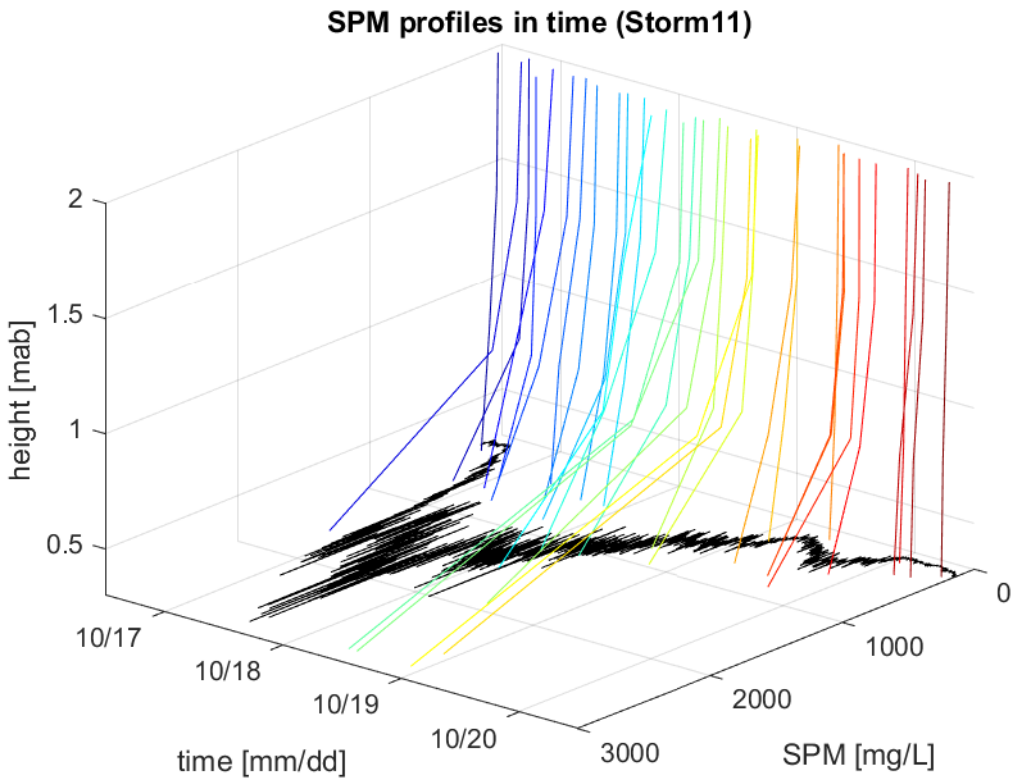

Figure 81: Sediment concentration profiles from the peak of each tide (ebb/flood) in rainbow, and the wave height scaled by 1000 in black

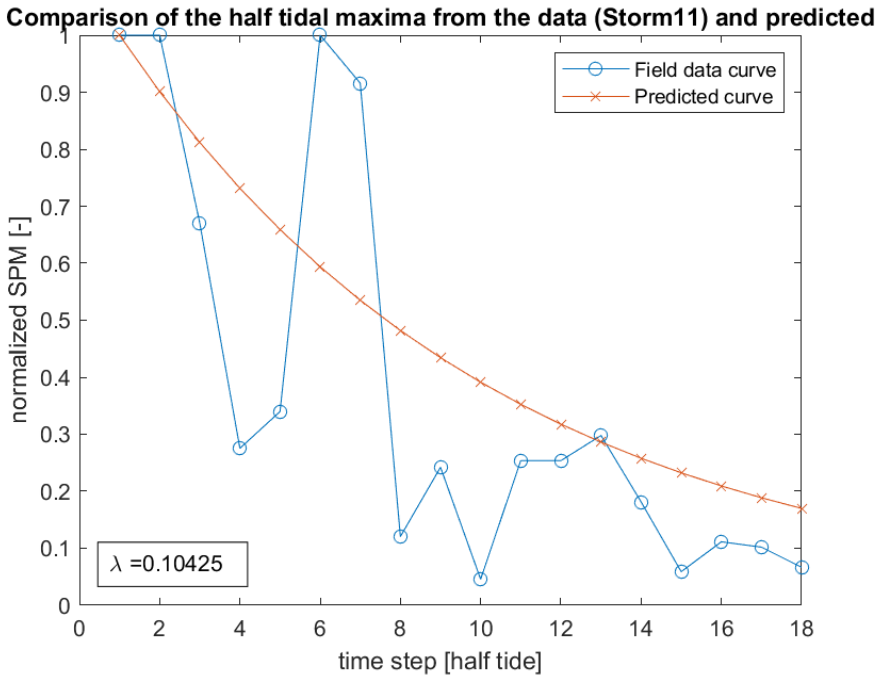

Figure 82: Predicted decay curve calculated with λ as shown in the figure, and data decay points. Each point represents the maximum SPM per tide (ebb/flood) normalized by the SPM peak due to the storm

STORM 12

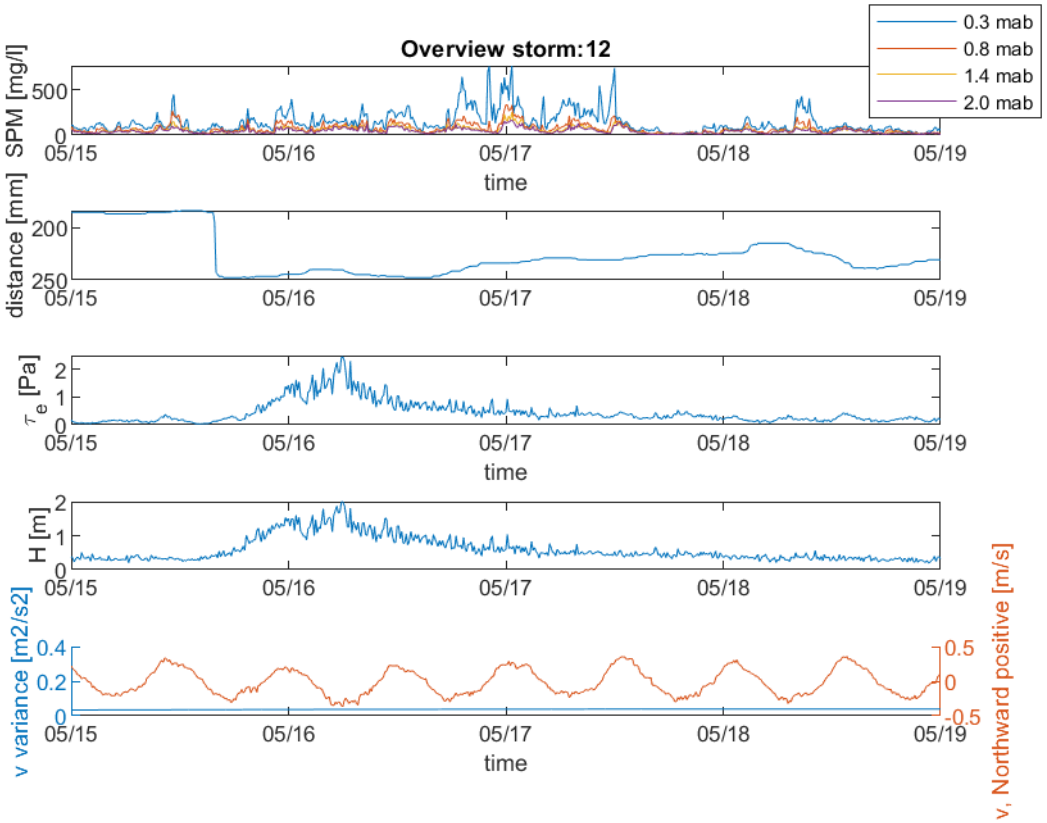

Figure 83: Storm overview. From top to bottom: suspended sediment concentration, distance to bed, shear stress, median wave height, near bed velocity, and velocity variance

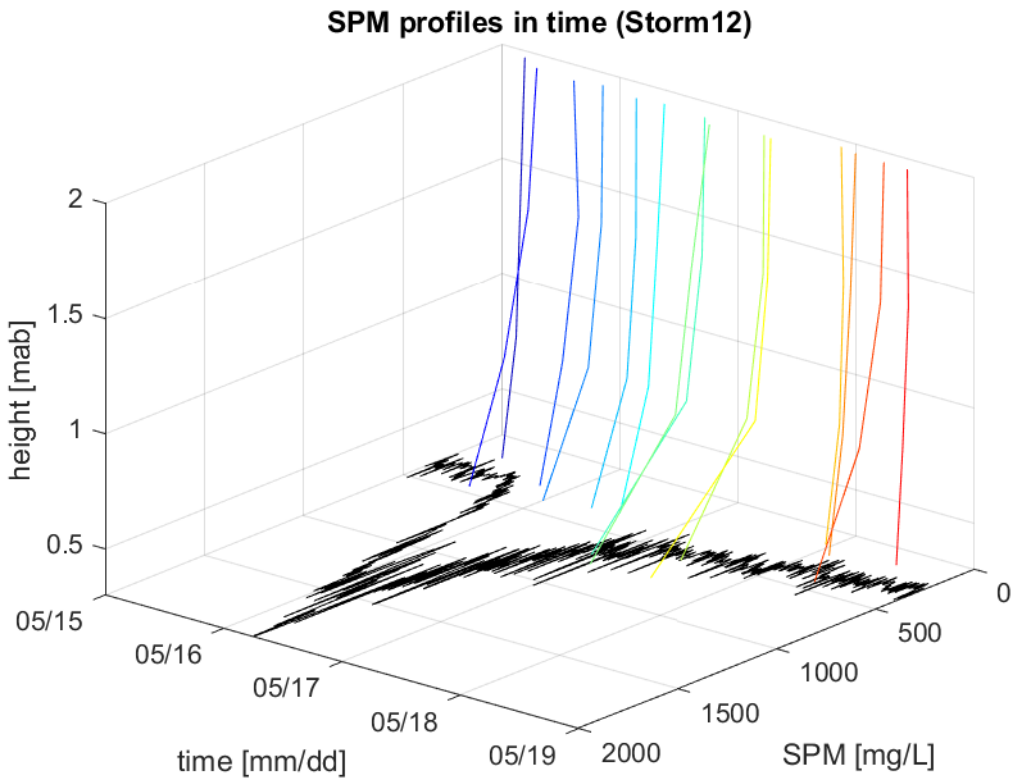

Figure 84: Sediment concentration profiles from the peak of each tide (ebb/flood) in rainbow, and the wave height scaled by 1000 in black

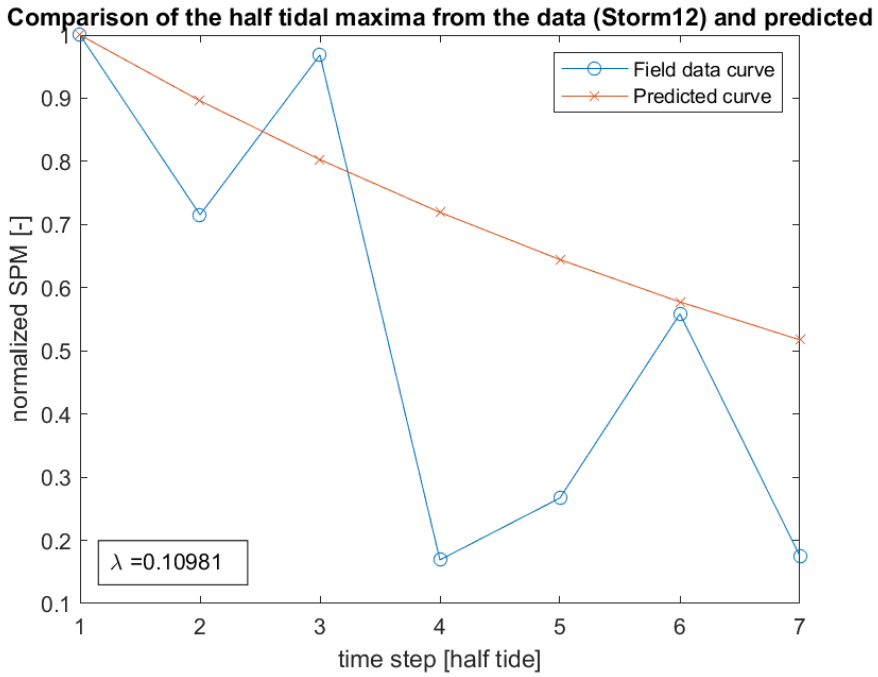

Figure 85: Predicted decay curve calculated with λ as shown in the figure, and data decay points. Each point represents the maximum SPM per tide (ebb/flood) normalized by the SPM peak due to the storm

STORM 13

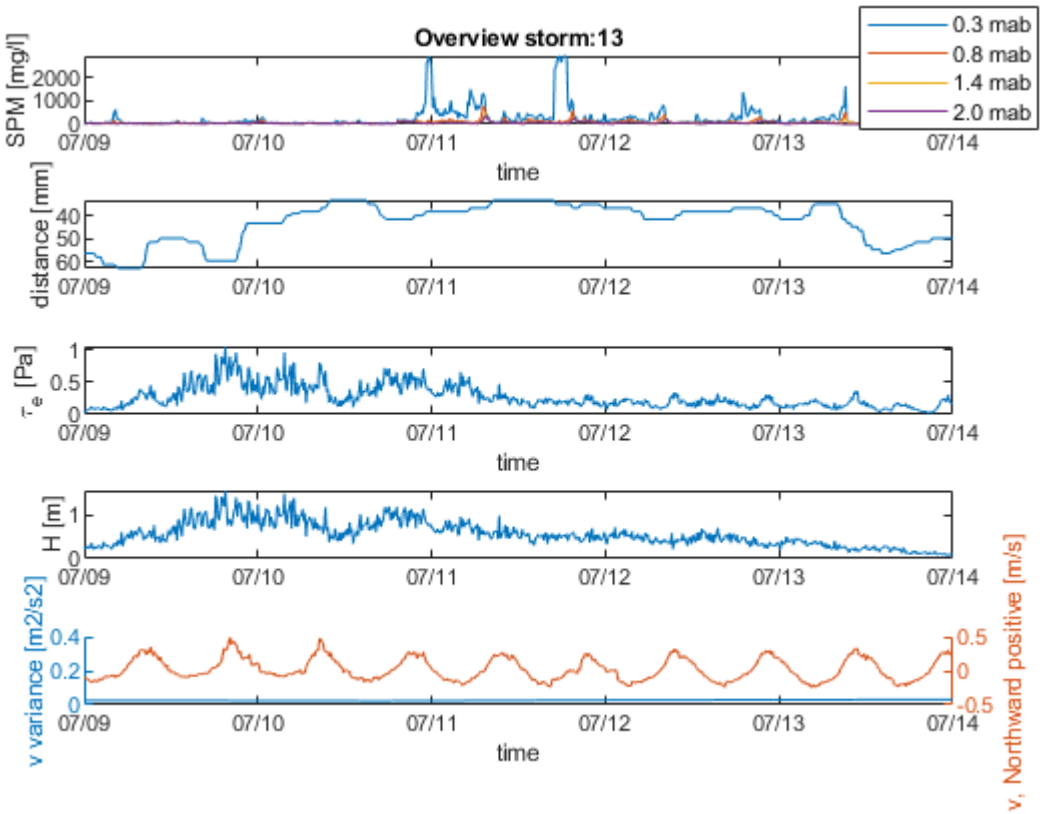

Figure 86: Storm overview. From top to bottom: suspended sediment concentration, distance to bed, shear stress, median wave height, near bed velocity, and velocity variance

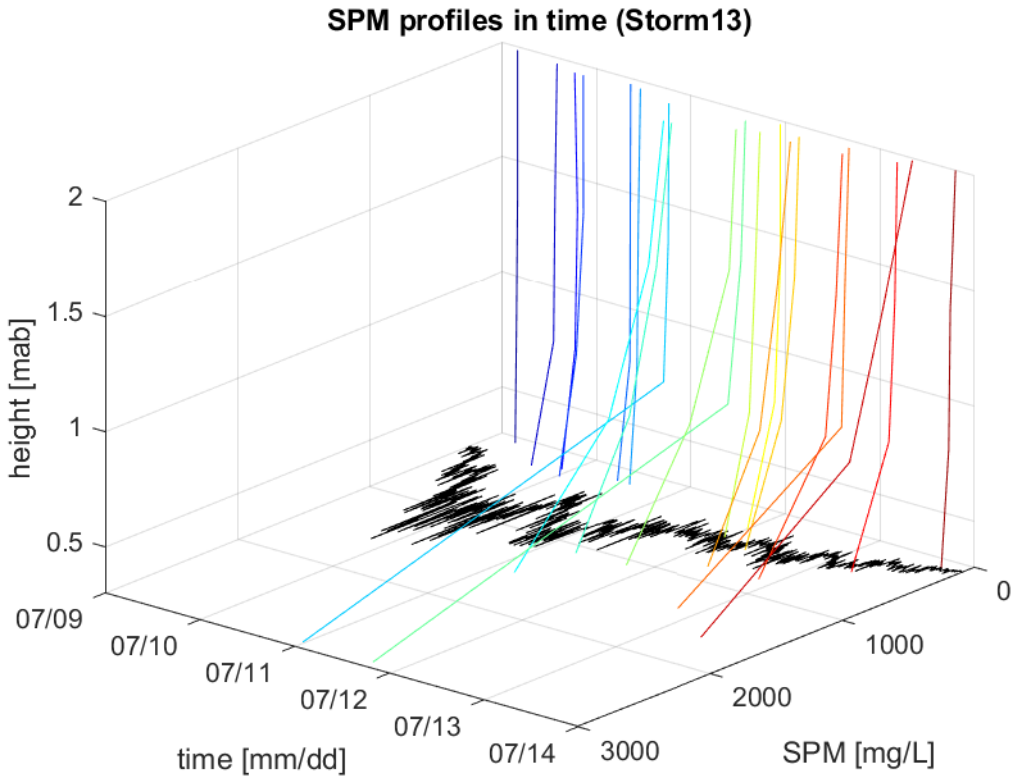

Figure 87: Sediment concentration profiles from the peak of each tide (ebb/flood) in rainbow, and the wave height scaled by 1000 in black

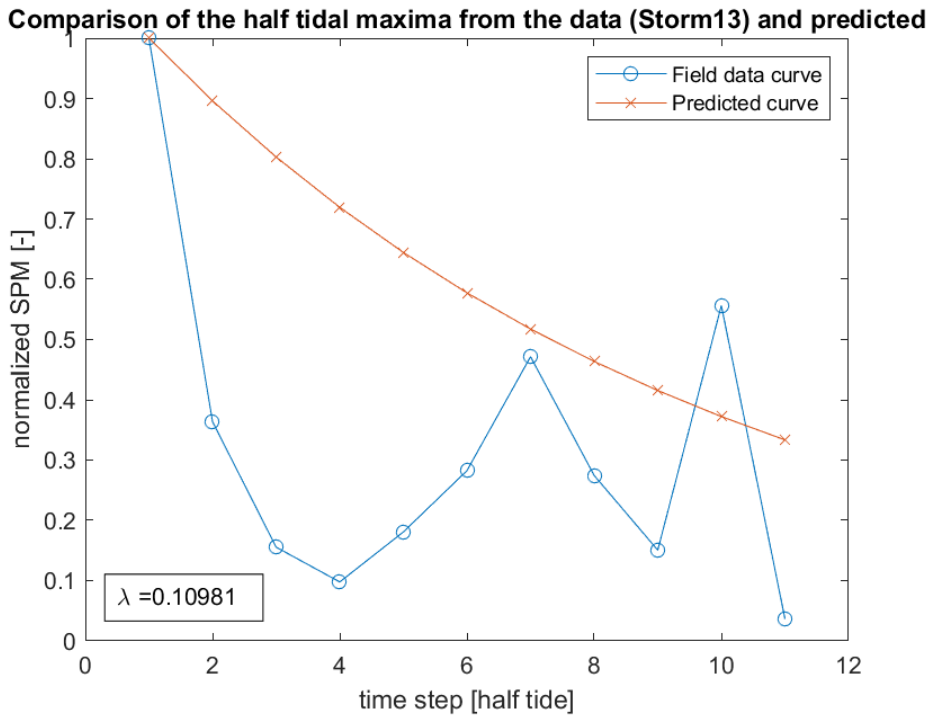

Figure 88: Predicted decay curve calculated with λ as shown in the figure, and data decay points. Each point represents the maximum SPM per tide (ebb/flood) normalized by the SPM peak due to the storm

APPENDIX C: MODEL STORMS

MODEL STORM 1

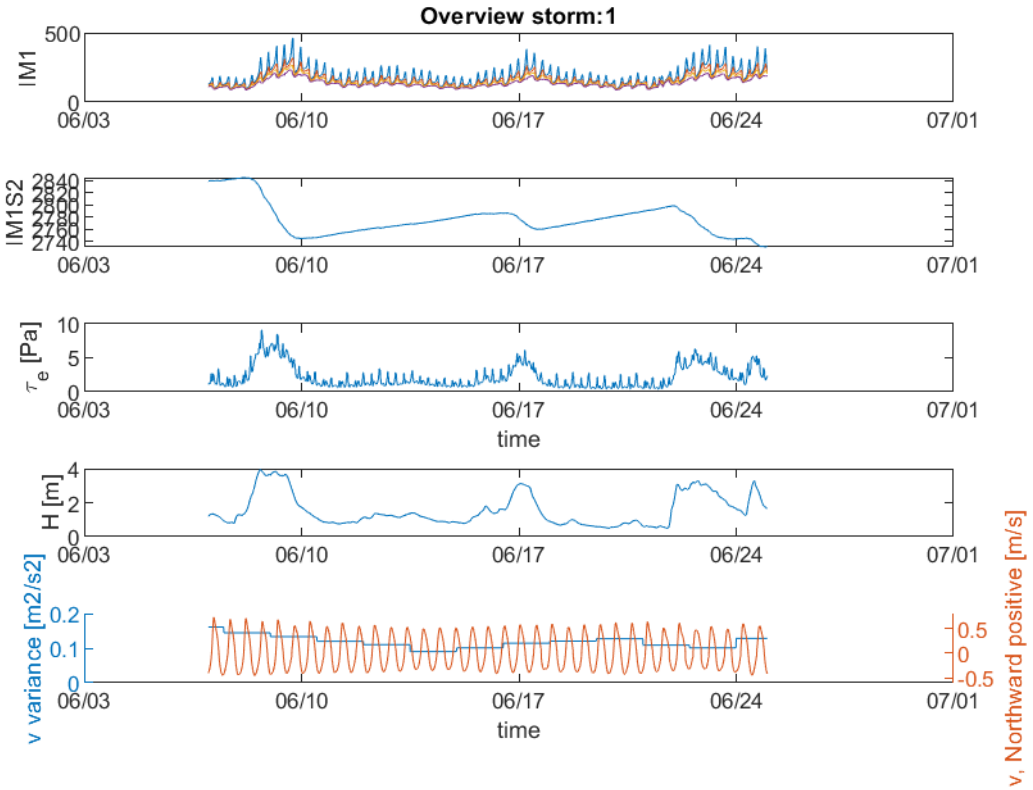

Figure 89: Storm overview from the North Sea model. These time series have a week added to either side, so are 2 weeks longer than the field data storms. From top to bottom: suspended sediment concentration, concentration in the 0.3 m thick buffer layer, shear stress, median wave height, near bed velocity and velocity variance

MODEL STORM 2

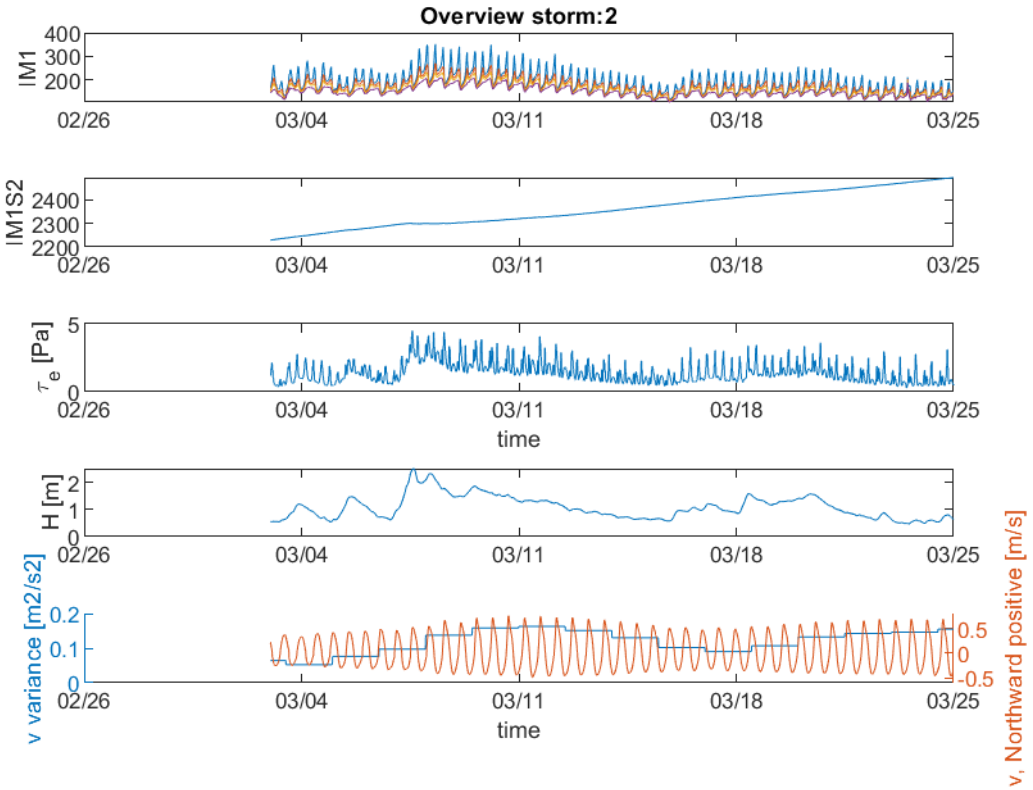

Figure 90: Storm overview from the North Sea model. These time series have a week added to either side, so are 2 weeks longer than the field data storms. From top to bottom: suspended sediment concentration, concentration in the 0.3 m thick buffer layer, shear stress, median wave height, near bed velocity and velocity variance

MODEL STORM 3

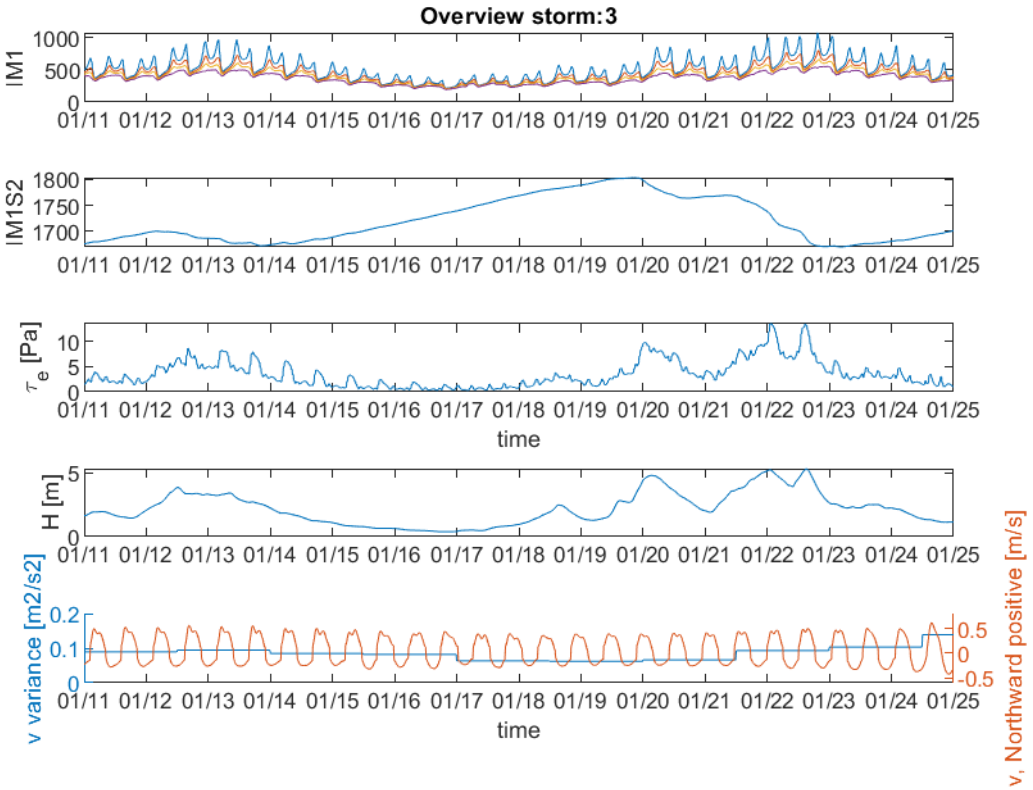

Figure 91: Storm overview from the North Sea model. These time series have a week added to either side, so are 2 weeks longer than the field data storms. From top to bottom: suspended sediment concentration, concentration in the 0.3 m thick buffer layer, shear stress, median wave height, near bed velocity and velocity variance

MODEL STORM 4

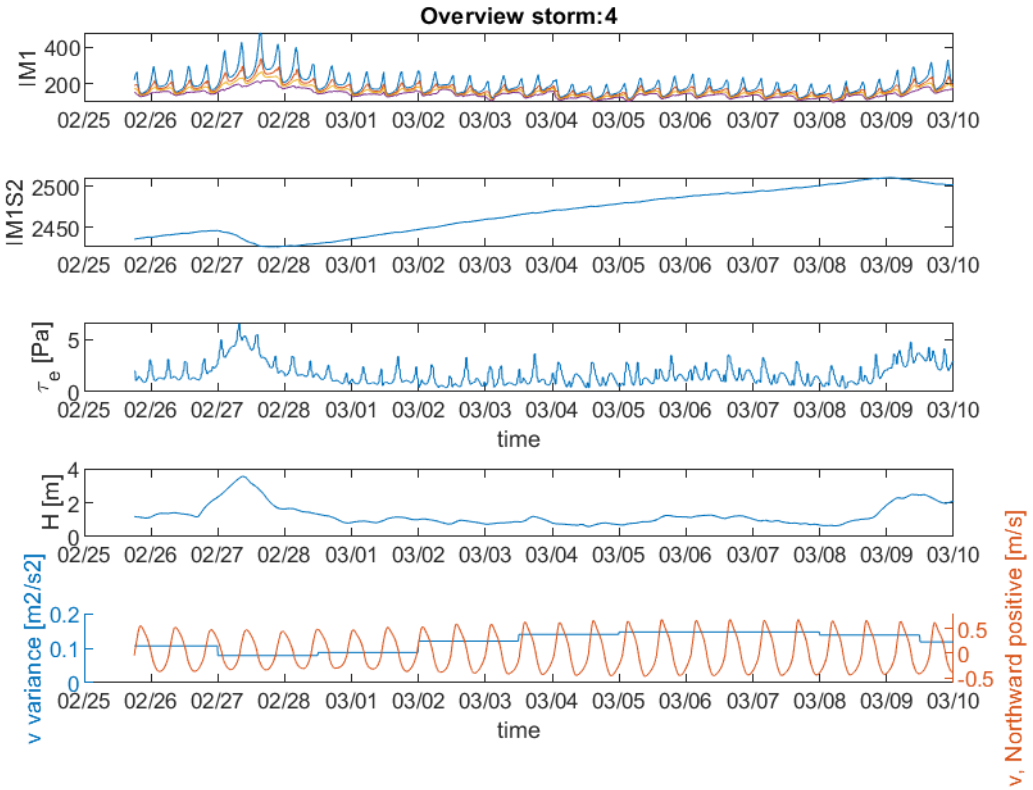

Figure 92: Storm overview from the North Sea model. These time series have a week added to either side, so are 2 weeks longer than the field data storms. From top to bottom: suspended sediment concentration, concentration in the 0.3 m thick buffer layer, shear stress, median wave height, near bed velocity and velocity variance

MODEL STORM 5

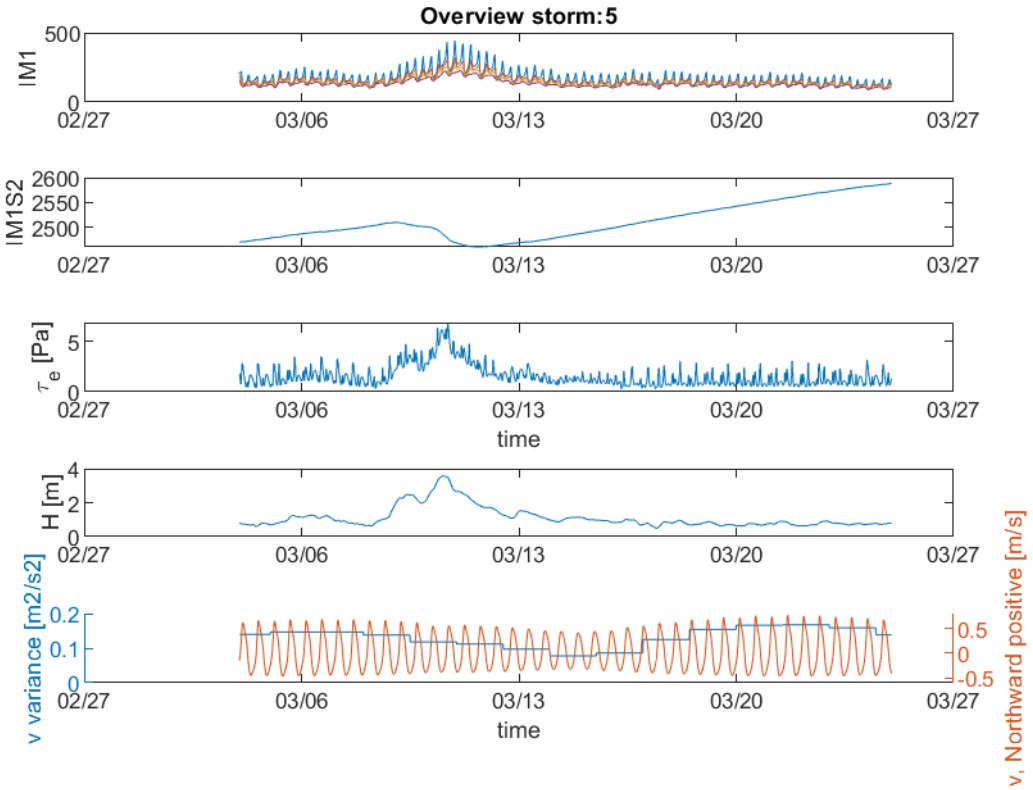

Figure 93: Storm overview from the North Sea model. These time series have a week added to either side, so are 2 weeks longer than the field data storms. From top to bottom: suspended sediment concentration, concentration in the 0.3 m thick buffer layer, shear stress, median wave height, near bed velocity and velocity variance

MODEL STORM 6

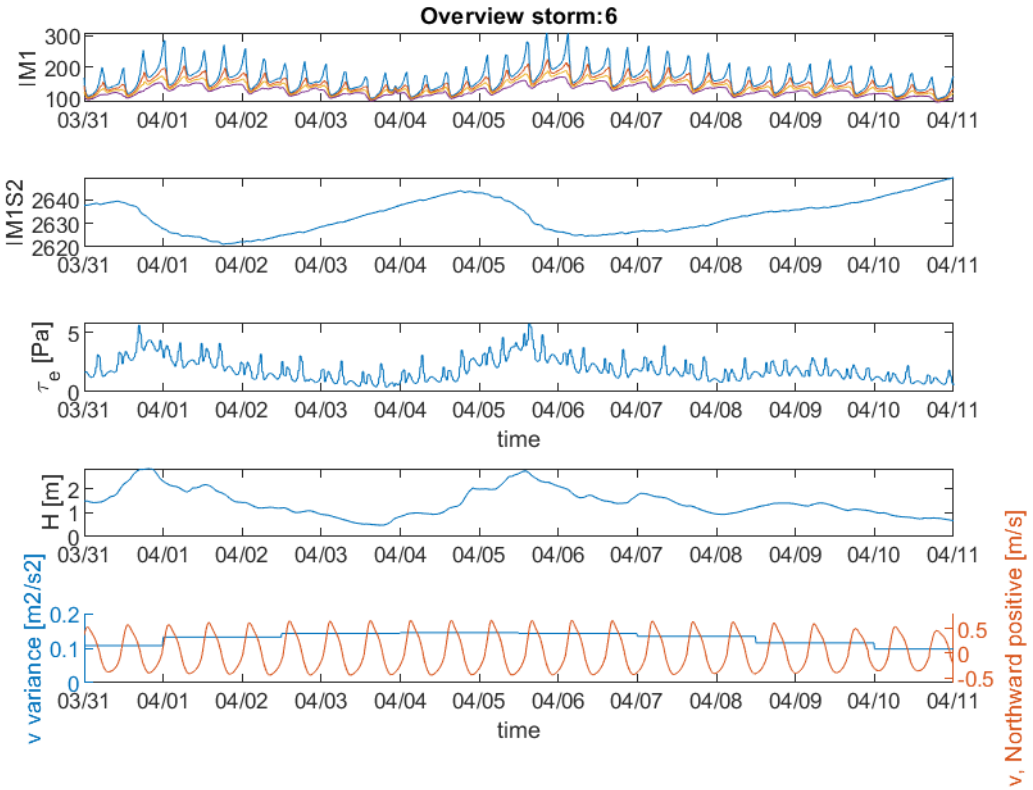

Figure 94: Storm overview from the North Sea model. These time series have a week added to either side, so are 2 weeks longer than the field data storms. From top to bottom: suspended sediment concentration, concentration in the 0.3 m thick buffer layer, shear stress, median wave height, near bed velocity and velocity variance

MODEL STORM 7

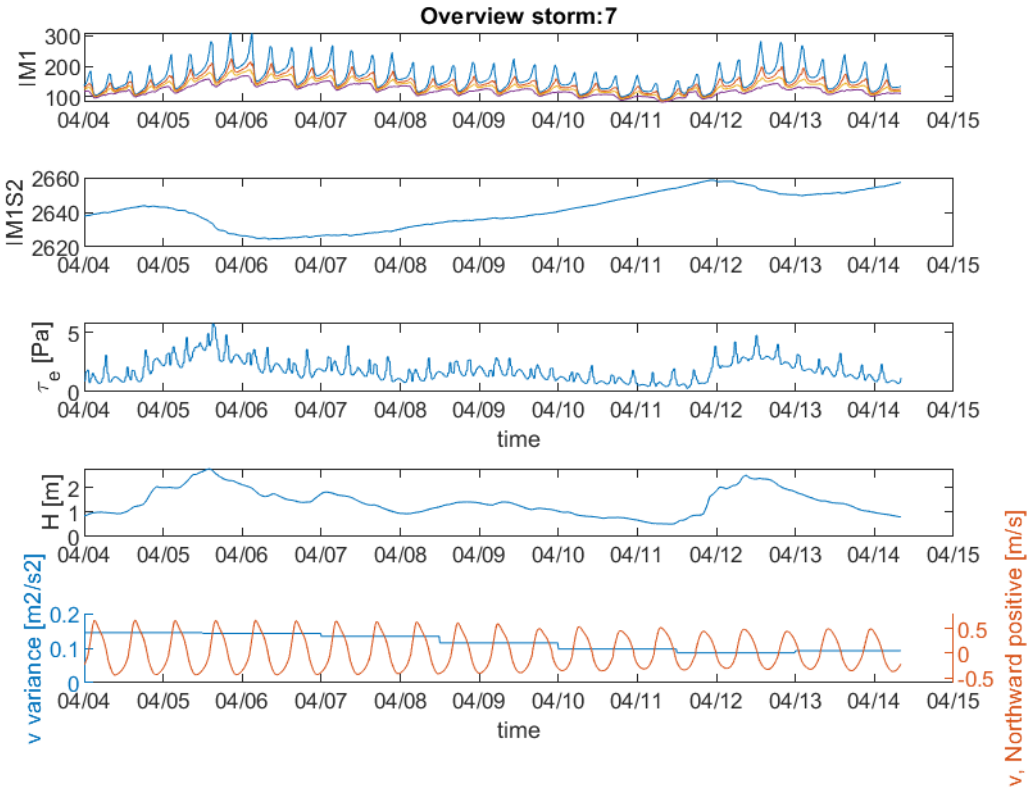

Figure 95: Storm overview from the North Sea model. These time series have a week added to either side, so are 2 weeks longer than the field data storms. From top to bottom: suspended sediment concentration, concentration in the 0.3 m thick buffer layer, shear stress, median wave height, near bed velocity and velocity variance

MODEL STORM 8

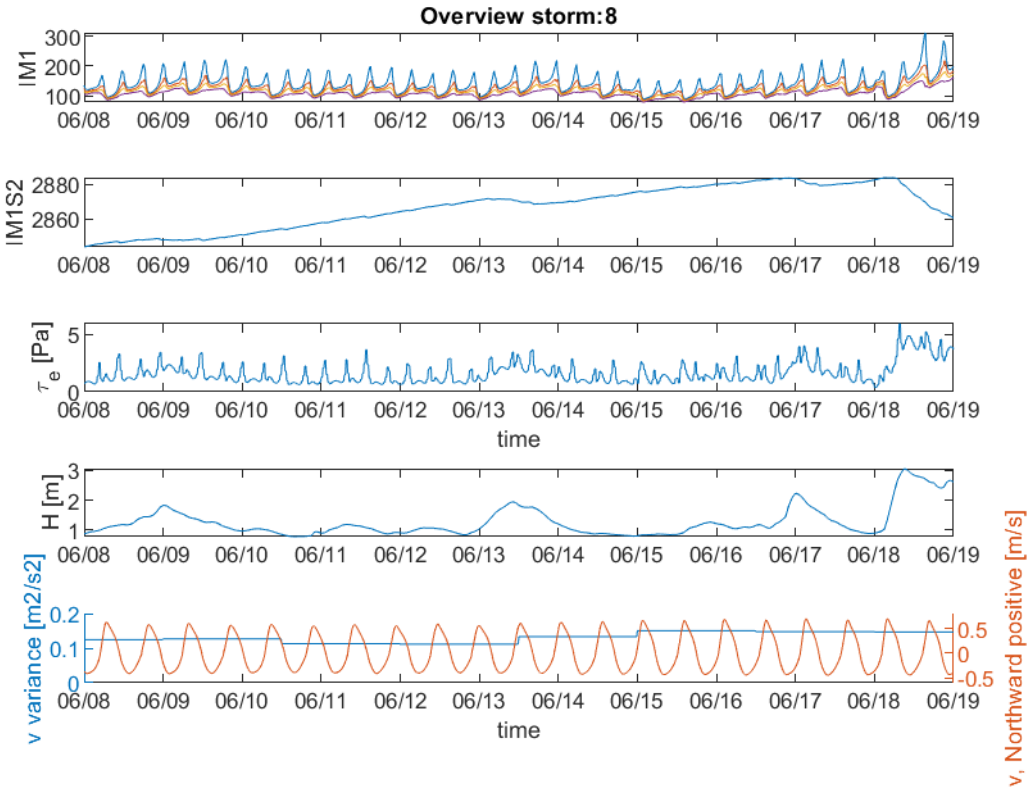

Figure 96: Storm overview from the North Sea model. These time series have a week added to either side, so are 2 weeks longer than the field data storms. From top to bottom: suspended sediment concentration, concentration in the 0.3 m thick buffer layer, shear stress, median wave height, near bed velocity and velocity variance

MODEL STORM 9

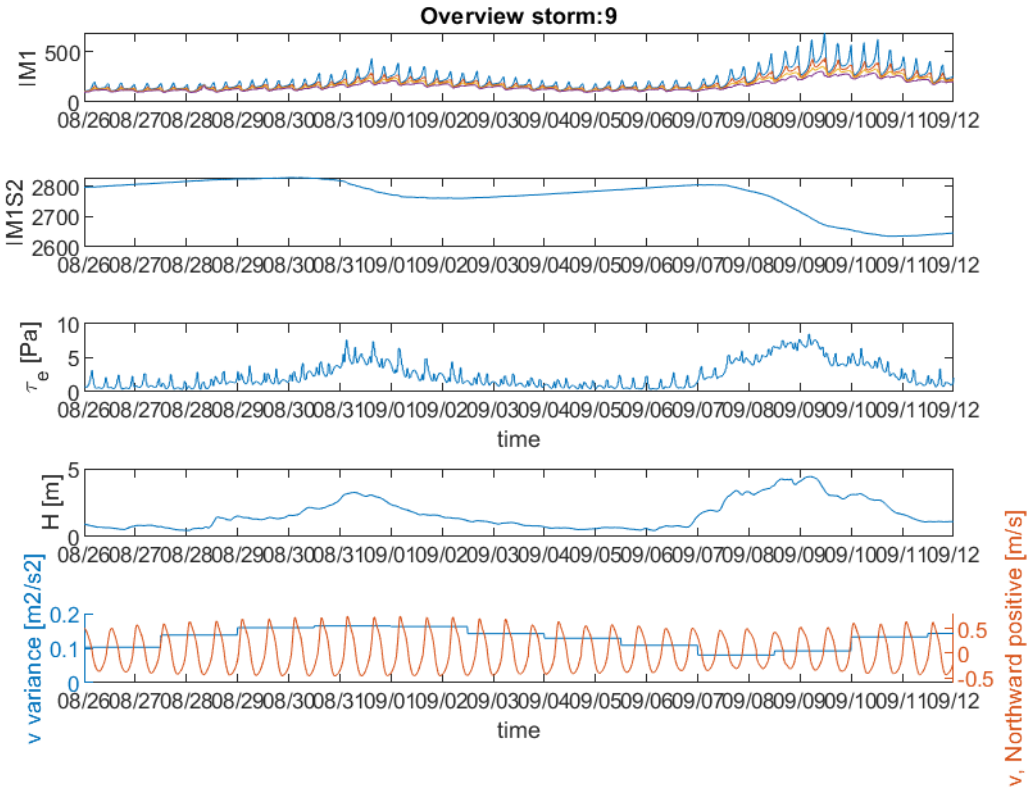

Figure 97: Storm overview from the North Sea model. These time series have a week added to either side, so are 2 weeks longer than the field data storms. From top to bottom: suspended sediment concentration, concentration in the 0.3 m thick buffer layer, shear stress, median wave height, near bed velocity and velocity variance

MODEL STORM 10

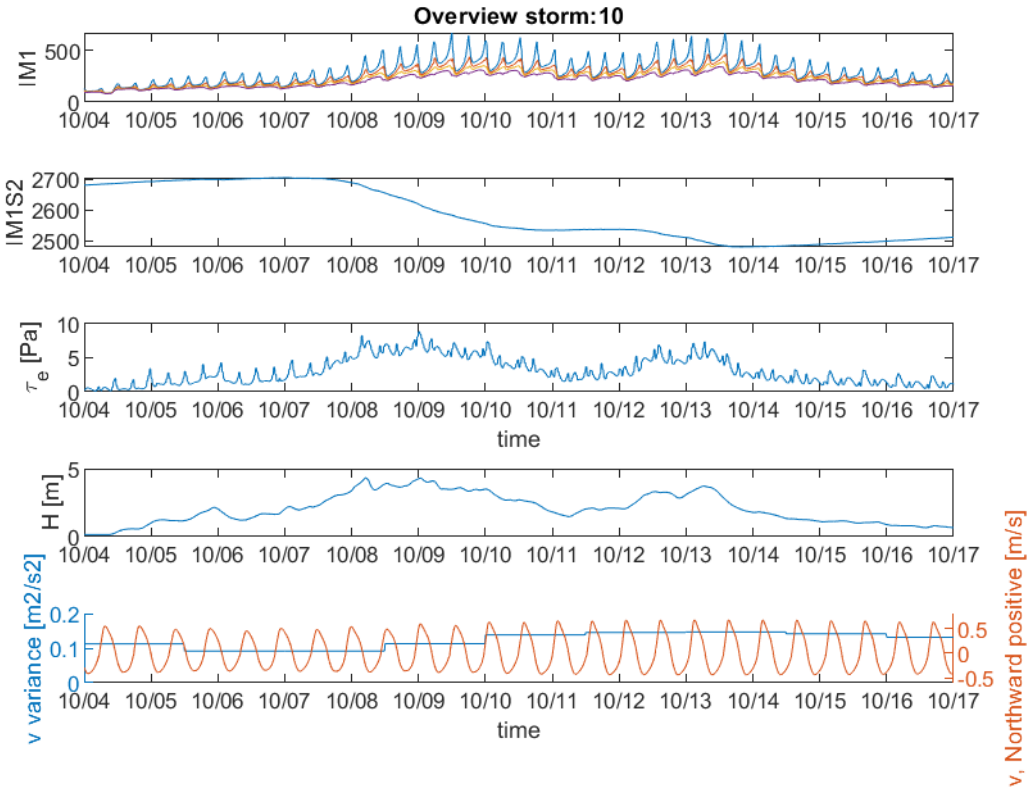

Figure 98: Storm overview from the North Sea model. These time series have a week added to either side, so are 2 weeks longer than the field data storms. From top to bottom: suspended sediment concentration, concentration in the 0.3 m thick buffer layer, shear stress, median wave height, near bed velocity and velocity variance

MODEL STORM 11

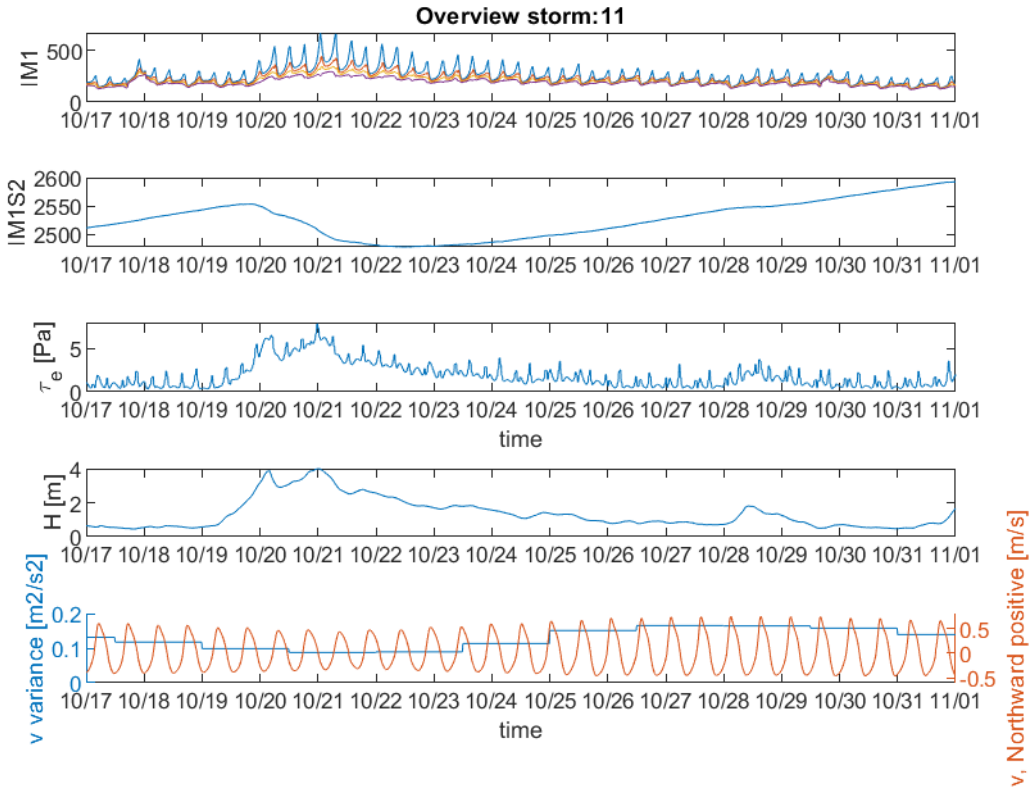

Figure 99: Storm overview from the North Sea model. These time series have a week added to either side, so are 2 weeks longer than the field data storms. From top to bottom: suspended sediment concentration, concentration in the 0.3 m thick buffer layer, shear stress, median wave height, near bed velocity and velocity variance

MODEL STORM 12

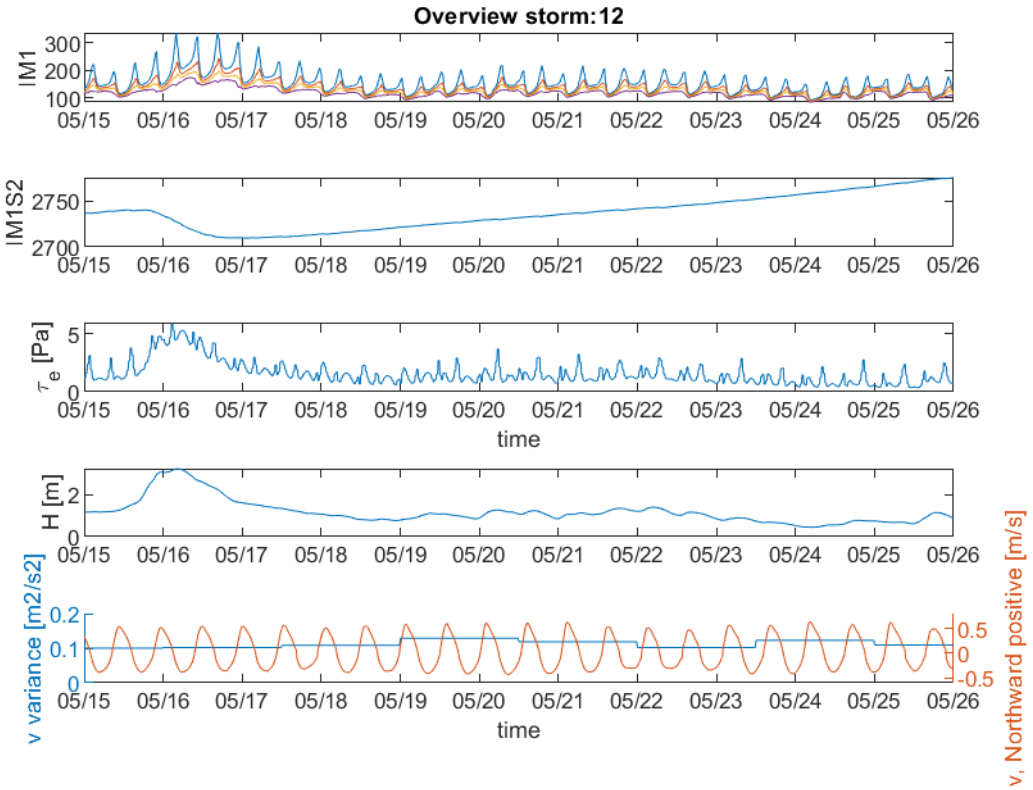

Figure 100: Storm overview from the North Sea model. These time series have a week added to either side, so are 2 weeks longer than the field data storms. From top to bottom: suspended sediment concentration, concentration in the 0.3 m thick buffer layer, shear stress, median wave height, near bed velocity and velocity variance

MODEL STORM 13

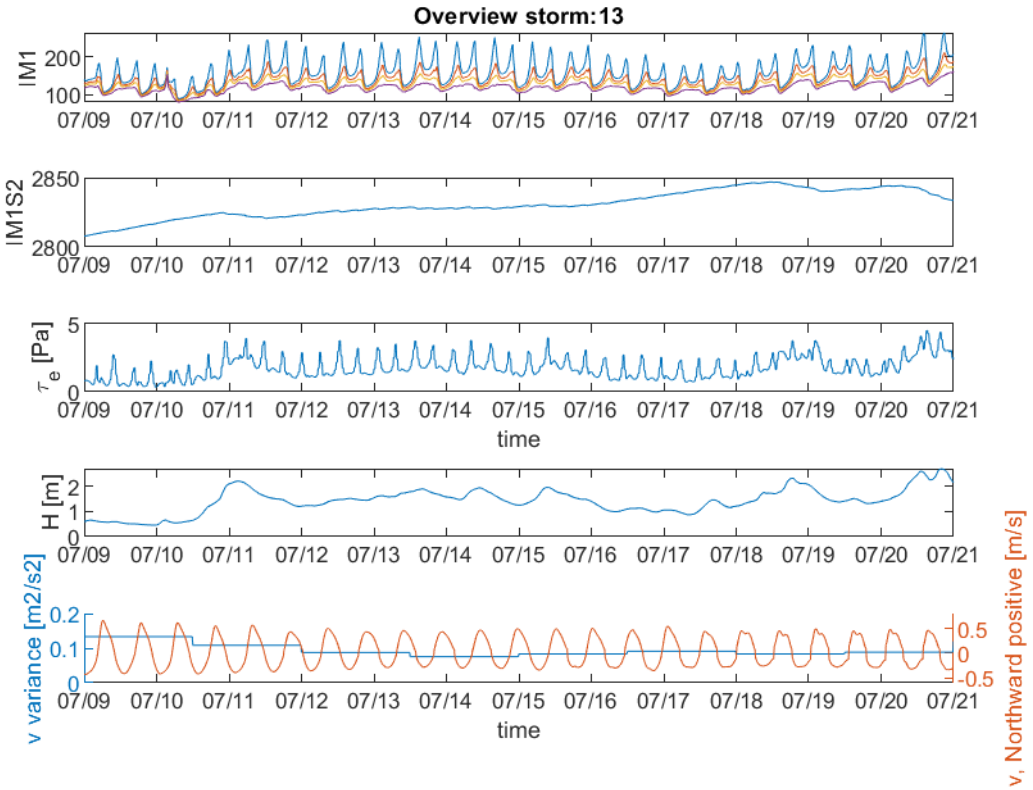

Figure 101: Storm overview from the North Sea model. These time series have a week added to either side, so are 2 weeks longer than the field data storms. From top to bottom: suspended sediment concentration, concentration in the 0.3 m thick buffer layer, shear stress, median wave height, near bed velocity and velocity variance